UNIVERSITY OF SZEGED
DEPARTMENT OF PHYSIOLOGY, SCHOOL OF MEDICINE
DOCTORAL SCHOOL OF THEORETICAL MEDICINE

Molecular Mechanisms of Hypoxic-Ischemic Encephalopathy in Newborn Piglets

Ph.D. Thesis

Viktória Éva Varga

Supervisor: Dr. Ferenc Domoki

Szeged

2018

Publications related to the PhD thesis

I. Viktória Varga, János Németh, Orsolya Oláh, Valéria Tóth-Szűki, Viktória Kovács, Gábor Remzső, and Ferenc Domoki: Asphyxia-induced neuronal cyclooxygenase-2 expression is alleviated by molecular hydrogen in newborn pigs. *Acta Pharmacol Sin* [Epub ahead of print] doi: 10.1038/aps.2017.148 2018.
IF: 3.223

II. Viktória Kovács, Valéria Tóth-Szűki, János Németh, Viktória Varga, Gábor Remzső, and Ferenc Domoki: Active forms of Akt and ERK are dominant in the cerebral cortex of newborn pigs that are unaffected by asphyxia. *Life Sci* 192:1-8 2018.
IF: 2.936

Contents

Ph.D. Thesis 1
Publications related to the PhD thesis 2
List of Figures and Tables 5
List of abbreviations 6
Summary 7
1. Introduction 8
1.1. Perinatal asphyxia and hypoxic-ischemic encephalopathy 8
1.2. Potential therapeutic interventions 9
1.3. PA/HIE piglet models to study H_2–induced neuroprotection 10
1.4. Cyclooxygenase-2 13
1.5. Microglial activation 16
1.6. ERK and Akt 18
2. Aims 20
3. Materials and Methods 21
3.1. Immunohistochemical analysis 21
3.1.1. Experimental groups and tissue sampling 21
3.1.2. Histology 22
3.1.3. COX-2 immunohistochemistry 22
3.1.4. 8-OHdG and Iba-1 immunohistochemistry 23
3.2. Western blot study 24
3.2.1. Experimental groups and surgical preparation 24
3.2.2. ERK and Akt kinase inhibitors 24
3.2.3. Western blot analysis 25
3.3. Statistical analysis 26
4. Results 28
4.1. Neuronal COX-2 expression in the time controls 28
4.2. Effect of asphyxia and H_2 ventilation on neuronal COX-2 expression 29
4.3. Assessment of correlation between neuronal COX-2 expression and neuronal damage 33
4.4. Assessment of correlation between neuronal COX-2 expression and oxidative DNA damage 35

4.5. Microglial activation and its correlation with COX-2 expression 36
4.6. Activation of ERK/Akt signalling pathways 37
5. Discussion 41
6. Conclusion 47
7. Acknowledgements 48
8. References 49

List of Figures and Tables

Table 1. Scoring system of cortical neuronal damage 11

Fig. 1. Comparison of some physiological parameters at the nadir of experimentally induced asphyxia and the grade of neuronal injury.....12

Fig. 2. COX-derived arachidonic acid metabolites in neurons.....15

Fig. 3. Activation of microglia and the following immune response 17

Fig. 4. The signalling pathway of Akt and ERK 19

Fig. 5. Experimental groups of immunohistochemical studies.....21

Fig. 6. Experimental groups of Western blot analysis.....25

Fig. 7. The ratio of neocortical COX-2 immunopositive neurons is decreased over time under normoxic conditions in anesthetized time control animals 28

Fig. 8. The effect of perinatal asphyxia and neuroprotective molecular H_2 on the ratio of COX-2 immunopositive neurons determined at 24 h survival.....30

Fig. 9. Representative photomicrographs showing COX-2 immunopositive neurons.....32

Fig. 10. High ratios of COX-2 immunopositive neurons/total neurons in cortical and hippocampal regions 34

Fig. 11. 8-OHdG immunopositivity in the parietal cortex 35

Fig. 12. Iba-1 immunopositivity in the parietal cortex.....36

Fig. 13. Ratio of phosphorylated and of total ERK and Akt levels in the cerebral cortex of the different experimental groups.....38

Fig. 14. Ratio of phosphorylated and of total ERK and Akt levels in the normoxic, non-asphyxiated cerebral cortex after inhibition.....39

Fig. 15. Ratio of phosphorylated and of total ERK and Akt levels in the assessed brain regions from the untreated and 48h asphyxia groups 40

List of abbreviations

8-OHdG – 8-hidroxy-2'-deoxyguanozine

aCSF – artificial cerebrospinal fluid

ADP – adenosine diphosphate

Akt - RAC-alpha serine/threonine-protein kinase / protein kinase B

BDNF – brain derived neurotrophic factor

COX – cyclooxygenase

DMSO – dimethyl-sulfoxide

EDTA – ethylenediaminetetraacetic acid

EGTA – ethylene glycol -bis (β-aminoethyl ether)-NNN'N'-tetraacetic acid

ERK – extracellular signal related kinase

H_2 – molecular hydrogen

HFS – high frequency stimulation

HIE – hypoxic-ischemic encephalopathy

HRP – horseradish peroxidase

LTP – long term potentiation

MAPK – mitogen activated protein kinase

mRNA – messenger ribonucleic acid

NF-κB – nuclear factor kappa-light-chain-enhancer of activated B cells

NMDA – N-methyl-D-aspartate

PA – perinatal asphyxia

PA/HIE – perinatal asphyxia-induced hypoxic-ischemic encephalopathy

PARP – poly (ADP-ribose) polymerase

PG – prostaglandin

PI-3-K – phosphatidylinositide-3-kinase

pMCAO – permanent medial cerebral arterial occlusion

PMSF – phenylmethanesulfonyl fluoride

PVDF – polyvinylidene difluoride

ROS – reactive oxygen species

SDS – sodium dodecyl sulphate

Summary

Perinatal asphyxia (PA) is among the most common causes of neonatal deaths. In the survivors, PA may result in multi-organ damage including hypoxic-ischemic encephalopathy (HIE) that often leads to life-long disabilities. Understanding the pathophysiological mechanisms of HIE is key to the development of neuroprotective therapies, and large animal PA/HIE models can help to bridge the translational gap between studies at the molecular/cellular level and the cotside management.

Our research group has previously shown that 8- or 20-min-long PA resulted in incrementally severe HIE in newborn pigs and that neuronal-vascular injury was alleviated by molecular H_2 ventilation in these models. Our purpose was to address several hypotheses related to the mechanisms of neuronal injury as well as H_2-induced neuroprotection using brain samples chiefly obtained from these previous studies.

First, we investigated the abundance of cyclooxygenase-2 (COX-2) immunopositive neurons in our samples, as COX-2 is known to be an important source of reactive oxygen species in the neonatal brain, however, induction of neuronal COX-2 by PA has not yet been shown in piglets. Oxidative cellular (DNA) damage was visualized with 8-hydroxy-deoxyguanozin immunohistochemistry and was correlated with neuronal COX-2 expression. Second, microglia were visualized with Iba-1 immunohistochemistry in order to detect PA-induced neuroinflammatory changes in microglial morphology quantified by the so-called ramification index. Third, the ratio of active (phosphorylated) and total forms of ERK and Akt kinases were determined using Western blots to assess the activity and PA-induced changes of these important antiapoptotic signal transduction mechanisms.

PA increased neuronal COX-2 expression neurons in several brain regions, where high percentage of COX-2 positive neurons always coincided with severe neuronal damage. In the parietal cortex, neuronal COX-2 abundance correlated both with oxidative damage and microglial activations.H_2 attenuated all of these PA-induced changes. Erk and Akt displayed high degree of phosphorylation in controls that was unaffected by PA in any studied region.

In conclusion, PA-induced neuronal COX-2 induction, oxidative damage and neuroinflammation all contribute to neuronal injury and are reduced by H_2, however, induction of antiapoptotic pathways appear to have a minor neuroprotective capacity in our HIE model.

1. Introduction

1.1. Perinatal asphyxia and hypoxic-ischemic encephalopathy

Perinatal asphyxia (PA) affects 1 to 6 newborns per 1000 full-term live births and represents the third most common cause of neonatal death (23%) right after preterm birth and severe infections[1]. PA is the medical condition resulted from impaired exchange of the respiratory gases – resulting in hypoxemia and hypercapnia – during birth to a newborn infant that lasts long enough to cause damage to the infant's organs, including the heart, lungs, liver, guts, kidneys and the brain[2].

The clinical presentation of PA-induced brain injury is hypoxic-ischemic encephalopathy (HIE) that is a sub-set of neonatal encephalopathy cases with a good evidence of a recent hypoxic-ischemic cause (including but not limited to PA), characterized as "a clinically defined syndrome of disturbed neurological function in the earliest days of life in the term infant, manifested by difficulty with initiating and maintaining respiration, depression of tone and reflexes, subnormal level of consciousness, and often by seizures"[3]. The prognosis depends on the severity of the hypoxic-ischemic insult[2]. HIE cases can be graded into 3 clinical stages: mild, moderate and severe encephalopathy according to the Sarnat scoring system[4]. Whereas few infants survive even severe HIE without a handicap, many of them develop life-long complications[5]. 10% of the survivors of moderate to severe HIE suffers in cerebral palsy and the risk is threefold if there is a history of neonatal seizures[6]. 80% of dyskinetic cerebral palsy can be associated to PA at term[7]. HIE may also result in sensory deficits including hearing loss[8] or abnormal visual function[9]. Learning difficulties, impairments in episodic memory associated with reduced hippocampal volume have all been found in children following HIE[10]. Reductions in school readiness and attention, as well as increased irritability have been shown in survivors of moderate encephalopathy without further disabilities[11]. Children who were affected by HIE have lower working memory, reading accuracy and comprehension scores, and increased requirement for educational support at the age of 8-11[12]. There is also a reported increase in behavioural difficulties among these children: hyperactivity[13] and increase in autistic spectrum disorders and an increased risk of psychotic symptoms including schizophrenia[14] are reported.

Although these studies are based on data of high-income developed countries, unquestionably the burden of this disease is the most severe in the developing countries[15]. Lack

of modern healthcare results in 8 times higher mortality in low income countries than in the developed regions[1].

We need to strive for an effective, reliable and inexpensive therapeutic intervention to alleviate the threats of PA/HIE.

1.2. Potential therapeutic interventions

Though therapeutic cooling is an acknowledged treatment for newborns who suffered from PA/HIE[16,17], a modern servo-controlled cooling set-up is expensive and inaccessible for many underprivileged medical institutions[18], whereas the cooling-rewarming procedure should be thoroughly controlled[19,20]. Even when performed with state-of-the-art technique, therapeutic hypothermia can offer no full neuroprotection, however, the whole-body hypothermia may cause various side effects, including bradycardia, hypotension or thrombogenesis[21]. Therefore, new studies aim to establish alternative/ complementary therapies, including the ventilation with "inert" gases[22].

We chose molecular hydrogen (H_2) as a putative neuroprotective agent based on the original report of Ohsawa et al. in an adult stroke rat model, where inhalation of 2-4 % H_2 proved to be the most effectively neuroprotective dose[23]. H_2 is a small membrane-soluble gas molecule, therefore inhaled H_2 can easily penetrate the blood-brain barrier, indeed, H_2 has been successfully used for measuring cerebral blood flow in hydrogen clearance technique since the 1960's[24] and this method was even adopted in piglets[25-27]. After rapid equilibration with the blood, the inhaled 2.1% H_2 in our studies is expected to result in approximately 10-20 μmol/l brain H_2 levels, similar to the levels determined in both rats and humans[23,28]. The neuroprotective effect of H_2 may be partly based on its antioxidant nature: it has been reported that H_2 selectively eliminates free radicals such as $OH^{\cdot}$ and $ONOO^{-}$[23], though there are suggestions of other, albeit little-known additional pharmacological targets. For instance, a recent study suggests, that beside its radical scavenger role, H_2 may have a mitohormetic effect[29], increasing the expression of anti-oxidative enzymes underlying the Nrf2-pathway[29], and there can be further yet unknown direct targets of H_2. H_2 is readily available, inexpensive, safe (not flammable in neuroprotective concentrations) and easy to apply, and shown to be harmless both in piglets and humans[28,30,31] . In this study we strived to gain a better understanding about the mechanisms lying behind the neuroprotective effect of H_2.

1.3. PA/HIE piglet models to study H_2–induced neuroprotection

The newborn piglet is an accepted large animal model of the term human neonates as the brain of the newborn piglet has similarly gyrencephalic structure, its developmental state and metabolic rate are matching around birth in the two species[32].

Our Experimental Neonatology Research Group performed two sets of subacute (24 h survival) experiments to study the neuroprotective potential of H_2 against PA/HIE in term newborn piglets: in the first study PA was induced with 8-minute long trachea-occlusion, in the second study with 20-minute long ventilation of a hypoxic-hypercapnic gas mixture, completed with respective time control and H_2 treated asphyxia groups[30,32]. The animals were similarly monitored in the two studies, the recorded physiological parameters, the observed neuronal injury and the neuroprotection afforded by H_2 in these PA/HIE models have been previously published[30,33]. However, as the major aim of the present thesis was to study the mechanisms of PA/HIE-induced neuronal injury in brain samples obtained from these animals, I would like to summarize the most important findings and also provide a little meta-analysis of these studies in the following paragraphs.

The physiological parameters (heart rate, arterial blood pressure, O_2 saturation, core temperature), blood gas and blood glucose levels at baseline were always in the physiological range[34] in all animals, in the normoxic time control animals also throughout the whole experiment, Asphyxia induced severe mixed respiratory and metabolic acidosis, characterized by elevated lactate and reduced base excess levels[33]. Our meta-analysis showed that by the end of the asphyxia, acidosis, hypercapnia, and hyperglycemia was more severe in the 20-min-long PA model (Figure 1).

We used cell counting in the first[30] and a neuropathology scoring system (0-9) in the second study to assess the extent of cortical lesions (Table 1.)[33]. In the latter method, from each region 20 fields of view of hematoxylin-eosin stained sections were assessed by two independent observers. In each field of view, the pattern of neuronal lesions was described as none, scattered, grouped/laminar or panlaminar. The neuropathology score was determined by the incidence of the most severe lesion observed. If the most severe lesions represented less than 20% of the total lesions, the scores were 1, 4, or 7; if 20-50%, 2, 6, or 8; and if more than 50%, 3, 6, or 9, respectively. Thus, higher scores represented increasingly severe neuronal damage[33]. In order to be able to compare the cortical neuronal injury in the two PA models, we

re-analyzed now the slides from the first study to also determine the corresponding neuropathological scores. We could demonstrate that neuropathological scores were significantly higher in the second study representing more severe cerebrocortical lesion in the 20-min-long asphyxiated animals. In a similar fashion, more severe neuronal injury was observed in the hippocampus and in the basal ganglia as well (Figure 1.)

score	morphology of cortical damage	percentage of damage in the given area
0	no damage	
1	scattered	<20 %
2		21-50%
3		50%<
4	grouped/laminar	<20 %
5		21-50%
6		50%<
7	panlaminar	<20 %
8		21-50%
9		50%<

Table 1. – Scoring system of cortical neuronal damage[33]

In summary, we can state that PA in the first study elicited mild-moderate whereas in the second study moderate-severe HIE. Thus, the 20-min-long PA was more appropriate to demonstrate the neuroprotective potential of H_2, indeed, H_2 treatment decreased the lesion to the level of the time controls in virtually all assessed regions: the cerebral cortex, the hippocampus, the basal ganglia, the thalamus, and cerebellum as well showing remarkable neuroprotection[33]. In the following sections, three potential factors of neuronal cell death/survival are introduced that could play a role in the pathomechanism of HIE.

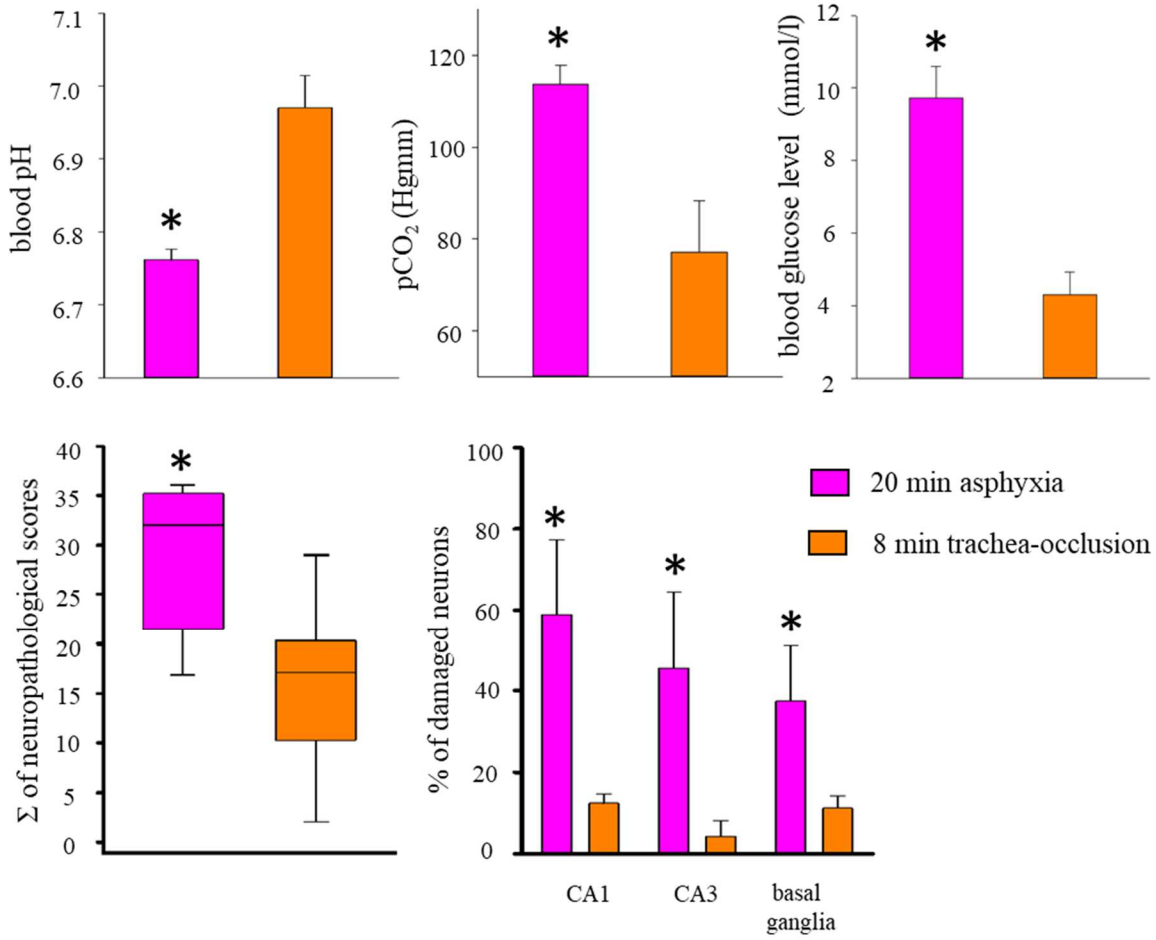

*Fig. 1. Comparison of some physiological parameters at the nadir of experimentally induced asphyxia and the grade of neuronal injury between the untreated asphyxia groups of our two previous studies[30,33]. The 20 min asphyxia resulted in significantly more severe acidosis, hypercapnia, and hyperglycemia. Neuropathological scoring revealed more severe injury 24h after the 20 min asphyxia, neuropathological scores (0-9) from the frontal, parietal, temporal and occipital cortices have been summated and plotted on the box plot showing median, 25th-75th as well as 10th-90th percentiles (line, box, as well as whiskers, respectively). The percentage of neuronal damage was also markedly larger in the CA1 and CA3 fields of the hippocampus, and in the basal ganglia as well. (n=7-7, * vs. 8-min trachea-occlusion; t-test / Mann-Whitney U-test, $p < 0.05$)*

1.4. Cyclooxygenase-2

Cyclooxygenases (COXs) are the rate-limiting enzymes catalysing the first committing step of prostaglandin (PG) production, i.e. the conversion of arachidonic acid released from membrane phospholipids by phospholipase-A2 to PGH_2[35]. PGH_2 is then further converted to biologically active prostaglandins, including PGD_2, PGE_2, $PGF_{2\alpha}$, PGI_2 and thromboxane-A_2[35] (Fig. 2.). There have been at least two COX isoforms described in the central nervous system, COX-1 and COX-2[36]. They are both membrane-associated enzymes with 71kDa molecular weight and they maintain 63% homology in their amino acid sequence[37]. Although they have similar catalytic activity, they differ in their pharmacological properties, as well as in cellular and tissue distribution[38]. Originally COX-1 was considered to be the constitutively expressed while COX-2 to be the inducible isoform[39]. In contrast, both COX-1 and COX-2 are constitutively expressed in the central nervous system[36], furthermore, COX-2 proved to be the dominant isoform of COXs in the neonatal brain[40], providing up to 80% of the total brain COX activity[41]. Whereas COX-1 is constitutively expressed in most brain regions[36], COX-2 is especially enriched in the hippocampus and the cortex[42]. The tissue distribution of COX-2 raised the issue whether COX-2 derived prostanoids have any modulatory role in the regulation of synaptic transmission and neural plasticity. Yamagata et al. found that the basal expression of COX-2 is regulated by NMDA receptor-dependent synaptic activity and COX-2 expression is upregulated by high-frequency stimulation (HFS) associated with the induction of long-term potentiation (LTP)[42]. The putative connection was confirmed by the observation that specific COX-2 inhibitors reduced the HFS-induced LTP at hippocampal synapses[43]. This result suggests that the COX-2 is involved in hippocampal long-term synaptic plasticity. Hippocampal LTP found to be potentiated in COX-2 transgenic mice[44], meanwhile the HFP-induced LTP was not significantly different in COX-2 knockout mice[45], presumably due to compensatory COX-1 response[46,47].

The function of COX-2 in synaptic transmission is verified by the reports that COX-2 is localized in the dendritic spines of neurons as well[48]. COX-2 also participates in the flow-metabolism coupling, e. g. in the functional hyperemia in the barrel-cortex following whisker stimulation[49]: COX-2 produces PGH_2 which is then further converted to PGE_2 which has vasodilatory effect[50].

Additionally, expression of COX-2 is well-known to be upregulated by various deleterious stimuli including brain trauma[51,52], cerebral ischemia[53,54], and proinflammatory insults[55]. The neuronal induction of COX-2 expression suggests the enzyme's participation in neuroinflammation, the pathogenesis of neurodegenerative diseases, traumatic brain injury, and ischemia-induced neuronal damage and epileptogenesis[56].

Studies have shown that the stroke volume and neurological deficit is decreased by the deletion of COX-2 gene or specific COX-2 inhibitors[57,58].

During prostaglandin production, reactive oxygen species (ROS) are released by COX-2[56,59] (Fig. 2.), which are eliminated by endogenous antioxidants - like superoxide dismutase[60] or glutathione peroxidase[61] - in physiological conditions, though neonates are particularly sensitive for ROS due their organs' structural and functional immaturity, the overloading of aerobic metabolism with rapidly growing energy demand, the reduced ability to induce efficient homeostatic mechanisms, as well as the lack of effective antioxidant systems that mature during the first year of life in human neonates[62].

COX-2 has an undeniable role in the pathogenesis of HIE. A study showed that the administration of COX-2 inhibitors before as well as soon after the ischemic insult provided neuroprotection in a rat HIE model[63]. Additionally, human neonatal brain ischemia has been also linked to high level of neuronal COX-2 expression by a human autopsy study[64]. Therefore, the role of COX-2 in the pathomechanism of HIE could be best investigated in a translational large animal model that could also be used to establish neuroprotective treatments.

COX-2 has been extensively researched in newborn piglets as well. It has been shown that anoxic stress increases COX-2 but not COX-1 mRNA and protein levels both in the cerebral vascular endothelium[65] as well as in the cortical and hippocampal neurons, meanwhile this elevation was not successfully evoked by asphyxia within 2-8 hours of survival[54]. The regional distribution of COX-2 immunopositive neurons in piglet brain was already described by our group, however within 4 hours following trachea-occlusion no change in COX-2 immunopositivity occurred[66]. This study raised the question about whether a more effective asphyxia induction or longer time window of observation was needed.

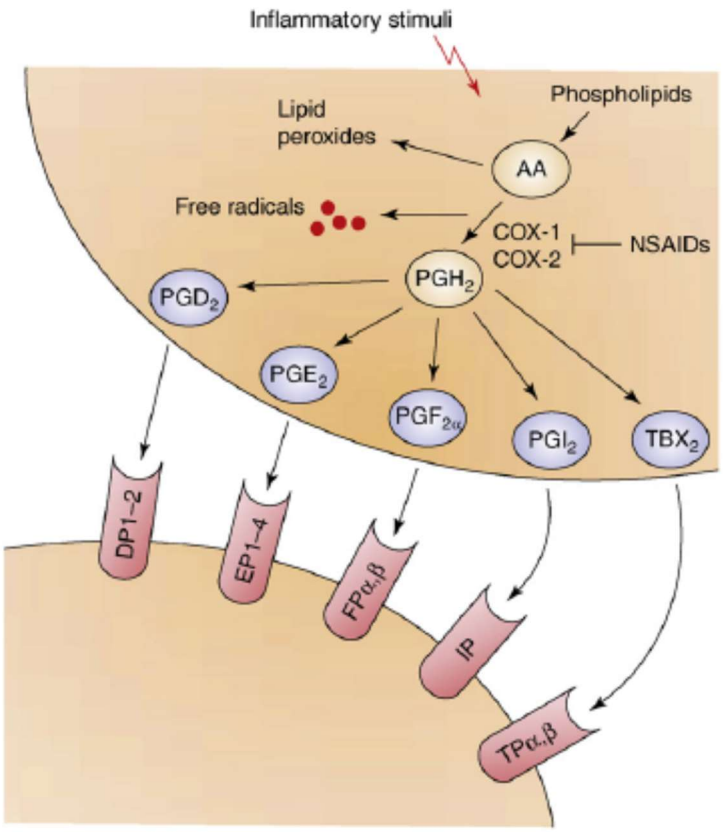

Fig. 2. COX-derived arachidonic acid (AA) metabolites in neurons[56]

Note that in an equimolar concentration with prostanoids, oxygen free radicals are produced! (PGD_2, PGE_2, $PGF_{2\alpha}$, PGH_2, PGI_2, TBX_2 – prostanoids; DP1-2, EP1-4, FPα,β, IP, TPα,β – corresponding prostanoid receptors, NSAIDs – non-steroid anti-inflammatory drugs)

1.5. Microglial activation

Microglia are the resident immune-competent cells of the brain tissue, derived from monocytes and entering the brain during the early embryonic brain development[67]. They total up to 5-12% of the glia population[68]. Microglia develop a ramified phenotype and constantly monitor their environment[69]. They may get activated by any changes in the brain homeostasis or a pathological event [70]. Although there are different proposed models of morphological changes occurring due to microglial activation, they all agree that the process results in de-ramification[70]. Therefore, the activational state of microglial cell can be characterized with the so-called ramification index, published by Faulkner et al. in 2011[22]. The ramification index takes into account the number of microglial cells and their branches in a given area. The lower the value of the ramification index is, the more activated the microglia are.

Microglia have a contrasting role in neuroinflammation. Depending on their subtype they can activate either pro- or anti-inflammatory pathways[71]. The M1 subtype, which is co-activated by ROS, nevertheless releases pro-inflammatory cytokines and produces further ROS meanwhile blocking the anti-inflammatory effects of the M2 subtype[71] (Fig. 3.).

The microglial activation and polarization is influenced by the mechanism, location, and severity of the injury and the age at which the injury occurs[72,73], therefore it is necessary to describe the microglial activation in the given model of a neurodegenerative disease.

Previous reports about microglial activation in the piglet model of PA/HIE were inconsistent[22,74]. We sought to determine whether we can detect activated microglia after 24 hours of survival in our recent PA/HIE model.

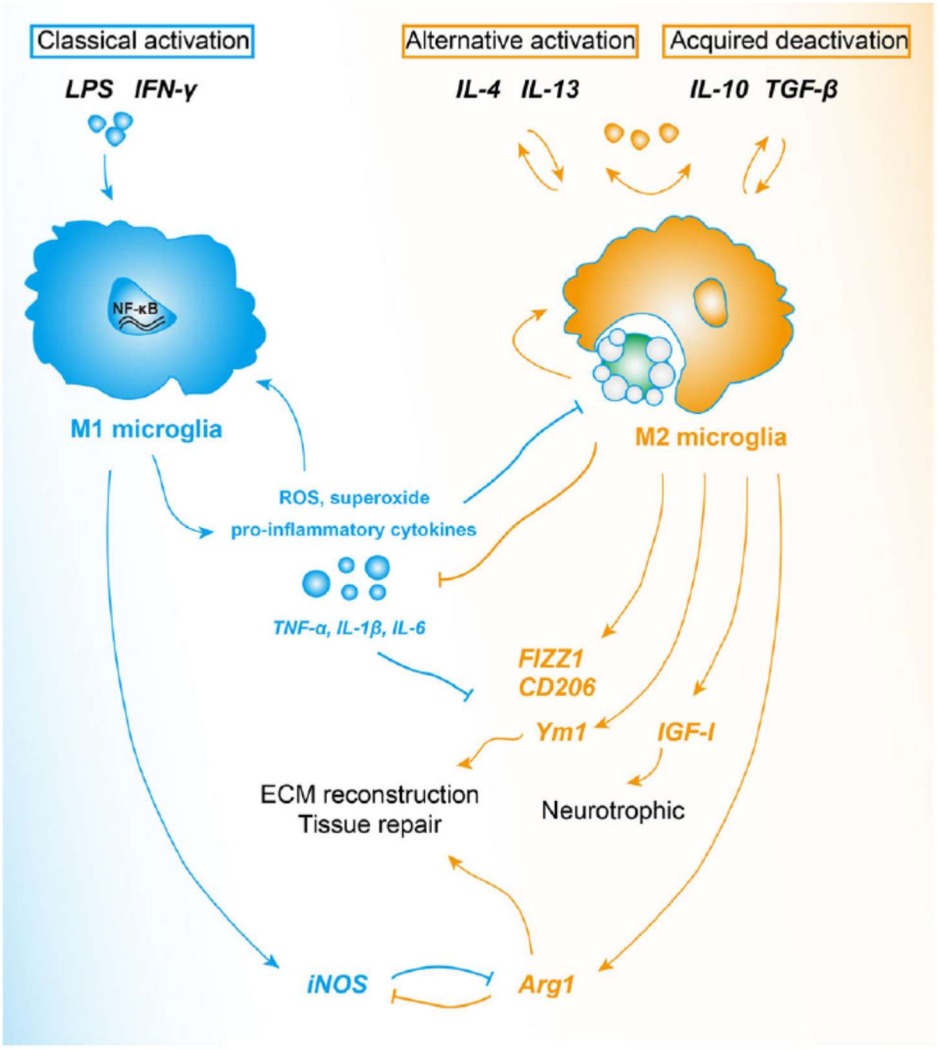

Fig. 3. Activation of microglia and the following immune response[71]

The pro-inflammatory M1 subtype of microglia is co-activated by ROS and inhibits the anti-inflammatory effects of the M2 subtype. (LPS – lipopolysaccharide, IFN-γ – interferon-γ, IL – interleukin, TGF-β – tumor growth factor-β, ROS – reactive oxygen species, TNF-α – tumor necrosis factor-α, FIZZ1 – =RETNLB - resistin like beta,CD206 – mannose receptor C-type 1, Ym1 – chitinase-like 3, IGF-1 – insulin like growth factor 1, Arg1 – arginase 1, iNOS – inducible nitric oxide synthase, ECM – extracellular matrix)

1.6. ERK and Akt

While PA/HIE causes severe neuronal damage, many, sometimes the majority of the neurons still survive the insult, but the role of antiapoptotic mechanisms in neuronal survival is still not fully revealed. As the antiapoptotic mechanisms work in the favour of preserving the neurons, therefore they can serve in theory as potential targets for neuroprotective strategies.

Neurotrophins activate different intracellular pathways (Fig. 4.) that may exert neuroprotective effect[75,76]. Brain-derived neurotrophic factor (BDNF) belongs to the neurotrophic factor family and plays an important role in neuronal development and maturation in the central nervous system[77]. BDNF proved to be neuroprotective against hypoxic-ischemic injury in rodents[78,79]. The neuroprotective effects of BDNF are mediated either by the mitogen-activated protein kinase (MAPK) or phosphatidylinositide-3-kinase (PI-3-K) pathway[80] depending on environmental conditions and cellular stimuli. The activation of PI-3-K can be detected by the phosphorylation of the RAC-alpha serine/threonine-protein kinase (Akt) which regulates cell survival, proliferation, growth, and glycogen metabolism[81,82]. Among MAPKs, the extracellular signal related kinase (ERK) has been identified as a possible contributor to neuroprotection[83]. Intracerebroventricular administration of BDNF to postnatal day 7 rats elevated the phosphorylation level of ERK1/2 and Akt kinases[84]. Pharmacological inhibition of ERK increased the tissue loss after the hypoxic-ischemic insult in rodents[84], however little is known about the activation of these pathways in a newborn large animal model after hypoxic-ischemic injury.

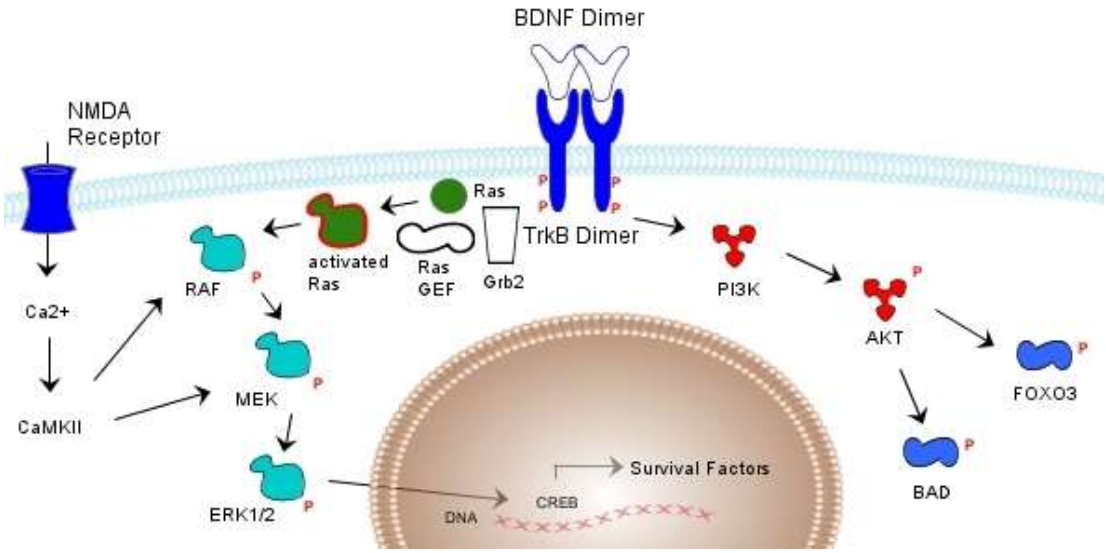

Fig. 4. The signalling pathway of Akt and ERK[85]

The receptor binding of BDNF dimer activates Akt and ERK kinase cascades which lead to cell survival.

(BDNF – brain derived neurotrophic factor, NMDA – N-methyl-D-aspartate, CAMKII – calmodulin kinase II. – RAF – [rapidly accelerated fibrosarcoma] kinase family, MEK – mitogen activated protein kinase kinase, ERK – extracellular signal-regulated kinase, Ras – [rat sarcoma] small GTPase proteins, GEF – guanine nucleotide exchange factor, Grb2 – growth factor receptor-bound protein 2, TrkB – tyrosine kinase receptor-B, PI3K – phosphoinositide 3- kinase, AKT – protein kinase-B, FOXO3 – forkhead box O3, BAD – Blc-2-associated death promoter, DNA – deoxyribonucleic acid, CREB – cAMP response element-binding protein)

2. Aims

Our group has successfully constructed translational piglet PA/HIE models, in which the applied PA protocols induced mild or moderate-severe HIE. These models were also adequate to test and to demonstrate the neuronal-vascular protection afforded by H_2 applied in the reventilation period after PA. However, the molecular mechanisms responsible for the observed neuronal cell death, as well as the effector mechanism of the neuroprotective H_2 have still many yet unmapped areas. To better describe our model, and also to tackle some of the cellular events of the developing HIE, our aims were to answer the following questions:

1.) Regional differences in neuronal COX-2 expression have been previously reported[66]. We therefore asked if the 24 h observation of the anesthetized animals would *per se* influence the percentage of COX-2 immunopositive neurons?
2.) Does PA induce neuronal COX-2 after 24 hours of survival? Are there any regional differences in the response to PA?
3.) Is there any correlation between the percentage of COX-2 immunopositive neurons and the severity of the neuronal lesion?
4.) Is there any correlation between the percentage of COX-2 immunopositive neurons and the oxidative damage of neurons?
5.) Can microglial activation be demonstrated in our PA/HIE model? Is there any correlation between the percentage of COX-2 immunopositive neurons and the degree of microglial activation?
6.) Can the neuroprotective H_2 treatment interfere with the effect of PA on the percentage of COX-2 immunopositive neurons or affect the microglial response?
7.) Can the activation of the Akt and ERK play an important role in neuronal survival in 24-48 hours after PA?

3. Materials and Methods

3.1.Immunohistochemical analysis

3.1.1. Experimental groups and tissue sampling

For immunohistochemistry, we used the brain samples of newborn male Large-White piglets (age < 24 h at beginning of experiments, body weight: 1.5-2.5 kg, n=47; Pigmark Ltd., Co., Szeged, Hungary) obtained mainly from the previous studies[30,33]. The major difference between the two studies was the induction method and the duration of PA: asphyxia was elicited by 8 minutes of trachea-occlusion and suspended ventilation in the first, and by 20-minute-long ventilation with hypoxic-hypercapnic gas mixture (6% O_2, 20% CO_2) in the second study. The animals were divided into the following 3-3 groups in both studies (Fig. 5.):

1.) normoxic time control groups (n=7-7) ventilated with air
2.) asphyxiated control groups (n=7-7) reventilated with air for 24 hours
3.) and asphyxiated groups reventilated with air containing 2.1% H_2 for 4 hours, followed by air for the remaining (20 hours) survival time (n=7-7).

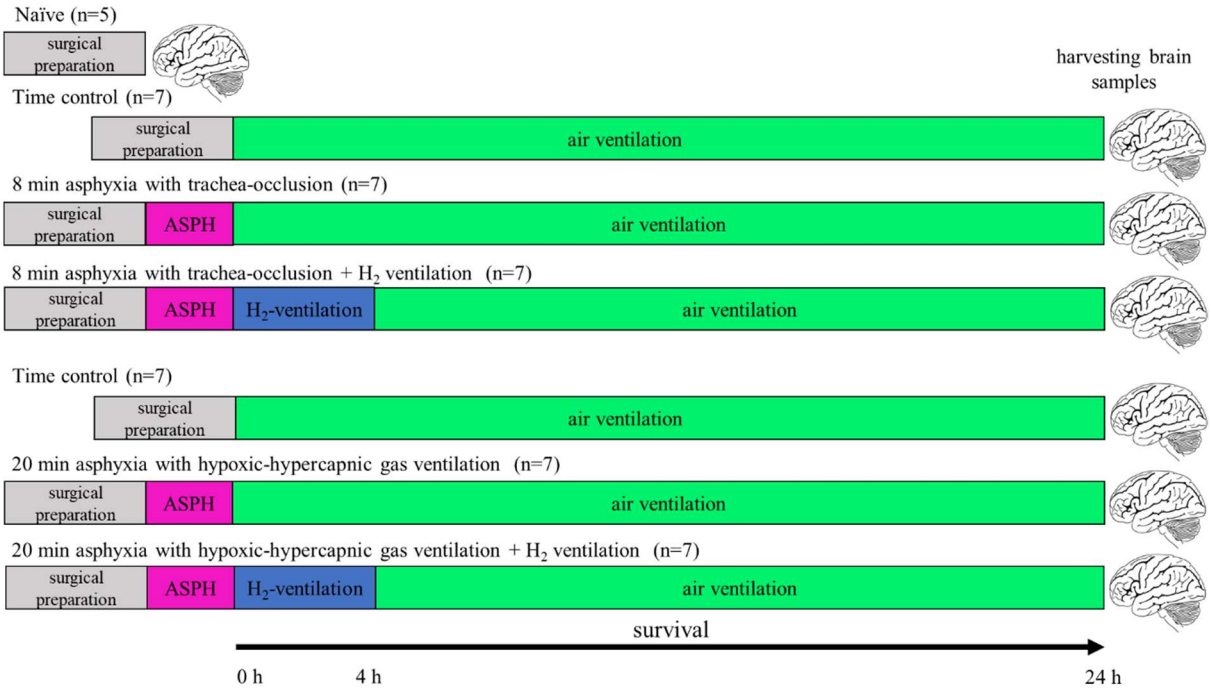

Fig. 5. Experimental groups of immunohistological studies (ASPH – asphyxia)

We also included an additional naïve control group to study baseline levels of the different markers. In the naïve control group, piglets (n=5) were anesthetized with sodium thiopental (45 mg/kg; ip.; Sandoz, Kundl, Austria), and the brains were immediately perfused with 100 ml cold physiological saline solution through the catheterized common carotid arteries and harvested for immunohistochemical analysis.

All procedures were approved by the Animal Care and Use Committee of the University of Szeged. Animal care and handling were in accordance with the National Institutes of Health guidelines.

3.1.2. Histology

The brain tissue was immersion fixed with 4%, 4°C paraformaldehyde for 2 weeks. Paraffin-embedded, 4 μm sections were produced using a microtome (Leica Microsystems, Wetzlar, Germany). The sections were mounted on sylanized slides. Haematoxylin-eosin staining was performed to determine the degree of neuronal lesion, which was determined with cell counting in most areas. In the cerebral cortex, however, neuropathology scores were determined (0-9) in each region, as previously described.

3.1.3. COX-2 immunohistochemistry

COX-2 immunohistochemistry was performed using Leica Bond Max automated immunostainer (Leica Microsystems, Wetzlar, Germany): the slides were dewaxed at 72°C, and antigen retrieval was performed at pH: 6. The slides were then incubated with a 1:100 rabbit monoclonal antibody against COX-2 (clone SP21, Labvision, Fremont, California, USA) for 30 min followed by horseradish peroxidase-conjugated anti-rabbit antibody (EnVision®; Dako, Glostrup, Denmark). 3,3'-diaminobenzidine (DAB) tetrahydrochloride solution was used for visualization, then the slides were counterstained with haematoxylin to visualize the cell nuclei. The slides were dehydrated in ascending alcohol series, cleared in xylene and covered with a coverslip, then scanned in a slide scanner (Pannoramic MIDI, 3DHISTECH Ltd., Budapest, Hungary) and visualized on a personal computer using the Pannoramic Viewer software (3DHISTECH Ltd.) at 20x magnification. Areas of interest were randomly selected and photomicrographs were taken from each observed regions: 10-10 images of the frontal, temporal, parietal and occipital cortex, 3-3 of the CA1, CA3 subfields and the dentate gyrus of

the hippocampus, 10-10 of the thalamus and the basal ganglia, and 15 images of the cerebellar cortex for the study of Purkinje-cells. Cells were manually counted with the help of the ImageJ software (Wayne Rasband, NIH, Bethesda, Maryland, USA) by two independent observers. Neurons were identified by their shape and size. The ratio of COX-2 immunopositive to all neurons were determined, the averages/cerebral areas/animals were counted.

3.1.4. 8-OHdG and Iba-1 immunohistochemistry

Based on the results of our COX-2 studies, the parietal cortex has been selected for further studies. Tissue microarrays from the parietal cortex were produced from using a custom-made stainless steel tissue puncher (3 mm) from the paraffin embedded tissue blocks of the second study (time control, 20 min asphyxia, 20 min asphyxia+H_2 groups). The microarrays were also sectioned at 4 μm, mounted on sylanized slides and processed for immunohistochemistry. To test the oxidative damage of the neurons, 8-OHdG immunohistochemistry was performed[33]. Slides were incubated with a 1:200 dilution of mouse monoclonal primary antibody against 8-OHdG (JaICA Inc., Fukuroi, Japan) for 20 min followed by horseradish peroxidase-conjugated rabbit anti-mouse secondary antibody for 15 minutes (n = 6-6-6). To assess microglial activation, Iba-1 immunohistochemistry was performed (n = 7-6-6). Slides were incubated with rabbit anti-Iba-1 antibody (Wako Chemicals GmbH, Neuss, Germany) for 30 min, followed by horseradish peroxidase-conjugated anti-rabbit antibody (EnVision®; Dako, Glostrup, Denmark) for 15 min. In both cases 3,3'-diaminobenzidine was used to visualize the immunostaining, then the slides were counterstained with haematoxylin, to visualize the cell nuclei. The slides were covered with a coverslip then scanned in the slide scanner, and visualized on a personal computer using the Pannoramic Viewer software at 40x magnification. As a sign of oxidative damage, homogenous, strong nuclear 8-OHdG immunoreactivity was considered. The ratio of these nuclei to the total neuronal nuclei was determined using the ImageJ software, similarly to the previously described method. The average/sample was plotted on box plots. The groups were compared with one-way ANOVA on ranks followed by Student-Newman-Keuls *post hoc* test ($p<0.05$). Microglial activation was characterized by determining the so-called ramification index (RI). We applied a 0.20 x 0.25 mm grid to the microphotographs of 3 randomly selected areas/sample at 40x magnification. The immunopositive cell bodies (CBD) in the grid were

counted as well as the microglial branches (B) crossing the gridlines. From these data, RI was defined according to the following equation: $RI = B^2/CBD$.

3.2. Western blot study

3.2.1. Experimental groups and surgical preparation

Anaesthesia was induced by intraperitoneal injection of sodium thiopental (45 mg/kg; Sandoz, Kundl, Austria). Piglets (n=20) were intubated via tracheotomy and artificially ventilated with humified, warmed room air (21% O_2, balance N_2; respiratory rate: 30-35 1/min, peak inspiratory pressure: 120-135 mmH_2O). A catheter was introduced into the right femoral vein to maintain anaesthesia/analgesia with a bolus injection of morphine (100 µg/kg; Teva, Petach Tikva, Izrael) and midazolam (250 µg/kg; Torrex Pharma, Vienna, Austria), followed by continuous infusion of morphine (10 µg/kg/h) and midazolam (250 µg/kg/h), as well as 5% glucose and 0,45% NaCl 3-5 ml/kg/h) throughout the whole experiment. Another catheter was placed either into the right femoral artery or into the right carotid artery for continuous monitoring of arterial blood pressure and heart rate and take arterial blood samples for determining the blood gas and blood sugar levels and certain time points of the experiment.

The animals used in the Western blot study were divided to naïve, time control and asphyxia groups with both 24 and 48 hours of survival (Fig. 6.). Asphyxia was elicited by 20-minute-long ventilation with hypoxic-hypercapnic gas mixture (6% O_2, 20% CO_2). Based on our preliminary Western blot results, we added two special MAPK/ERK or Akt1/2 kinase inhibitor treated groups to our Western blot study.

3.2.2. ERK and Akt kinase inhibitors

A custom-made closed cranial window with 3 injectable ports was inserted over the left frontoparietal region, then filled with artificial cerebrospinal fluid (aCSF; 126.6 mM NaCl, 3 mM KCl, 1.5 mM $CaCl_2$, 1.2 mM $MgCl_2$, 24.5 mM $NaHCO_3$, 6.7 mM urea, 3.7 mM glucose bubbled with 95% O_2 and 5% CO_2 to achieve a constant pH of 7.4). The *dura mater* was opened. After the implantation we allowed a 45-min-long stabilization period. Both the MEK inhibitor U0126 and the Akt1/2 kinase inhibitor A-6730 drugs were dissolved in dimethyl-sulfoxide

(DMSO) to a 10 mM stock solution then further diluted in aCSF to obtain 10 µM drug solutions (final DMSO concentration was 0.01%). In the respective experimental groups, the drugs were applied topically onto the cerebral cortex with continuous superfusion through one of the injectible ports at a rate of 0.5 ml/min for 40 min. The other two ports allowed continuous efflux of the aCSF. The cortex below the cranial window as well as the corresponding contralateral untreated cortex were collected and processed as described in the following section.

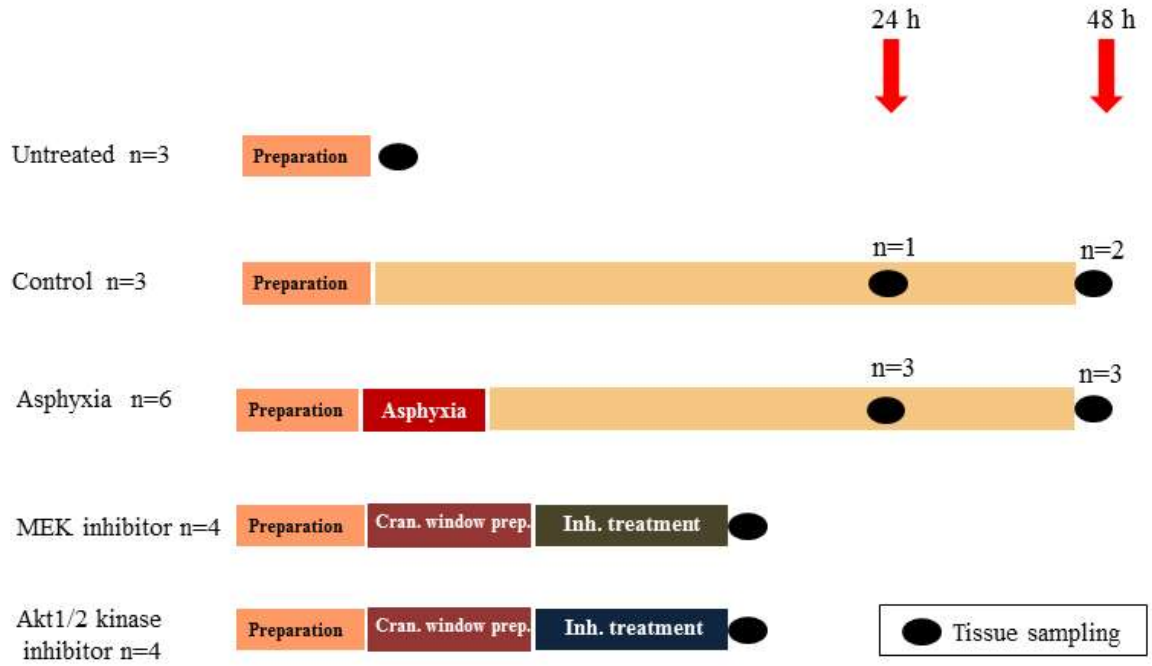

Fig. 6. Experimental groups of Western blot analysis

3.2.3. Western blot analysis

Thawed samples were homogenized and harvested in ice-cold lysis buffer (50 mM Tris-base, pH 7.4, 150 mM NaCl, 10% glycerol, 1mM EGTA, 1 mM Na-orthovanadate, 5 µM $ZnCl_2$, 100 mM NaF, 10 µg/ml aprotinin, 1 µg/ml leupeptin, 1mM phenylmethylsulfonyl fluoride (PMSF), 1% Triton X-100). The homogenate was centrifuged at 40,000 x g at 4°C for 30 min and the protein concentration of the supernatant was determined (Bio-Rad Protein Assay Dye Reagent Concentrate, Bio-Rad, Hercules, CA, USA). Samples prepared from equal amounts (50 µg) of protein were mixed with Laemmli buffer (1M Tris-HCl, pH 6.8, glycerol, SDS, 100

mM EDTA, 100mM EGTA and 1% bromophenolblue) and denatured by boiling. Subsequently, they were loaded for 12% SDS-containing polyacrylamide gel and separated based on molecular size. The gels were electroblotted for polyvinylidene difluoride (PVDF) membranes (Hybond-P, GE Healthcare, United Kingdom). Detection of the protein of interest was carried out by first blocking the membrane in 3% nonfat dry milk in Tris Buffered Saline -Tween (10 mM Tris-base, 150 mM NaCl, 0.2% Tween-20, pH 8.0; TBS-Tween). Membranes were probed overnight at 4°C with antibodies recognizing the following antigens: phospho-p44/42 MAP kinase to detect phospho-ERK1/2, total p44/42 MAP kinase, anti-Akt and phospho-Akt (Ser473), (Cell Signalling Technology, Danvers, MA, USA), diluted 1:1000 in the blocking solution. Excess antibody was removed by five washes of TBS-Tween. Membranes were incubated with a horseradish-peroxidase (HRP)-conjugated goat anti-rabbit secondary antibody (Cell Signalling Technology, Danvers, MA, USA) diluted 1:1000 in blocking solution at room temperature for 2 hours. Five washes in TBS-Tween were followed by detection of the enhanced chemiluminescent signal (WesternBright ECL, Advansta, USA) on X-ray films. The relative protein expressions were determined using densitometry (ImageJ software, National Institutes of Health, USA). Each experiment has been performed at least three times.

3.3. Statistical analysis

COX-2 immunopositivity was plotted on box plots using R 3.3.1 software (The R Foundation for Statistical Computing, Vienna, Austria) as the data followed a non-normal distribution tested by Shapiro-Wilk normality test. For statistical analysis, ANOVA on ranks followed by Student-Newman-Keuls *post hoc* test was performed using SigmaPlot 12.0 (Systat Software Inc., Chicago, Illinois, USA). $P<0.05$ was considered statistically significant. The ratio of COX-2 immunopositive neurons was correlated with the previously determined histopathological score[33], and the result was plotted on a dot plot using R 3.3.1 software.

The RI values of each field of view were plotted on box plots and the groups were compared with one-way ANOVA on ranks followed by Dunn's *post hoc* test. Correlations were plotted and tested using the R 3.3.1 software (Pearson's correlation, $p<0.05$).

The Western blot results were plotted using SigmaPlot (v12.0, Systat Software Inc., San Jose, CA., USA). Statistical comparisons include one-way analysis of variance (ANOVA) as

well as two-way repeated measures ANOVA followed by the Holm-Sidak *post hoc* test for pairwise comparisons. Neuropathology scores were expressed as median, 25-75 percentiles. For non-parametric data Mann-Whitney U test was applied. P values <0.05 were considered to be significant.

4. Results

4.1. Neuronal COX-2 expression in the time controls

Neuronal COX-2 expression showed marked regional differences: in the naïve animals the highest percentage of COX-2 positive neurons could be observed in the frontal and parietal cortices similar to our previous results in time controls at 4 hours of survival, as described previously[66]. However, this regional expression pattern appeared markedly changed in the 24h time controls, as the COX-2 expression was significantly reduced in all neocortical regions compared to naïve or 4h survival animals (Fig. 7.). This reduction was found limited to the neocortex: the ratio of COX-2 immunopositive neurons remained unchanged in the hippocampus (Fig. 7.).

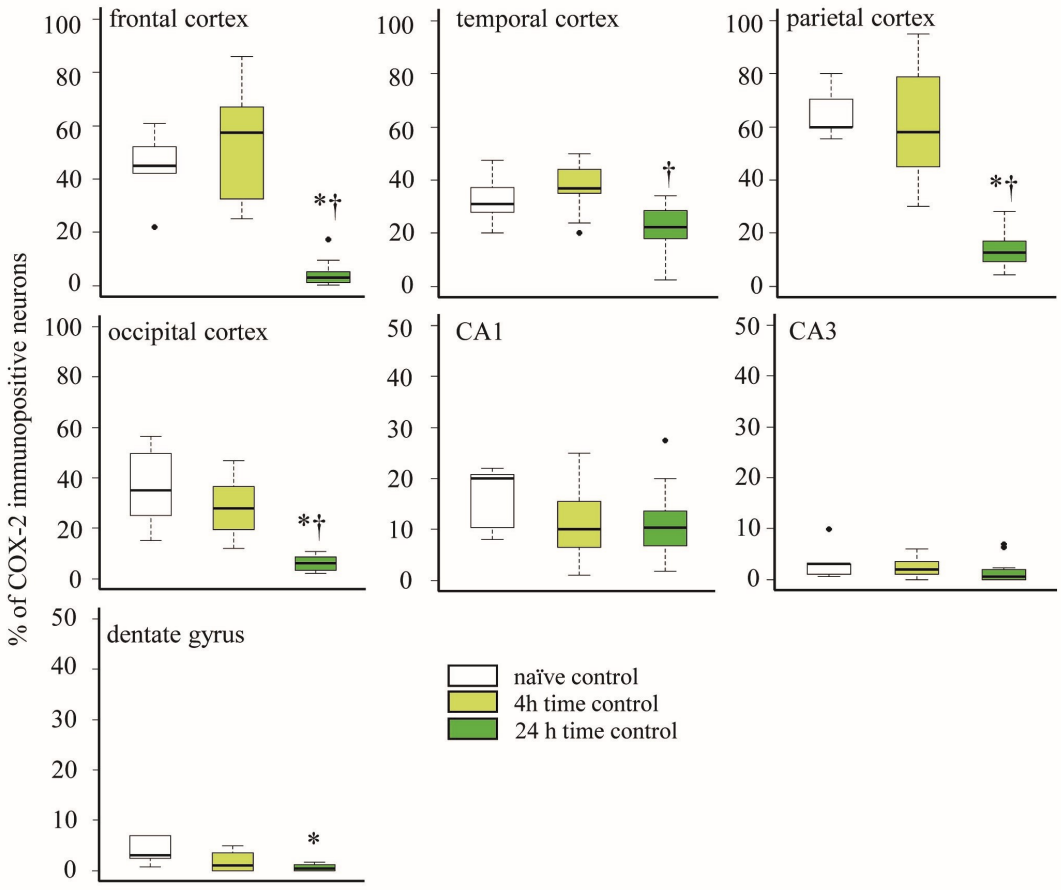

Fig. 7. The ratio of neocortical COX-2 immunopositive neurons is decreased over time under normoxic conditions in anesthetized time control animals. In the different cortical lobes, the percentage of COX-2 immunopositive cells determined in samples from naïve animals (brains

harvested immediately after anaesthesia n=5), as well as from normoxic time controls with 4 hours of survival after anaesthesia (n=12) displayed similar COX-2 expression in accordance with previous data showing regional differences among the regions[66]. However, the percentage of COX-2 immunopositive neurons in the 24h survival time control group (n=14) has been significantly reduced compared to both the naïve and the 4h time control groups in all neocortical regions. Interestingly this reduction did not to affect the CA1 and CA3 hippocampal subfields. (vs. naïve animals, † vs. 4 h time control; ANOVA on ranks, Dunn's post hoc test, $p<0.05$; bold line, box, and whiskers represent the median, 25^{th}-75^{th}, and 10^{th}-90^{th} percentiles, respectively; black dots are outliers.)*

4.2. Effect of asphyxia and H_2 ventilation on neuronal COX-2 expression

In the brain regions obtained from the study of 8-minute-long asphyxia, there was no significant alteration in neuronal COX-2 expression (Fig. 8.) as no difference was noted between the time control and asphyxiated groups in any of the observed regions (Fig. 8.). In contrast, 20-minute-long asphyxia elicited significant increases in neuronal COX-2 immunopositivity in the parietal and occipital cortices, as well as in the hippocampal CA3 region (Fig. 8.). Furthermore, a tendency of asphyxia-induced elevation in COX-2 immunopositive neurons could also be observed in the frontal and temporal cortices and in the basal ganglia too, albeit these changes did not reach statistical significance in these regions (Fig. 8.). In the H_2-treated group, despite exposure to the same level of asphyxia, the ratio of COX-2 immunopositive cells was similar to the time control group (Fig. 8.).

In contrast to the CA3 subfield, the hippocampal CA1 region and the dentate gyrus displayed low percentage of COX-2 immunopositive neurons in time controls, and the ratio of immunopositive neurons were unchanged by asphyxia, they were similar in all three groups. In a similar fashion, COX-2 was present in about 30% of the cerebellar Purkinje cells in all experimental groups (Fig. 8.).

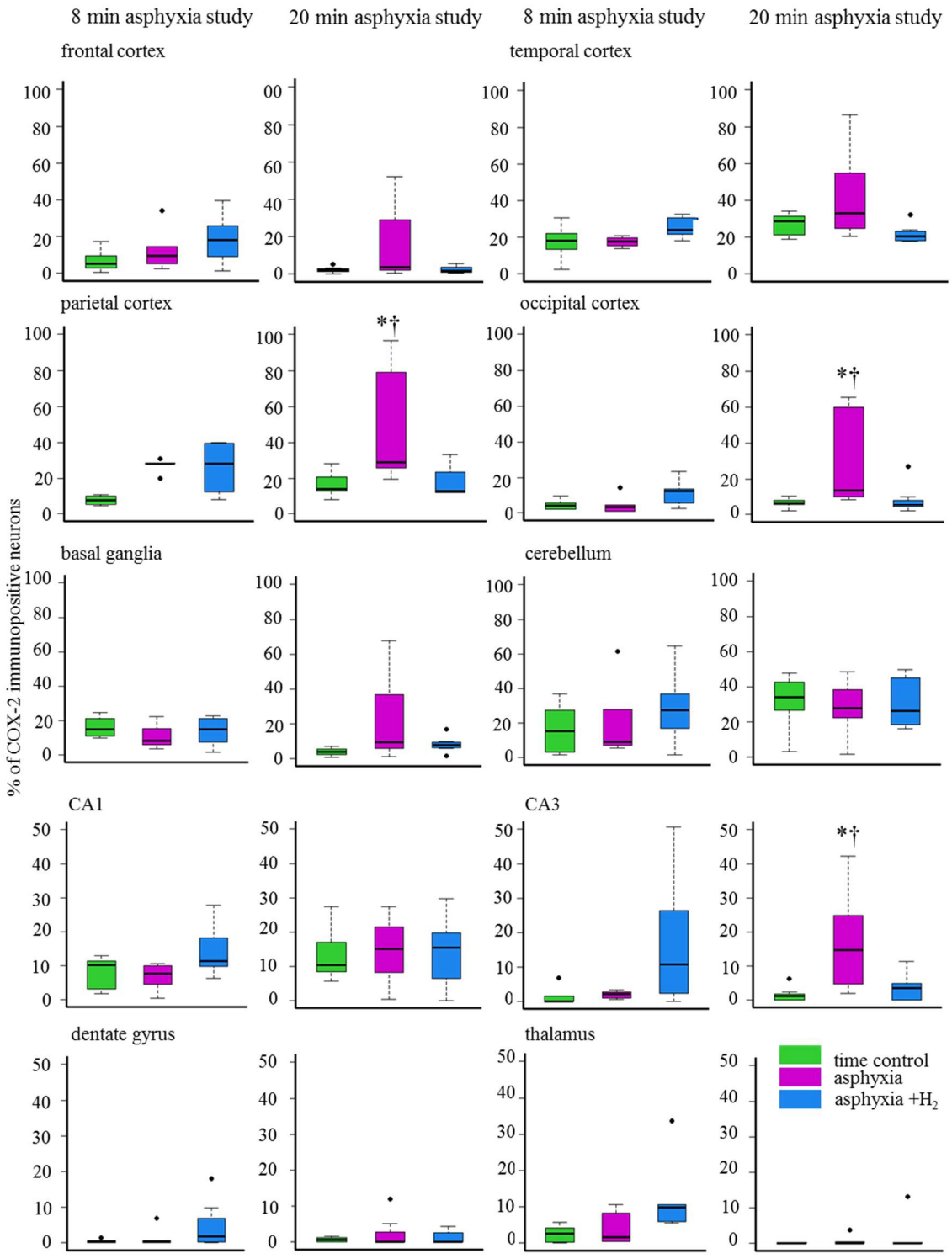

Fig. 8. The effect of perinatal asphyxia and neuroprotective molecular H_2 on the ratio of COX-2 immunopositive neurons determined at 24h survival. Two levels of perinatal asphyxia of different duration (8 and 20 min) were studied, and both asphyxia groups (n=7-7) were

compared to the corresponding time control (n=7-7) and H_2-treated asphyxia groups (n=7-7). In the first study using 8 min asphyxia, the neuronal COX-2 expression was not significantly affected neither in the asphyxia nor in the H_2-treated asphyxia groups. On the other hand, in the second study using 20 min asphyxia, the asphyxia elicited significant elevations in the ratio of COX-2 immunopositive neurons in the parietal and occipital cortices, as well as in the hippocampal CA3 region. The trends of increased COX-2 expression could also be observed in the frontal and temporal cortices along with the basal ganglia, though the differences did not reach statistical significance in these regions. The hippocampal CA1 region and dentate gyrus, as well as the thalamus showed low immunopositivity, which was unaffected both by asphyxia and H_2-treatment. About one third of cerebellar Purkinje-cells were COX-2 immunopositive, no marked difference was detected among the three groups. (vs. time control, † vs. asphyxia+H_2; ANOVA on ranks, Student-Newman-Keuls post hoc test, $p<0.05$; bold line, box, and whiskers represent the median, 25^{th}-75^{th}, and 10^{th}-90^{th} percentiles, respectively; black dots are outliers)*

Notably, strong COX-2 immunopositive areas were only recorded in the asphyxia group of animals (Fig. 9.).

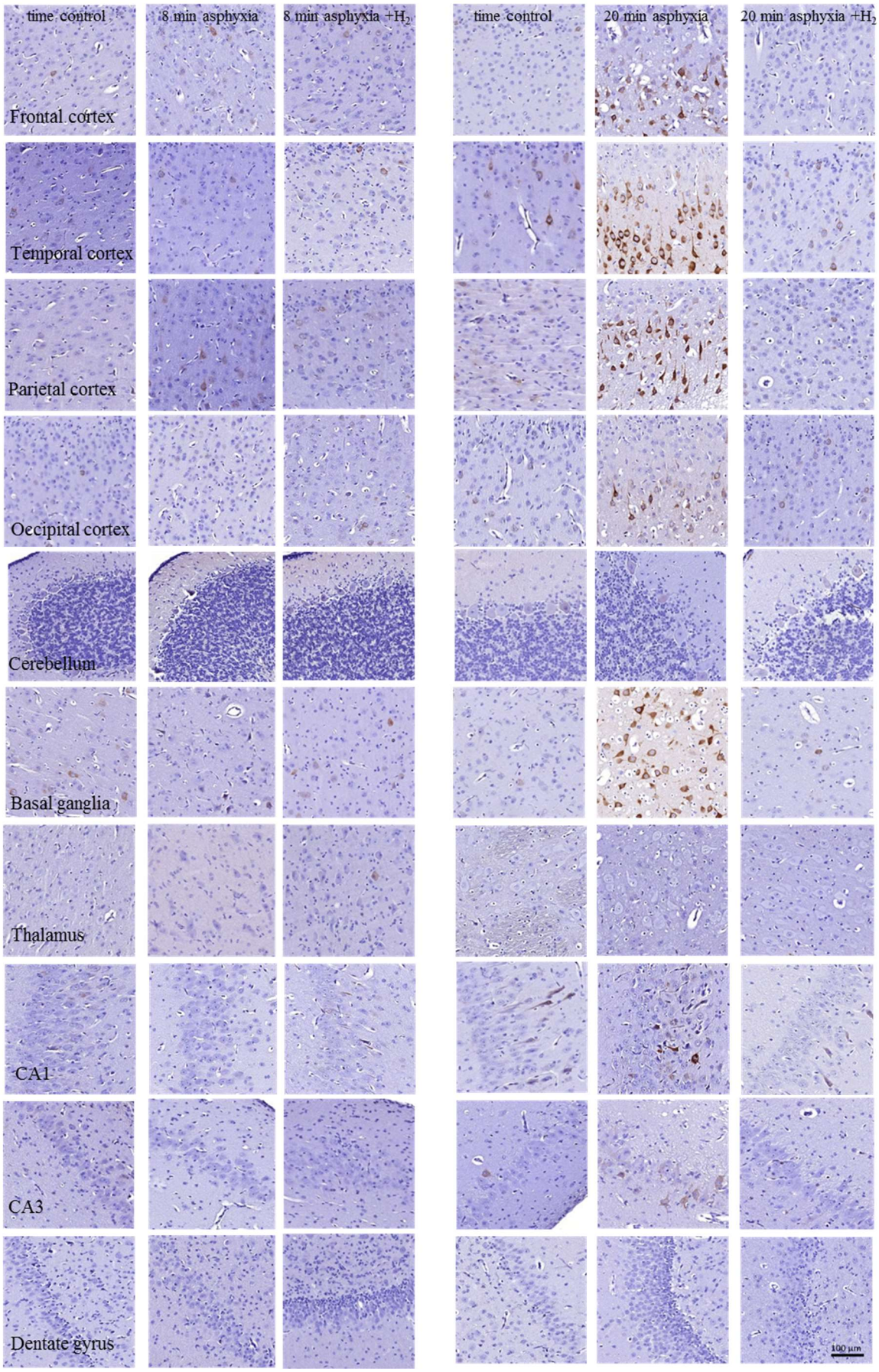
time control
8 min asphyxia
8 min asphyxia +H2
time control
20 min asphyxia
20 min asphyxia +H2
Frontal cortex
Temporal cortex
Parietal cortex
Oecipital cortex
Cerebellum
Basal ganglia
Thalamus
CA1
CA3
Dentate gyrus
100 μm

Fig. 9. Representative photomicrographs (20x) showing cyclooxygenase-2 (COX-2) immunopositive neurons (brown-stained neurons) from the assessed brain regions in the matching time control, asphyxia and asphyxia+H_2 groups of the 8 min asphyxia and the 20 min asphyxia studies. The displayed fields of views were selected from the 10 analyzed fields of views of those animals that yielded the median values of the respective groups in Fig. 8. No remarkable difference can be detected among the experimental groups of 8 min asphyxia study, the increased abundance of COX-2 immunopositive neurons is striking in virtually all neocortical areas, in the CA3 hippocampal region and in the basal ganglia from the 20 min asphyxia group.

4.3. Assessment of correlation between neuronal COX-2 expression and neuronal damage

As neuronal COX-2 expression was affected by 20-minute-long asphyxia only, we performed all subsequent studies on these animals. We first investigated whether the ratio of COX-2 immunopositive neurons correlated with the previously determined neuropathology scores, higher scores reflecting more severe neuronal damage in the cortex (Fig.10.). We found no correlation between the neuropathology scores and neuronal COX-2 expression ($r=0.38$; $p<0.01$), however, we could clearly identify 3 expression patterns: low neuropathology scores were always associated with low-moderate levels of neuronal COX-2 expressions; high neuropathology scores were associated either with high or with low COX-2 expression levels. Notably, low neuropathology score never coincided with high COX-2 expression level (Fig. 10.).

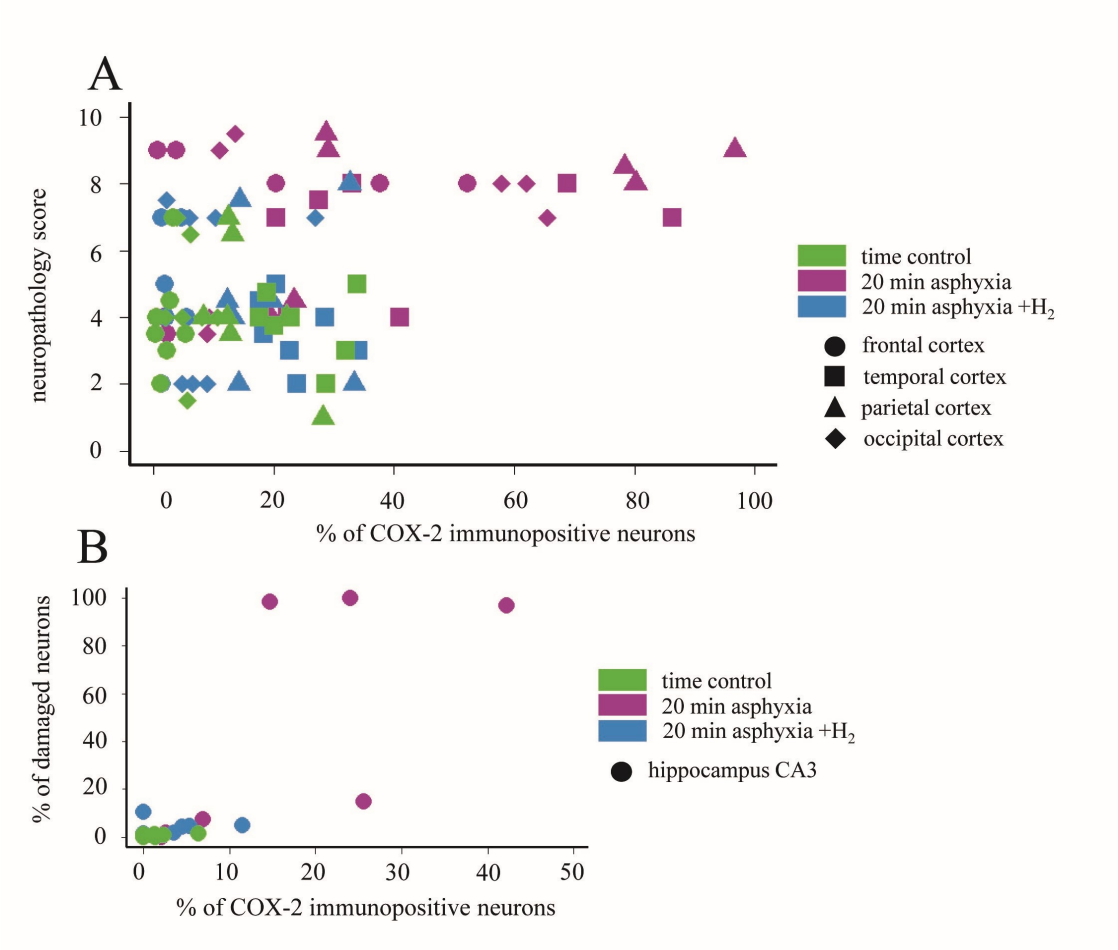

Fig. 10. High ratios of COX-2 immunopositive neurons/ total neurons are exclusively found in severely damaged cortical and hippocampal regions. A) In the cortical regions of normoxic time control group (n=7), neuropathology scores are usually low and associated with low levels of COX-2 immunopositive neurons. Similar observations can be made for the 20 min asphyxia+H_2 group (n=7) as well. However, in the 20 min asphyxia group (n=7), severe neuronal lesion may or may not be associated with high percentage of COX-2 immunopositive neurons. Importantly, high COX-2 immunpositivity is not associated with low neuropathology scores in any animals/regions B) In the hippocampal CA3 subfield, the highest number COX-2 immunopositive neurons are from the 20 min asphyxia group with largest degree of neuronal damage.

4.4. Assessment of correlation between neuronal COX-2 expression and oxidative DNA damage

In the parietal cortex, 20-minute-long asphyxia significantly increased the ratio of 8-OHdG immunopositive neuronal nuclei (Fig.11/A, B) compared to both the time control and the H_2-treated asphyxia group indicating oxidative stress induced by asphyxia and the mitigating effect of molecular H_2 (Fig.11/A, B). By assessing the correlation between the ratios of COX-2 and 8-OHdG immunopositive neurons (Fig. 11/C), we found a marked tendency (r = 0.71), either considering data from all groups or from the 20 min asphyxia group alone.

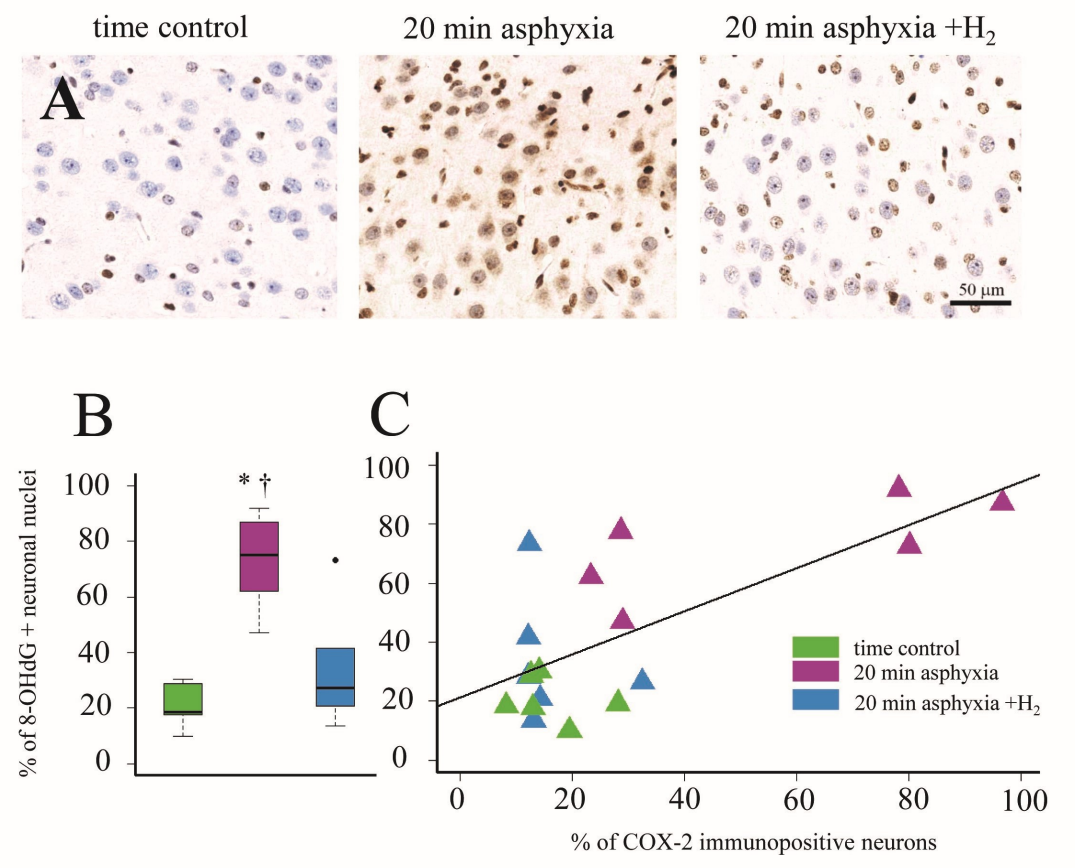

Fig. 11. 8-OHdG immunopositivity in the parietal cortex of the matching time control, 20 min asphyxia and 20 min asphyxia+H_2 groups. Representative photomicrographs (A) demonstrate the oxidative damage of nuclei (40x) in the 20 min asphyxia group compared to the time control and the 20 min asphyixa+H_2 groups. The ratio of 8-OHdG immunopositive neuronal nuclei/ total neuronal nuclei (B) is markedly increased in 20 min asphyxia group compared to time control and 20 min asphyxia+H_2 groups (n=6-6-6, ANOVA on ranks, Student-Newman-Keuls

post hoc test, $p<0.05$; bold line, box, and whiskers represent the median, 25^{th}-75^{th}, and 10^{th}-90^{th} percentiles, respectively; black dots are outliers) Correlating the 8-OHdG and COX-2 immunopositivity (C), we can detect a significant tendence (Pearson's method, $r = 0.71$, $p<0.05$).

4.5. Microglial activation and its correlation with COX-2 expression

The Iba-1 immunohistochemistry visualized the distribution and morphology of microglia in the parietal cortex (Fig. 12/A). Microglial activation is associated with reduced branching and assuming an amoeboid shape, and this change was quantified by RI determination. We found that RI was significantly lower in the group subjected to 20 min asphyxia, than in the time control group (Fig. 12/B). However, there was no statistical difference between the time controls and the H_2-treated asphyxiated animals. When considering all data points, RI showed no correlation with neuronal COX-2 expression ($r = -0.56$, $p<0.05$, Fig. 12/C), but when regarding exclusively the 20 min asphyxia group significant negative correlation ($r = -0.75$, $p<0.05$) was observed.

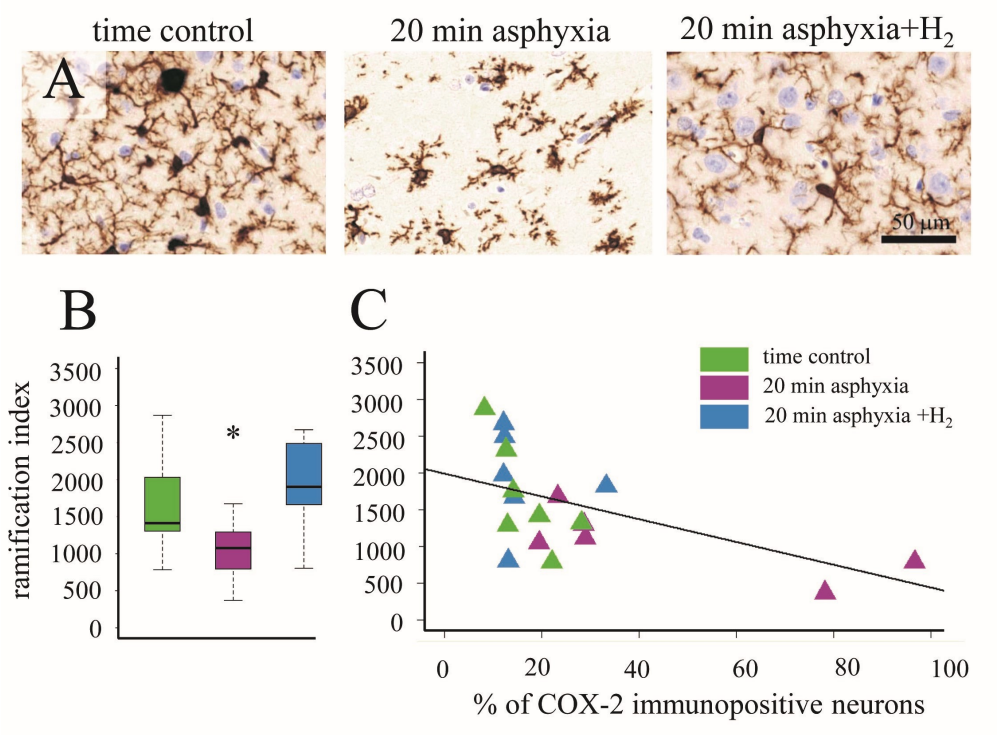

Fig. 12. Iba-1 immunopositivity and microglial ramification index in the parietal cortex of the matching time control, 20 min asphyxia and 20 min asphyxia+H_2 groups. Representative photomicrographs (A) show that while in time control and 20 min asphyxia+H_2 groups the shape of microglial cells is ramified, in 20 min asphyxia group the microglial cells are getting activated and start assuming a more amoeboid shape (40x). The ramification index (B) is evidently decreased in the 20 min asphyxia group compared to the time control group, however, the 20 min asphyxia+H_2 group is more similar to the time control group (n=7-6-6, ANOVA on ranks, Dunn's post hoc test, p=0.015). The correlation between the ramification index and neuronal COX-2 expression (% of total neurons) (C) considering all 3 groups is less pronounced (Pearson's method, r = -0.56, p<0.05), however, when regarding the 20 min asphyxia group only, we can detect a significant negative correlation (r = -0.75).

4.6. Activation of ERK/Akt signalling pathways

Total ERK levels in the frontoparietal cortex were remarkably similar in all experimental groups. In addition, the levels of phosphorylated ERK (P-ERK) were also similar to the total levels; therefore the ratio of the P-ERK to total ERK was typically between 80-100 % indicating high degree of activation of the pathway (Fig. 13.). The results concerning total and phosphorylated Akt (P-Akt) levels, the ratio of P-Akt to total Akt levels were also remarkably high and there were no statistical differences among the groups, despite a slight tendency of activation by asphyxia (Fig 13.).

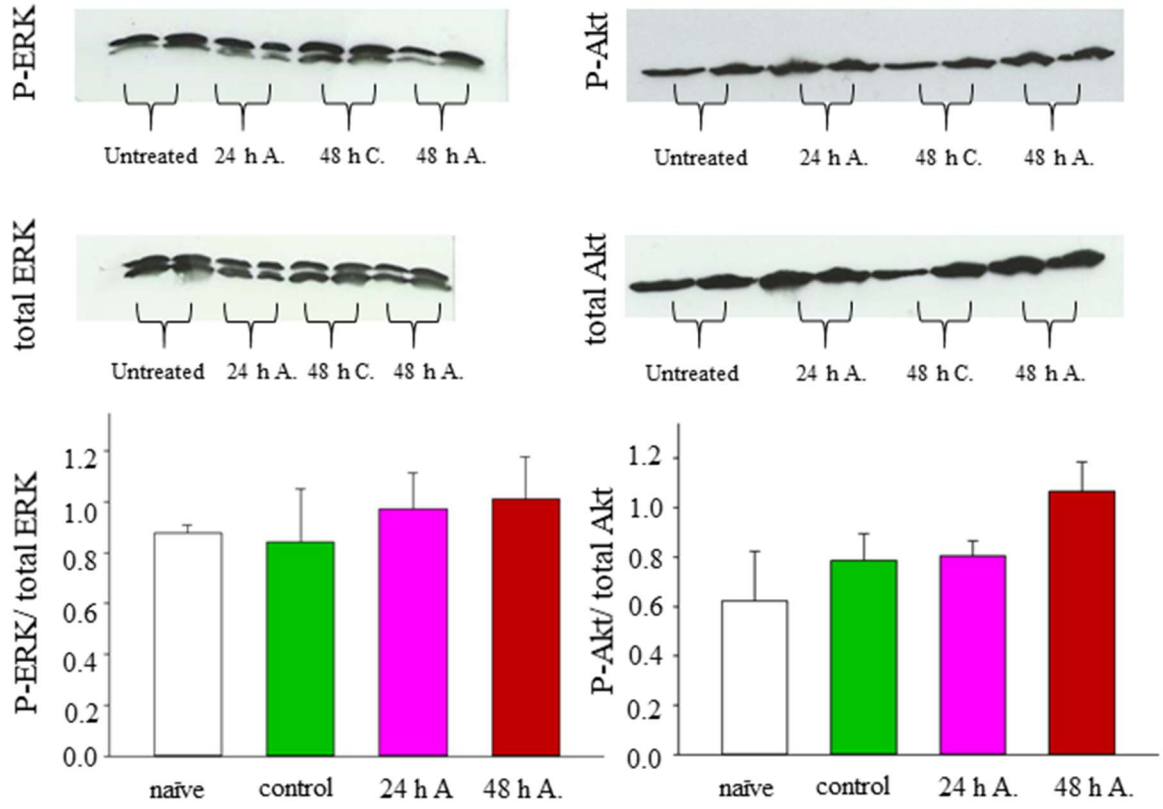

Fig. 13. Ratio of phosphorylated (P-ERK, P-Akt) and levels of total ERK and Akt in the cerebral cortex of the different experimental groups (bar graphs) with representative blots. There were no significant differences among the different groups. Untreated – untreated group; Control, C – time control animals without asphyxia; A – asphyxia group, 24 h - 48 h – length of survival.

High degree of ERK and Akt phosphorylation in the frontoparietal cortex was also demonstrated in the samples taken from the control side in our short-term experiments (Fig. 14.). However, under normoxic conditions, local, topical *in vivo* treatment with the MEK inhibitor U0126 and the Akt1/2 kinase inhibitor A-6730 resulted in significant inhibition of ERK and Akt phosphorylation, respectively (Fig. 14.).

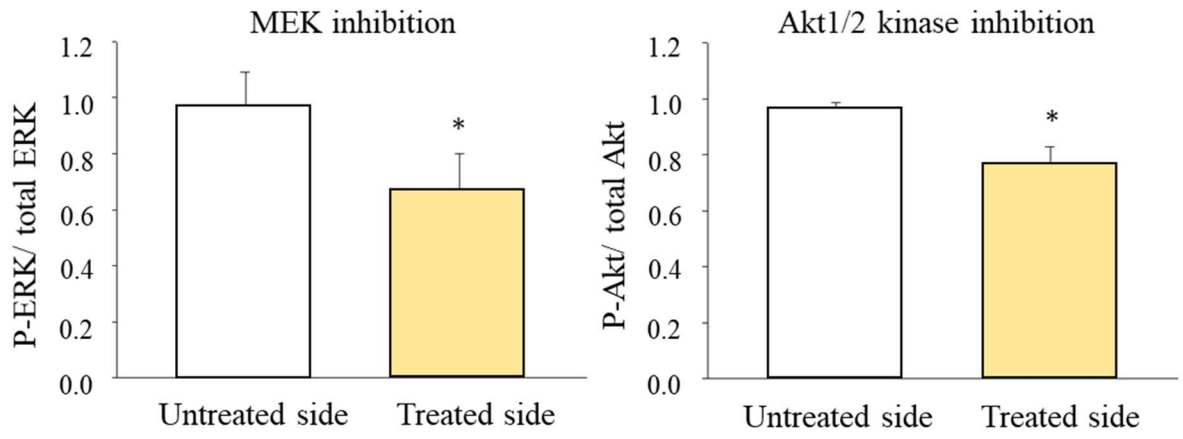

Fig. 14. Ratio of phosphorylated (P-ERK, P-Akt) and levels of total ERK and Akt in the normoxic, non-asphyxiated cerebral cortex after inhibition with the MEK inhibitor U0126 and the Akt1/2 kinase inhibitor A-6730, respectively. Both inhibitors significantly reduced phosphorylation compared to the contralateral untreated side. ($p<0.05$ compared to the untreated side)*

The ratios of P-ERK/total ERK and the P-Akt/total Akt in the other assessed brain regions were remarkably similar to the values determined in the neocortex (Fig. 15.). In the untreated as well as in the 48 h asphyxia animals, the phosphorylation ratios were remarkably high and there were no statistical differences among the groups, indicating no effect of asphyxia.

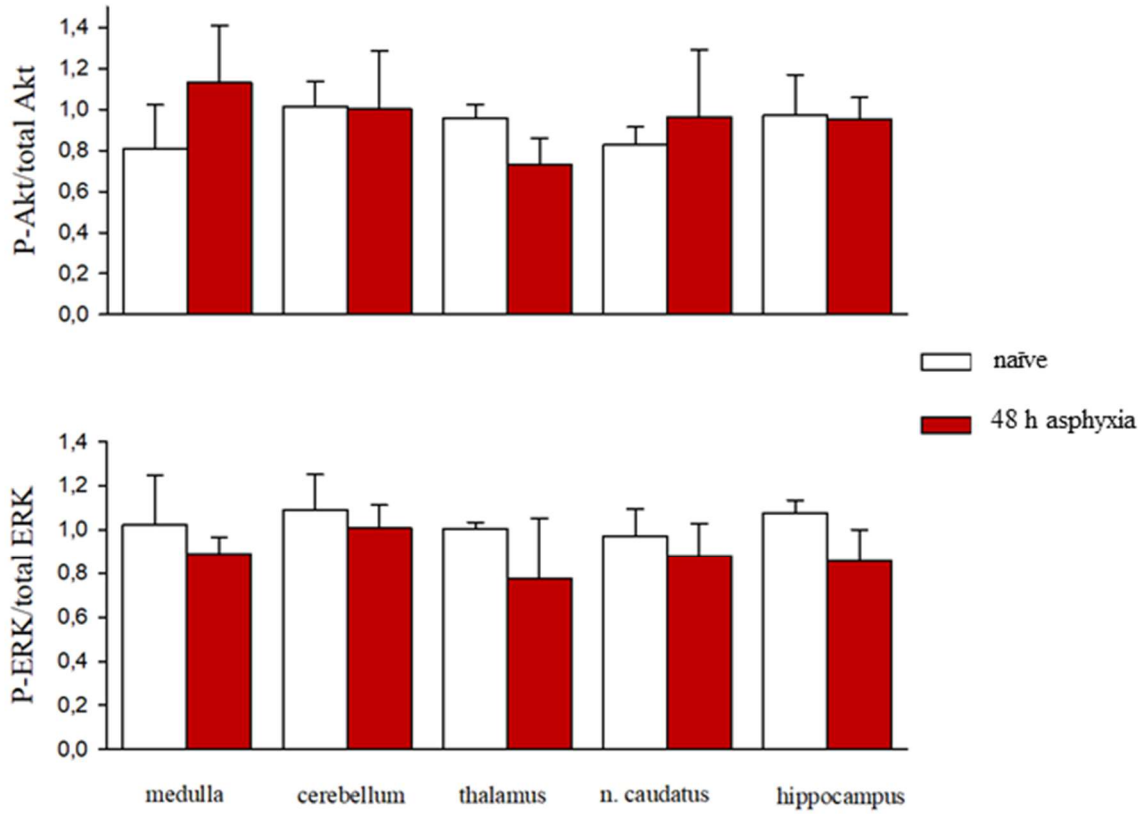

Fig. 15. Ratio of phosphorylated (P-ERK, P-Akt) and of total ERK and Akt levels in the assessed brain regions from the untreated and 48 h asphyxia groups (n=3-3). Assessment of the different brain regions yielded essentially similar data: both ERK and Akt displayed high degree of phosphorylation that was unaffected by asphyxia, there were no significant differences among the different groups. (naïve – untreated group; 48 h asphyxia - asphyxia group with 48 h of survival)

5. Discussion

The major findings of the present study are as follows:

1) region-specific neuronal COX-2 expression in the neocortical areas is maintained at 4 hours, but greatly reduced at 24 hours of survival in anaesthetized time controls;

2) 20-min, but not 8-min-long PA can significantly elevate the number of COX-2 positive neurons in the neocortex and the hippocampal CA3 subfield but not in the assessed subcortical areas or other hippocampal structures;

3) high ratios of COX-2 immunopositive neurons are always associated with severe neuronal lesion;

4) the ratio of COX-2 expressing neurons correlates with the oxidative damage of the neurons in the parietal cortex;

5) microglial activation can be detected in our HIE model already after 24 hours of survival in the parietal cortex, and the ratio of COX-2 immunopositive neurons correlates with microglial activation;

6) the neuroprotective H_2 administration prevents the upregulation of neuronal COX-2 expression in all sensitive brain regions, reduces oxidative damage, and alleviates microglial activation after PA;

7) both ERK and Akt are constitutively phosphorylated/ active in the cerebral cortex and all other assessed brain regions of newborn pigs irrespective of the length of anaesthesia and/or exposure to asphyxia; meanwhile we proved that the high cerebrocortical ERK and Akt phosphorylation levels under normoxic conditions can be *in vivo* modulated by specific inhibitors.

We believe to be the first to describe the induction of neuronal COX-2 expression following asphyxia in a translational subacute piglet PA/HIE model. Previously, we extensively characterized the effect of 20-min asphyxia elicited in newborn (<1 day old) piglets by ventilation with a hypoxic-hypercapnic (6% O_2 - 20% CO_2) gas mixture on hemodynamics, blood gases, metabolites, electroencephalogram and neuropathology[33]. The applied insult resulted in alterations that matched both human pathology and naturally occurring birth asphyxia in swine[66] and corresponded to moderate to severe HIE in all of the animals. Our present results elucidated the confounding results from previous studies in which elevations in

COX-2 levels were reported after 10 min of global cerebral ischemia but not 10 min of asphyxia[54]. Our current results suggest that this reported difference was due to the more severe hypoxic/ischemic insult elicited by global cerebral ischemia, and in the present study, the longer asphyxia duration rather than the shorter treatment elicited conditions similar to those observed with global ischemia, which resulted in the upregulation of COX-2.

In the present study, neuronal COX-2 abundance was conspicuously reduced in all neocortical areas of the 24 h time control animals compared with the values previously reported in our 4 h survival study[66]. This difference cannot be attributed to differences in methodology such as for COX-2 immunostaining or cell counting, as the values obtained from the naïve animals in the present study yielded virtually identical data to the previously published values. The decreased number of COX-2-expressing neurons may be in part explained by the inactivation of cortex due to anaesthesia, as COX-2 expression is stimulated by neuronal activity[86]. The applied anaesthetic/analgesic drugs could exert an inhibitory effect on COX-2 expression by interacting with the nuclear transcription factor NF-κB signalling pathway, which is a well-known transcriptional regulator of COX-2[87]. Although morphine has been reported to have ambiguous stimulatory and inhibitory effects on NF-κB activation[88,89], midazolam is unequivocally known to inhibit the NF-κB pathway[90]. The applied anaesthetic regimen was chosen to enhance the translational potential of our animal model, as morphine/midazolam analgesia/sedation is routinely used in the management of human neonates affected by PA/HIE[91]. Furthermore, experimental data suggested that morphine analgesia may be an important permissive factor by allowing neuroprotective therapies such as therapeutic hypothermia to be effective; mild hypothermia failed to exhibit neuroprotection in the absence of anaesthesia and analgesia in newborn pigs[92]. Our current results suggested that this “supportive” analgesia may have a beneficial effect on neuronal survival in part through the attenuation of COX-2 expression. Our findings also suggested a time-dependent role of COX-2-derived ROS and prostanoids in the pathomechanism of HIE development in different brain regions, as COX-2 activity-dependent neuronal injury in the early reventilation/ reoxygenation phase will be most likely pronounced in regions with high baseline COX-2 expression (especially the frontoparietal neocortex). However, in the delayed secondary energy failure phase, COX-2 will likely remain a more important pathogenic factor for neuronal injury in those areas where the asphyxia-induced elevation dominates over the anaesthesia-induced depression of COX-2 levels.

The present data thus suggest that at least in the neocortical areas, two factors affect neuronal COX-2 abundance. Long-term anaesthesia tends to decrease the enzyme levels, whereas asphyxia elevates them. Both the increase in COX-2 levels and the increase in the level of neuronal injury were variable in the piglets subjected to asphyxia, in accordance with the spectrum of human HIE severity. We found that very high percentages of COX-2-immunopositive neurons were inevitably accompanied by the most severe types of cortical neuronal damage. In some cases, however, similarly high neuropathology scores coincided with rather low COX-2 immunopositivity. These areas may perhaps represent those severely damaged areas where the hypoxia/ischemia-induced translational blockade might have prevented the expression of COX-2. Thus, the areas displaying very high neuronal COX-2 levels may represent those areas that were still able after asphyxia to translate new proteins, and the deleterious effects of COX-2 may have contributed most in these areas to the observed neuronal damage.

We assessed the effect of a neuroprotective (2.1%) concentration of H_2 on neuronal COX-2 expression. In addition to our previous studies[30,33,66], this concentration was found to be neuroprotective in a number of other disease models as well[23,93,94].

Our current results concerning the correlation of nuclear 8-OHdG immunoreactivity with COX-2 expression and the remarkable efficacy of molecular H_2 inhalation to attenuate elevations in both 8-OHdG and COX-2 levels after asphyxia suggest a role for ROS in the mechanism of COX-2 expression. 8-OHdG is used as a biomarker of oxidative modifications to DNA[95-97] and is one of the most studied catabolites. Guanine is the best electron donor that has the lowest oxidation potential among the DNA bases[95,98]. 8-Hydroxylation in the guanine base occurs after an attack by hydroxyl radicals under oxidative stress. Thus, elevations in the number of 8-OHdG-positive nuclei indirectly indicate significant oxidative stress imposed by hydroxyl radicals. Importantly, as molecular H_2 was originally described as a selective hydroxyl radical scavenger[23], the efficacy of H_2 to attenuate elevations in 8-OHdG levels after asphyxia further confirms the presence of significant oxidative stress perhaps characterized by significant production of hydroxyl radicals in our present PA/HIE piglet model. The connection between this oxidative stress and the observed induction of COX-2 expression may be the activation of NF-κB, which is a transcription factor known to be induced by ROS and inhibited by antioxidants[99]. The general physiological functions of NF-κB include the regulation of

apoptosis, cell growth, cellular stress responses and intracellular signalling[100]. NF-κB affects various brain functions as well as neuronal development, inflammation and neurodegeneration[101]. Brain injury has been shown to increase NF-κB activity[102]. The COX-2 gene is a neuronal target of NF-κB[87], and therefore the asphyxia-induced increase in neuronal COX-2 expression is very likely mediated via NF-κB. A recent report in neonatal rats demonstrated reduced NF-κB activation in H_2-treated rat pups[103], which lends experimental support to our hypothesis.

Our results with Iba-1 immunohistochemistry that was used to visualize microglia to determine the RI as an indicator of microglial activation are also in favour of the above-mentioned mechanism. We found that microglia were activated by asphyxia only but not by asphyxia followed by H_2. As microglial activation has also been reported to be accompanied by NF-κB activation[104], hydroxyl radicals may have activated the microglia by promoting NF-κB activity in the present study.

The efficacy of molecular H_2 to prevent increases in COX-2 levels after asphyxia suggest that the ROS responsible for triggering COX-2 induction were produced during the early reventilation/reoxygenation phase, as H_2 was administered only in the first four hours of survival. This is interesting, as ROS may arise at later time points as well, for instance from mitochondria during the secondary energy failure[105], from COX activity itself[106], or from the activated microglia[107].

ROS also trigger mitochondrial dysfunction and DNA fragmentation leading to apoptosis[108]. Therefore, another possible neuroprotective therapy would be the prevention of neuronal cell death through the activation of antiapoptotic signalization. This therapeutic approach can be used before the secondary energy failure giving us approximately 3-6 hours after the asphyxia[109]. Both endogenous and exogenous BDNF could exert neuroprotection through stimulation of neuronal survival and inhibition of apoptosis in this period. BDNF might be involved in the endogenous neuroprotective response after PA, as BDNF mRNA levels detected at 48 h survival were significantly increased in all brain areas compared to naïve animals in a newborn piglet HIE model[110]. Furthermore, exogenous BDNF was found neuroprotective in a rat HIE model[84]. Neuroprotection elicited by intracerebroventrical administration of BDNF to postnatal day 7 rat pups was causally linked to pronounced and rapid increases in the phosphorylation/activation of ERK and Akt kinases lasting up to at least

12 h[84]. Furthermore, ERK activation was specifically shown to reduce apoptotic neuronal death assessed with cleaved caspase-3 immunohistochemistry[84]. In addition to BDNF, other growth factors such as basic fibroblast growth factor have been identified as a factor promoting cell survival and neurogenesis, through activation of the ERK pathway[111]. In addition, Cohen-Armon et al. demonstrated that ERK2 phosphorylation can be modulated by poly (ADP-ribose) polymerase-1 (PARP-1) which catalyze a posttranslational modification of nuclear proteins by polyADP-ribosylation[112]. PARP-1 activation could play a role in our model as it has been found to be induced by hypoxia in newborn piglets[113]. The importance of the activation of the PI3K/Akt signalling pathway has been demonstrated in an adult rat stroke model[114], where cerebral infarct was elicited with permanent middle cerebral artery occlusion (pMCAO). Again, BDNF could reduce infarct size via the phosphorylation of Akt[114]. Wortmannin, a selective PI3K inhibitor, could reverse the increment in p-Akt level and the afforded neuroprotection[114]. The transient elevation in p-Akt levels was also noted in adult mice within hours of MCAO[115], and this endogenous activation was regarded as neuroprotective. Our current study yielded markedly different results concerning the phosphorylation levels of both ERK and Akt. Unlike in the previously cited adult or P7 neonatal rodent studies, ERK and Akt phosphorylation was virtually complete also in the cortex of untreated naïve animals, and it was not changed significantly for at least 48 h either in the normoxic time controls or the animals subjected to PA. This high degree of baseline phosphorylation/activation of untreated animals was also observed in virtually all of the assessed brain regions, not only in the neocortex, but also in the hippocampus, the caudate nucleus, the thalamus, cerebellum, and the medulla oblongata suggesting a general phenomenon. Similarly, high phosphorylation levels were maintained also at 48 h after asphyxia. Given the high basic activation of these neuroprotective kinases, H_2-induced neuroprotection is unlikely to accomplish neuroprotection via further Akt or ERK activation. Our pharmacological experiments proved that our results cannot be simply attributed to technical limitations. We could show in the neocortex, where local pharmacological treatment through the closed cranial window was possible that the MEK and Akt1/2 kinase inhibitors could reduce rapidly and statistically significantly the ratio of the phosphorylated forms of ERK and Akt, respectively. The background of this substantial difference is unknown, but one can assume to be associated with the fact that the piglets in the present study were indeed in the perinatal period: they were all born < 24 h before the experiments. Vaginal

delivery even under physiological conditions is associated with mild asphyxia and perhaps this physiological amount of cerebral hypoxia is enough to trigger the observed activation of ERK and Akt. BDNF acts as a participant of neuroendocrine cascade of delivery[116], thus its level is elevated – measured in umbilical cord samples – and may interact through Akt and ERK signalisation. This situation may be in sharp contrast with most of the neonatal rodent HIE models. In these models P7–P8 pups are used because brain maturity is closest to the term human baby at this postnatal age[32]. However, our results suggest that in these models the effects of delivery on cerebral function may have already likely faded, and the activation levels of ERK and Akt may be significantly different from the immediate perinatal period. These results question the efficacy of therapeutic interventions aiming to activate these antiapoptotic signalling pathways to obtain neuroprotection. This suggestion is supported by the findings of Robertson et al., who studied melatonin-induced neuroprotection in a very similar newborn piglet 48 h survival HIE model[74]. Although melatonin was found neuroprotective, however, significant anti-apoptotic effect of melatonin using cleaved caspase-3 immunohistochemistry could not be shown in the cerebral cortex[74]. These results support the findings of Yue et al. describing that the cell death following hypoxia-ischemia is predominantly caused by necrosis[117].

We demonstrated in a translational newborn piglet model of PA/ HIE that the endogenous activations levels of ERK and Akt kinases critical in antiapoptotic signalling are already high in the cerebral cortex and all other assessed brain regions under baseline conditions and would not significantly change up to 48 h following an asphyxia capable to induce significant neuronal injury. We propose that further activation of these signalling pathways is difficult, and this limitation should be taken into consideration when designing rational neuroprotective treatments to mitigate the long-term adverse effects of HIE.

6. Conclusion

Our studies provide novel insight to the molecular mechanisms of HIE development in an established large animal model of PA/HIE. We showed that neuronal COX-2 abundance is dependent on the assessed brain region, the severity of PA, and even on the length of anaesthesia associated with the survival period. Our results suggest that neuronal COX-2 elicits oxidative stress that could be more severe in brain regions having larger baseline expression and can be worsened by further PA-induced increases. However, COX-2 induction can also be mitigated by anaesthesia/analgesia administered as a part of supportive care to infants exposed to PA. We showed in the parietal cortex, a region displaying both high baseline COX-2 expression as well as PA-induce elevations in COX-2 levels that neuronal COX-2 abundance correlates both with microglial activation and oxidative damage of the neurons. These findings all support the involvement of COX-2 derived ROS and neuroinflammatory mediators in the mechanism of neuronal injury. 2.1% H_2-ventilation in the early reventilation period after PA was previously found to be neuroprotective, however, the mechanism of this neuroprotective effect in this model was unknown. Our studies revealed that the applied H_2 prevented the upregulation of neuronal COX-2 that coincided with reduced oxidative damage and microglial activation, suggesting that the presence of H_2 in the early reventilation/ reoxygenation period may break the vicious circle of oxidative damage to cells leading to mitochondrial dysfunction and secondary energy failure culminating in neuronal cell death mainly through necrosis. This effect of H_2 is in accordance with its putative antioxidant effect. Our results with Akt and ERK kinases also emphasize indirectly the importance of necrosis in neuronal cell death. They appear to maintain a highly activated status in the newborn piglet brain and were found not to be further activated by PA; thus, the observed neuronal injury in our model takes place in the presence of highly activated anti-apoptotic pathways suggesting most neuronal cell death is via necrosis.

7. Acknowledgements

I am very thankful to my supervisor, Dr. Ferenc Domoki, who allowed me to join his research group and with his guidance and advices enabled me to complete my work and my thesis.

I would like to recognise the help of my colleagues in the Domoki lab: Dr. János Németh, Dr. Viktória Kovács, Gábor Remzső and Valéria Tóth-Szűki.

I would like to thank to Prof. Dr. Gábor Jancsó for accepting my application to the Theoretical Medicine Doctoral School.

I would like to thank to Prof. Dr. Gyula Sáry for enabling my work in the Department of Physiology.

On behalf of our research group, I would like to acknowledge and thank Prof. Péter Temesvári and Prof. Dr. Ferenc Bari for establishing molecular hydrogen research in the Department of Physiology 10 years ago.

I am very grateful to Prof. Dr. Zoltán Molnár, Anna Schoerder-Suabadissen, Kris Parley and every member of the Molnár Lab at the University of Oxford for their hospitality, kindness and support during my lab visit.

I would like to say thanks to Dr. Csaba Szigeti, Zsuzsa Ambrus and Olga Darányi for introducing me to the world of science and laboratory work.

I would like to appreciate the support and encouragement of Dr. Eszter Farkas and my fellow lab members: Orsolya Kiss, Írisz Szabó, Rita Frank, Dr. Dániel Varga, Dr. Ákos Menyhárt, and Dr. Orsolya M. Tóth.

And last, but not least, words can not describe how grateful I am to my family for their unbreakable love and support. I thank from the bottom of my heart to Olgi, Ágota, Betti, Dia and all of my friends for never letting me down.

8. References

1 Lawn, J. E., Cousens, S., Zupan, J. & Team, L. N. S. S. 4 million neonatal deaths: When? Where? Why? *The Lancet* **365**, 891-900 (2005).

2 Antonucci, R., Porcella, A. & Pilloni, M. D. Perinatal asphyxia in the term newborn. *Journal of Pediatric and Neonatal Individualized Medicine (JPNIM)* **3**, e030269 (2014).

3 Nelson, K. B. & Leviton, A. How much of neonatal encephalopathy is due to birth asphyxia? *Am. J. Dis. Child.* **145**, 1325-1331 (1991).

4 Sarnat, H. B. & Sarnat, M. S. Neonatal encephalopathy following fetal distress: a clinical and electroencephalographic study. *Arch. Neurol.* **33**, 696-705 (1976).

5 van Handel, M., Swaab, H., de Vries, L. S. & Jongmans, M. J. Long-term cognitive and behavioral consequences of neonatal encephalopathy following perinatal asphyxia: a review. *Eur. J. Pediatr.* **166**, 645-654, doi:10.1007/s00431-007-0437-8 (2007).

6 Dixon, G. *et al.* Early developmental outcomes after newborn encephalopathy. *Pediatrics* **109**, 26-33 (2002).

7 Rennie, J. M., Hagmann, C. F. & Robertson, N. J. in *Semin Fetal Neonatal Med.* 398-407 (Elsevier).

8 Jiang, Z. Long-term effect of perinatal and postnatal asphyxia on developing human auditory brainstem responses: peripheral hearing loss. *Int. J. Pediatr. Otorhinolaryngol.* **33**, 225-238 (1995).

9 Mercuri, E. *et al.* Visual function at school age in children with neonatal encephalopathy and low Apgar scores. *Arch Dis Child Fetal Neonatal Ed* **89**, F258-F262 (2004).

10 Gadian, D. G. *et al.* Developmental amnesia associated with early hypoxic–ischaemic injury. *Brain* **123**, 499-507 (2000).

11 Robertson, C. M. & Finer, N. N. Educational readiness of survivors of neonatal encephalopathy associated with birth asphyxia at term. *J. Dev. Behav. Pediatr.* (1988).

12 Odd, D. E., Whitelaw, A., Gunnell, D. & Lewis, G. The association between birth condition and neuropsychological functioning and educational attainment at school age: a cohort study. *Arch. Dis. Child.* **96**, 30-37 (2011).

13 Marlow, N., Rose, A., Rands, C. & Draper, E. Neuropsychological and educational problems at school age associated with neonatal encephalopathy. *Arch Dis Child Fetal Neonatal Ed* **90**, F380-F387 (2005).

14 De Haan, M. *et al.* Brain and cognitive-behavioural development after asphyxia at term birth. *Dev Sci* **9**, 350-358 (2006).

15 Haider, B. A. & Bhutta, Z. A. Birth asphyxia in developing countries: current status and public health implications. *Curr. Probl. Pediatr. Adolesc. Health Care* **36**, 178-188 (2006).

16 Azzopardi, D. *et al.* Effects of hypothermia for perinatal asphyxia on childhood outcomes. *N. Engl. J. Med.* **371**, 140-149 (2014).

17 Cornette, L. Therapeutic hypothermia in neonatal asphyxia. *Facts, views & vision in ObGyn* **4**, 133 (2012).

18 Sharma, D. & Pandita, A. Therapeutic Hypothermia in Asphyxiated Newborn: Its Applicability, Feasibility and Accessibility in Developing Country India: A Long Way to Go. *J Neonatal Biol* **3**, 1-3, doi:{10.4172/2167-0897.1000E111} (2014).

19 Gerrits, L. C., Battin, M. R., Bennet, L., Gonzalez, H. & Gunn, A. J. Epileptiform activity during rewarming from moderate cerebral hypothermia in the near-term fetal sheep. *Pediatr. Res.* **57**, 342 (2005).

20 Wang, B. *et al.* Rewarming from therapeutic hypothermia induces cortical neuron apoptosis in a swine model of neonatal hypoxic–ischemic encephalopathy. *J. Cereb. Blood Flow Metab.* **35**, 781-793 (2015).
21 Zanelli, S., Buck, M. & Fairchild, K. Physiologic and pharmacologic considerations for hypothermia therapy in neonates. *J. Perinatol.* **31**, 377 (2011).
22 Faulkner, S. *et al.* Xenon augmented hypothermia reduces early lactate/N-acetylaspartate and cell death in perinatal asphyxia. *Ann. Neurol.* **70**, 133-150 (2011).
23 Ohsawa, I. *et al.* Hydrogen acts as a therapeutic antioxidant by selectively reducing cytotoxic oxygen radicals. *Nat. Med.* **13**, 688 (2007).
24 Haining, J. L., Turner, M. D. & Pantall, R. M. Measurement of local cerebral blood flow in the unanesthetized rat using a hydrogen clearance method. *Circ. Res.* **23**, 313-324 (1968).
25 Park, T., Gidday, J. M. & Gonzales, E. Local cerebral blood flow response to locally infused 2-chloroadenosine during hypotension in piglets. *Dev Brain Res* **61**, 73-77 (1991).
26 Gidday, J. M. & Park, T. Effect of 2-chloroadenosine on cerebrovascular reactivity to hypercapnia in newborn pig. *J. Cereb. Blood Flow Metab.* **12**, 656-663 (1992).
27 Ruth, V. J., Park, T., Gonzales, E. R. & Gidday, J. M. Adenosine and cerebrovascular hyperemia during insulin-induced hypoglycemia in newborn piglet. *Am J Physiol Heart Circ Physiol* **265**, H1762-H1768 (1993).
28 Ono, H. *et al.* A basic study on molecular hydrogen (H 2) inhalation in acute cerebral ischemia patients for safety check with physiological parameters and measurement of blood H 2 level. *Med. Gas Res.* **2**, 21 (2012).
29 Murakami, Y., Ito, M. & Ohsawa, I. Molecular hydrogen protects against oxidative stress-induced SH-SY5Y neuroblastoma cell death through the process of mitohormesis. *PLoS One* **12**, e0176992 (2017).
30 Domoki, F. *et al.* Hydrogen is neuroprotective and preserves cerebrovascular reactivity in asphyxiated newborn pigs. *Pediatr. Res.* **68**, 387-392 (2010).
31 Tamura, T. *et al.* Feasibility and Safety of Hydrogen Gas Inhalation for Post-Cardiac Arrest Syndrome–First-in-Human Pilot Study–. *Circ. J.* **80**, 1870-1873 (2016).
32 Dobbing, J. & Sands, J. Comparative aspects of the brain growth spurt. *Early Hum. Dev.* **3**, 79-83 (1979).
33 Nemeth, J. *et al.* Molecular hydrogen affords neuroprotection in a translational piglet model of hypoxic-ischemic encephalopathy. *J. Physiol. Pharmacol.* **67**, 677-689 (2016).
34 Randall, G. pH values and blood-gas tensions in the normal piglet during the first 48 hours of life. *Neonatology* **20**, 68-73 (1972).
35 Smith, W. L., Garavito, R. M. & DeWitt, D. L. Prostaglandin endoperoxide H synthases (cyclooxygenases)-1 and− 2. *J. Biol. Chem.* **271**, 33157-33160 (1996).
36 Kaufmann, W. E., Andreasson, K. I., Isakson, P. C. & Worley, P. F. Cyclooxygenases and the central nervous system. *Prostaglandins* **54**, 601-624 (1997).
37 Vane, J., Bakhle, Y. & Botting, R. CYCLOOXYGENASES 1 AND 2. *Annu. Rev. Pharmacol. Toxicol.* **38**, 97-120 (1998).
38 Smith, W. L., DeWitt, D. L. & Garavito, R. M. Cyclooxygenases: structural, cellular, and molecular biology. *Annu. Rev. Biochem.* **69**, 145-182 (2000).
39 Hawkey, C. J. COX-2 inhibitors. *The Lancet* **353**, 307-314, doi:https://doi.org/10.1016/S0140-6736(98)12154-2 (1999).

40 Peri, K. G., Hardy, P., Li, D. Y., Varma, D. R. & Chemtob, S. Prostaglandin G/H synthase-2 is a major contributor of brain prostaglandins in the newborn. *J. Biol. Chem.* **270**, 24615-24620 (1995).
41 Weerasinghe, G. R., Coon, S. L., Bhattacharjee, A. K., Harry, G. J. & Bosetti, F. Regional protein levels of cytosolic phospholipase A2 and cyclooxygenase-2 in Rhesus monkey brain as a function of age. *Brain Res. Bull.* **69**, 614-621 (2006).
42 Yamagata, K., Andreasson, K. I., Kaufmann, W. E., Barnes, C. A. & Worley, P. F. Expression of a mitogen-inducible cyclooxygenase in brain neurons: regulation by synaptic activity and glucocorticoids. *Neuron* **11**, 371-386 (1993).
43 Chen, C., Magee, J. C. & Bazan, N. G. Cyclooxygenase-2 regulates prostaglandin E2 signaling in hippocampal long-term synaptic plasticity. *J. Neurophysiol.* **87**, 2851-2857 (2002).
44 Andreasson, K. I. *et al.* Age-dependent cognitive deficits and neuronal apoptosis in cyclooxygenase-2 transgenic mice. *J. Neurosci.* **21**, 8198-8209 (2001).
45 Yang, H., Zhang, J., Andreasson, K. & Chen, C. COX-2 oxidative metabolism of endocannabinoids augments hippocampal synaptic plasticity. *Mol. Cell. Neurosci.* **37**, 682-695 (2008).
46 Ballou, L. R., Botting, R. M., Goorha, S., Zhang, J. & Vane, J. R. Nociception in cyclooxygenase isozyme-deficient mice. *Proc Natl Acad Sci USA* **97**, 10272-10276 (2000).
47 Bosetti, F., Langenbach, R. & Weerasinghe, G. R. Prostaglandin E2 and microsomal prostaglandin E synthase-2 expression are decreased in the cyclooxygenase-2-deficient mouse brain despite compensatory induction of cyclooxygenase-1 and Ca2+-dependent phospholipase A2. *J. Neurochem.* **91**, 1389-1397 (2004).
48 Kaufmann, W. E., Worley, P. F., Pegg, J., Bremer, M. & Isakson, P. COX-2, a synaptically induced enzyme, is expressed by excitatory neurons at postsynaptic sites in rat cerebral cortex. *Proc Natl Acad Sci USA* **93**, 2317-2321 (1996).
49 Lecrux, C. *et al.* Pyramidal neurons are "neurogenic hubs" in the neurovascular coupling response to whisker stimulation. *J. Neurosci.* **31**, 9836-9847 (2011).
50 Ellis, E. F., Wei, E. P. & Kontos, H. A. Vasodilation of cat cerebral arterioles by prostaglandins D2, E2, G2, and I2. *Am J Physiol Heart Circ Physiol* **237**, H381-H385 (1979).
51 Strauss, K. I. *et al.* Prolonged cyclooxygenase-2 induction in neurons and glia following traumatic brain injury in the rat. *J. Neurotrauma* **17**, 695-711 (2000).
52 DASH, P. K., MACH, S. A. & MOORE, A. N. Regional expression and role of cyclooxygenase-2 following experimental traumatic brain injury. *J. Neurotrauma* **17**, 69-81 (2000).
53 Domoki, F. *et al.* Ischemia-reperfusion rapidly increases COX-2 expression in piglet cerebral arteries. *Am J Physiol Heart Circ Physiol* **277**, H1207-H1214 (1999).
54 Dégì, R. *et al.* Effects of anoxic stress on prostaglandin H synthase isoforms in piglet brain. *Dev Brain Res* **107**, 265-276 (1998).
55 Seibert, K. *et al.* Pharmacological and biochemical demonstration of the role of cyclooxygenase 2 in inflammation and pain. *Proc Natl Acad Sci USA* **91**, 12013-12017 (1994).
56 Choi, S.-H., Aid, S. & Bosetti, F. The distinct roles of cyclooxygenase-1 and-2 in neuroinflammation: implications for translational research. *Trends Pharmacol. Sci.* **30**, 174-181 (2009).

57 Candelario-Jalil, E. *et al.* Assessment of the relative contribution of COX-1 and COX-2 isoforms to ischemia-induced oxidative damage and neurodegeneration following transient global cerebral ischemia. *J. Neurochem.* **86**, 545-555 (2003).
58 Domoki, F., Perciaccante, J. V., Puskar, M., Bari, F. & Busija, D. W. Cyclooxygenase-2 inhibitor NS398 preserves neuronal function after hypoxia/ischemia in piglets. *Neuroreport* **12**, 4065-4068 (2001).
59 Marnett, L. J., Rowlinson, S. W., Goodwin, D. C., Kalgutkar, A. S. & Lanzo, C. A. Arachidonic acid oxygenation by COX-1 and COX-2 Mechanisms of catalysis and inhibition. *J. Biol. Chem.* **274**, 22903-22906 (1999).
60 Imaizumi, S., Woolworth, V., Fishman, R. A. & Chan, P. H. Liposome-entrapped superoxide dismutase reduces cerebral infarction in cerebral ischemia in rats. *Stroke* **21**, 1312-1317 (1990).
61 Weisbrot-Lefkowitz, M. *et al.* Overexpression of human glutathione peroxidase protects transgenic mice against focal cerebral ischemia/reperfusion damage. *Mol Brain Res* **53**, 333-338 (1998).
62 Perrone, S., Negro, S., Tataranno, M. L. & Buonocore, G. Oxidative stress and antioxidant strategies in newborns. *J. Matern. Fetal Neonatal Med.* **23 Suppl 3**, 63-65, doi:10.3109/14767058.2010.509940 (2010).
63 Fathali, N. *et al.* Cyclooxygenase-2 inhibition provides lasting protection against neonatal hypoxic-ischemic brain injury. *Crit. Care Med.* **38**, 572 (2010).
64 Toti, P. *et al.* Cyclooxygenase-2 immunoreactivity in the ischemic neonatal human brain. An autopsy study. *J. Submicrosc. Cytol. Pathol.* **33**, 245-249 (2001).
65 Busija, D. W., Thore, C., Beasley, T. & Bari, F. Induction of cyclooxygenase-2 following anoxic stress in piglet cerebral arteries. *Microcirculation* **3**, 379-386 (1996).
66 Oláh, O., Németh, I., Tóth-Szuki, V., Bari, F. & Domoki, F. Regional differences in the neuronal expression of cyclooxygenase-2 (COX-2) in the newborn pig brain. *Acta Histochem Cytoc* **45**, 187-192 (2012).
67 Katsumoto, A., Lu, H., Miranda, A. S. & Ransohoff, R. M. Ontogeny and functions of central nervous system macrophages. *J Immunol* **193**, 2615-2621 (2014).
68 Gomez-Nicola, D. & Perry, V. H. Microglial dynamics and role in the healthy and diseased brain: a paradigm of functional plasticity. *Neuroscientist* **21**, 169-184, doi:10.1177/1073858414530512 (2015).
69 Nimmerjahn, A., Kirchhoff, F. & Helmchen, F. Resting microglial cells are highly dynamic surveillants of brain parenchyma in vivo. *Science* **308**, 1314-1318, doi:10.1126/science.1110647 (2005).
70 Walker, F. R. *et al.* Dynamic structural remodelling of microglia in health and disease: A review of the models, the signals and the mechanisms. *Brain. Behav. Immun.* **37**, 1-14, doi:https://doi.org/10.1016/j.bbi.2013.12.010 (2014).
71 Tang, Y. & Le, W. Differential roles of M1 and M2 microglia in neurodegenerative diseases. *Mol. Neurobiol.* **53**, 1181-1194 (2016).
72 Raghupathi, R. & Huh, J. W. Age-at-injury effects of microglial activation following traumatic brain injury: implications for treatment strategies. *Neural Regen Res* **12**, 741 (2017).
73 Loane, D. J. & Byrnes, K. R. Role of microglia in neurotrauma. *Neurotherapeutics* **7**, 366-377 (2010).

74 Robertson, N. J. *et al.* Melatonin augments hypothermic neuroprotection in a perinatal asphyxia model. *Brain* **136**, 90-105 (2012).
75 Wu, D. Neuroprotection in experimental stroke with targeted neurotrophins. *NeuroRx* **2**, 120-128 (2005).
76 Nagahara, A. H. & Tuszynski, M. H. Potential therapeutic uses of BDNF in neurological and psychiatric disorders. *Nat Rev Drug Discov* **10**, 209 (2011).
77 Schwartz, P. M., Borghesani, P. R., Levy, R. L., Pomeroy, S. L. & Segal, R. A. Abnormal cerebellar development and foliation in BDNF−/− mice reveals a role for neurotrophins in CNS patterning. *Neuron* **19**, 269-281 (1997).
78 Chen, A., Xiong, L.-J., Tong, Y. & Mao, M. The neuroprotective roles of BDNF in hypoxic ischemic brain injury. *Biomed Rep* **1**, 167-176 (2013).
79 Almli, C. R. *et al.* BDNF protects against spatial memory deficits following neonatal hypoxia-ischemia. *Exp. Neurol.* **166**, 99-114 (2000).
80 Sun, X. *et al.* Neuroprotection of brain-derived neurotrophic factor against hypoxic injury in vitro requires activation of extracellular signal-regulated kinase and phosphatidylinositol 3-kinase. *Int. J. Dev. Neurosci.* **26**, 363-370 (2008).
81 Brazil, D. P., Park, J. & Hemmings, B. A. PKB binding proteins: getting in on the Akt. *Cell* **111**, 293-303 (2002).
82 Duman, R. S. & Voleti, B. Signaling pathways underlying the pathophysiology and treatment of depression: novel mechanisms for rapid-acting agents. *Trends Neurosci.* **35**, 47-56 (2012).
83 Hetman, M. & Gozdz, A. Role of extracellular signal regulated kinases 1 and 2 in neuronal survival. *Eur. J. Biochem.* **271**, 2050-2055 (2004).
84 Han, B. H. & Holtzman, D. M. BDNF protects the neonatal brain from hypoxic-ischemic injuryin vivo via the ERK pathway. *J. Neurosci.* **20**, 5775-5781 (2000).
85 Mitchell, E. Neuroprotection by physical activity. *Vanderbilt Rev* **1**, 76-81 (2010).
86 Niwa, K., Araki, E., Morham, S. G., Ross, M. E. & Iadecola, C. Cyclooxygenase-2 contributes to functional hyperemia in whisker-barrel cortex. *J. Neurosci.* **20**, 763-770 (2000).
87 Kaltschmidt, B., Linker, R. A., Deng, J. & Kaltschmidt, C. Cyclooxygenase-2 is a neuronal target gene of NF-κB. *BMC Mol. Biol.* **3**, 16 (2002).
88 Hou, Y.-N. *et al.* A μ-receptor opioid agonist induces AP-1 and NF-κB transcription factor activity in primary cultures of rat cortical neurons. *Neurosci. Lett.* **212**, 159-162 (1996).
89 Cadet, P. *et al.* Endogenous morphinergic signaling and tumor growth. *Front. Biosci.* **9**, 3176-3186 (2004).
90 Gupta, S. C., Sundaram, C., Reuter, S. & Aggarwal, B. B. Inhibiting NF-κB activation by small molecules as a therapeutic strategy. *Biochim Biophys Acta Gene Regul Mech* **1799**, 775-787 (2010).
91 Roka, A. *et al.* Serum S100B and neuron-specific enolase levels in normothermic and hypothermic infants after perinatal asphyxia. *Acta Paediatr.* **101**, 319-323 (2012).
92 Tooley, J., Eagle, R., Satas, S. & Thoresen, M. Significant head cooling can be achieved while maintaining normothermia in the newborn piglet. *Arch Dis Child Fetal Neonatal Ed* **90**, F262-FF266 (2005).
93 Xin, Y., Liu, H., Zhang, P., Chang, L. & Xie, K. Molecular hydrogen inhalation attenuates postoperative cognitive impairment in rats. *Neuroreport* **28**, 694-700 (2017).

94 Hayashida, K. *et al.* H2 gas improves functional outcome after cardiac arrest to an extent comparable to therapeutic hypothermia in a rat model. *J Am Heart Assoc* **1**, e003459 (2012).
95 Anjana Vaman, V., Tinu, S., Geetha, C., Lissy, K. & Mohanan, P. Effect of fibrin glue on antioxidant defense mechanism, oxidative DNA damage and chromosomal aberrations. *Toxicol. Mech. Methods* **23**, 500-508 (2013).
96 Villaño, D. *et al.* Effect of elite physical exercise by triathletes on seven catabolites of DNA oxidation. *Free Radic. Res.* **49**, 973-983 (2015).
97 Hintsala, H.-R. *et al.* NRF2/Keap1 pathway and expression of oxidative stress lesions 8-hydroxy-2'-deoxyguanosine and nitrotyrosine in melanoma. *Anticancer Res.* **36**, 1497-1506 (2016).
98 Nunomura, A. *et al.* Oxidative damage to RNA in aging and neurodegenerative disorders. *Neurotox. Res.* **22**, 231-248 (2012).
99 Calatroni, P. T.-D. S.-A. The antioxidant effect exerted by TGF-1 f-stimulated hyaluronan production reduced NF-kB activation and apoptosis in human fibroblasts exposed to FeSo plus ascorbate. *Mol. Cell. Biochem.* **311**, 167-177 (2008).
100 Hoffmann, A., Levchenko, A., Scott, M. L. & Baltimore, D. The IκB-NF-κB signaling module: temporal control and selective gene activation. *Science* **298**, 1241-1245 (2002).
101 O'Neill, L. A. & Kaltschmidt, C. NF-kB: a crucial transcription factor for glial and neuronal cell function. *Trends Neurosci.* **20**, 252-258 (1997).
102 Salminen, A., Liu, P. K. & Hsu, C. Y. Alteration of transcription factor binding activities in the ischemic rat-brain. *Biochem. Biophys. Res. Commun.* **212**, 939-944 (1995).
103 Shi, Y., Wang, G., Li, J. & Yu, W. Hydrogen gas attenuates sevoflurane neurotoxicity through inhibiting nuclear factor κ-light-chain-enhancer of activated B cells signaling and proinflammatory cytokine release in neonatal rats. *Neuroreport* **28**, 1170-1175 (2017).
104 Kaltschmidt, C. *et al.* Transcription factor NF-κB is activated in microglia during experimental autoimmune encephalomyelitis. *J. Neuroimmunol.* **55**, 99-106 (1994).
105 Indo, H. P. *et al.* Evidence of ROS generation by mitochondria in cells with impaired electron transport chain and mitochondrial DNA damage. *Mitochondrion* **7**, 106-118 (2007).
106 Phaniendra, A., Jestadi, D. B. & Periyasamy, L. Free radicals: properties, sources, targets, and their implication in various diseases. *Indian J. Clin. Biochem.* **30**, 11-26 (2015).
107 Block, M. L., Zecca, L. & Hong, J.-S. Microglia-mediated neurotoxicity: uncovering the molecular mechanisms. *Nat Rev Neurosci* **8**, 57 (2007).
108 Redza-Dutordoir, M. & Averill-Bates, D. A. Activation of apoptosis signalling pathways by reactive oxygen species. *Biochim Biophys Acta Mol Cell Res* **1863**, 2977-2992, doi:https://doi.org/10.1016/j.bbamcr.2016.09.012 (2016).
109 Lorek, A. *et al.* Delayed ("Secondary") Cerebral Energy Failure after Acute Hypoxia-Ischemia in the Newborn Piglet: Continuous 48-Hour Studies by Phosphorus Magnetic Resonance Spectroscopy. *Pediatr. Res.* **36**, 699, doi:10.1203/00006450-199412000-00003 (1994).
110 Olson, L. *et al.* Comparison of three hypothermic target temperatures for the treatment of hypoxic ischemia: mRNA level responses of eight genes in the piglet brain. *Transl Stroke Res* **4**, 248-257 (2013).
111 Takami, K. *et al.* Increase of basic fibroblast growth factor immunoreactivity and its mRNA level in rat brain following transient forebrain ischemia. *Exp. Brain Res.* **90**, 1-10 (1992).

112 Cohen-Armon, M. *et al.* DNA-independent PARP-1 activation by phosphorylated ERK2 increases Elk1 activity: a link to histone acetylation. *Mol. Cell* **25**, 297-308 (2007).
113 Mishra, O., Akhter, W., Ashraf, Q. & Delivoria-Papadopoulos, M. Hypoxia-induced modification of poly (ADP-Ribose) Polymerase and DNA polymerase β activity in cerebral cortical nuclei of newborn piglets: role of nitric oxide. *Neuroscience* **119**, 1023-1032 (2003).
114 Huang, H., Zhong, R., Xia, Z., Song, J. & Feng, L. Neuroprotective effects of rhynchophylline against ischemic brain injury via regulation of the Akt/mTOR and TLRs signaling pathways. *Molecules* **19**, 11196-11210 (2014).
115 Shibata, M. *et al.* Upregulation of Akt phosphorylation at the early stage of middle cerebral artery occlusion in mice. *Brain Res.* **942**, 1-10 (2002).
116 Flöck, A. *et al.* Determinants of brain-derived neurotrophic factor (BDNF) in umbilical cord and maternal serum. *Psychoneuroendocrinology* **63**, 191-197, doi:https://doi.org/10.1016/j.psyneuen.2015.09.028 (2016).
117 Yue, X. *et al.* Apoptosis and necrosis in the newborn piglet brain following transient cerebral hypoxia–ischaemia. *Neuropathol. Appl. Neurobiol.* **23**, 16-25 (1997).

APPENDIX

Publications related to the PhD thesis

I.

Acta Pharmacologica Sinica 2018: 1–11

www.nature.com/aps

Original Article

Molecular hydrogen alleviates asphyxia-induced neuronal cyclooxygenase-2 expression in newborn pigs

Viktória VARGA[1, *], János NÉMETH[1], Orsolya OLÁH[2], Valéria TÓTH-SZŰKI[1], Viktória KOVÁCS[1], Gábor REMZSŐ[1], Ferenc DOMOKI[1]

[1]*Department of Physiology, University of Szeged, School of Medicine, Szeged, Hungary*; [2]*Department of Pathology, University of Szeged, School of Medicine, Szeged, Hungary*

Abstract

Cyclooxygenase-2 (COX-2) has an established role in the pathogenesis of hypoxic-ischemic encephalopathy (HIE). In this study we sought to determine whether COX-2 was induced by asphyxia in newborn pigs, and whether neuronal COX-2 levels were affected by H_2 treatment. Piglets were subjected to either 8 min of asphyxia or a more severe 20 min of asphyxia followed by H_2 treatment (inhaling room air containing 2.1% H_2 for 4 h). COX-2 immunohistochemistry was performed on brain samples from surviving piglets 24 h after asphyxia. The percentages of COX-2-immunopositive neurons were determined in cortical and subcortical areas. Only in piglets with more severe HIE, we observed significant, region-specific increases in neuronal COX-2 expression within the parietal and occipital cortices and in the CA3 hippocampal subfield. H_2 treatment essentially prevented the increases in COX-2-immunopositive neurons. In the parietal cortex, the attenuation of COX-2 induction was associated with reduced 8'-hydroxy-2'-deoxyguanozine immunoreactivity and retained microglial ramifcation index, which are markers of oxidative stress and neuroinflammation, respectively. This study demonstrates for the first time that asphyxia elevates neuronal COX-2 expression in a piglet HIE model. Neuronal COX-2 induction may play region-specific roles in brain lesion progression during HIE development, and inhibition of this response may contribute to the antioxidant/anti-inflammatory neuroprotective effects of H_2 treatment.

Keywords: hypoxic-ischemic encephalopathy; COX-2; 8'-hydroxy-2'-deoxyguanozine; microglia; molecular hydrogen; neuroprotection; newborn pigs

Acta Pharmacologica Sinica advance online publication, 22 Mar 2018; doi: 10.1038/aps.2017.148

Introduction

In neonates, brain damage is most often associated with perinatal asphyxia (PA), which occurs in approximately 1–6 per 1000 live full-term births[1, 2]. PA may result in neonatal mortality, or depending on its severity, hypoxic-ischemic encephalopathy (HIE) may develop, which results in long-lasting neurodevelopmental motor and cognitive dysfunctions in approximately 25% of survivors[3].

Cyclooxygenases (COXs) are the rate-limiting enzymes that catalyze the conversion of arachidonic acid released from membrane phospholipids by phospholipase-A_2 to prostaglandin (PG)-H_2, which is further converted to biologically active prostaglandins, including PGD_2, PGE_2, $PGF_{2\alpha}$, PGI_2 and thromboxane A_2[4]. The two COX isozymes, COX-1 and COX-2, have similar catalytic activities but differ in their pharmacological properties and tissue distributions[5]. Although COX-1 and COX-2 are both constitutively expressed in the central nervous system[6], COX-2 is enriched in the hippocampus and the cerebral cortex[7]. Furthermore, COX-2 is the dominant isoform in the newborn brain[8], providing up to 80% of the total brain COX activity[9]. In the central nervous system, prostanoids modulate synaptic transmission and neurovascular coupling[10, 11]. Neuronal COX-2 plays an essential role in the modulation of excitatory glutamatergic synaptic transmission and long-term synaptic plasticity[10]. Simultaneously, COX-2-derived prostanoids also participate in flow-metabolism coupling, for instance in the local blood flow response to whisker stimulation in the barrel cortex[12]. Expression of the inducible COX-2 isoform is well-known to be upregulated by various deleterious stimuli including brain trauma[13, 14], cerebral ischemia[15, 16], and proinflammatory insults[17]. The neu-

*To whom correspondence should be addressed.
E-mail varga.viktoria.eva@med.u-szeged.hu
Received 2017-08-03 Accepted 2017-11-08

ronal induction of COX-2 suggests the enzyme's participation in neuroinflammation, the pathogenesis of neurodegenerative diseases, traumatic brain injury, and ischemia-induced neuronal damage and epileptogenesis[18].

COX-2 has an established role in the pathogenesis of HIE. For instance, a previous study showed that administration of COX-2 inhibitors before as well as soon after ischemic insult provided neuronal protection in a rat HIE model[19]. Furthermore, brain ischemia has been associated with high neuronal COX-2 levels also in the neonatal human brain in an autopsy study[20]. Therefore, the role of COX-2 in the mechanism of hypoxic-ischemic neuronal injury could perhaps be best studied in a translational large animal model that could also be used to establish possible neuroprotective treatments.

The newborn pig is an accepted large animal model for the human neonate, as brain size, gyrencephalic structure, neurodevelopmental state of the brain and cerebral metabolism at birth are similar in both species[21]. COX-2 has been quite extensively studied in the piglet model and has been identified as the major constitutive isoform in this species[8]. According to immunohistochemistry analysis, COX-2 expression in the brain and cerebral arteries of newborn piglets is markedly induced by global cerebral ischemia[15, 16] but, confoundingly, not by asphyxia[16, 22]. In these studies, global cerebral ischemia was induced by raising the intracranial pressure above the arterial pressure for 10 min while venous blood was withdrawn to control the blood pressure and asphyxia was induced by suspending ventilation for 10 min. The translational significance of the findings concerning the possible role of neuronal COX-2 induction in neuronal damage during HIE development has thus become difficult to determine, as the clinical presentation of HIE is associated with asphyxia and not global no-flow ischemia. Furthermore, animals in these studies survived only 4–8 h, so it was also possible that the expression changes after asphyxia would have occurred at a later and thus undetected time point.

In recent years, we established and published two piglet PA/HIE models of increasing severity[22, 23] to assess the neuroprotective effect of inhaled molecular hydrogen (H_2)[23, 24] that was first reported by *Ohsawa et al* in an adult rat stroke model[25]. H_2 was described as a neuroprotective agent that penetrates the blood–brain barrier and selectively reduces cytotoxic hydroxyl radicals[25]. H_2 was also found to be effective in rodent HIE models[26, 27] and in various other neuropathological conditions, such as Parkinson's disease[28], auditory neuropathy[29] and even stress-induced learning impairment[30]. The mechanistic details of H_2-induced neuroprotection are still unclear but likely involve inhibition of oxidative injury and inhibition of neuroinflammation[31]. However, we have virtually no information on the mechanism of H_2-induced neuroprotection in PA/HIE, let alone in a large animal model.

Therefore, the major purpose of the present study was to determine the effect of H_2 on asphyxia-induced neuronal COX-2 expression correlated with 8′-hydroxy-2′-deoxyguanozine[23] (8-OHdG) and Iba-1 immunohistochemistry markers of oxidative stress and neuroinflammation, respectively, in our translational PA/HIE piglet model.

Materials and methods

To study neuronal COX-2 expression, we used brain samples of newborn male Large-White piglets (age < 24 h at beginning of experiments, body weight: 1.5–2.5 kg, n=59), which were obtained mainly from previously published studies[23, 32]. In both studies, the anesthetized, artificially ventilated animals were divided into 3-3 experimental groups (n=7-7) including a normoxic time control group ventilated with room air, an asphyxiated group reventilated with room air for 24 h, and an asphyxiated group reventilated with room air containing 2.1% H_2 for 4 h followed by room air for the remaining (20 h) survival time. The major difference between the two previously published studies[23, 32] was the induction method and the duration of asphyxia. Asphyxia was elicited by 8 min of trachea occlusion and suspended ventilation in the first study and by 20 min of ventilation with a hypoxic-hypercapnic gas mixture (6% O_2, 20% CO_2) in the second study. Our preliminary results suggested that the length of anesthesia *per se* in the absence of asphyxia might have affected COX-2 expression, therefore we included an additional naïve control group to study baseline neuronal COX-2 expression. Furthermore, we also used brain samples from normoxic time control animals with 4 h survival from another previous study[24]. In the new naïve control group, piglets (n =5) were anesthetized with sodium thiopental (45 mg/kg, ip; Sandoz, Kundl, Austria), and the brains were immediately perfused with 100 mL cold physiological saline solution through the catheterized common carotid arteries and harvested for immunohistochemical analysis. All procedures were approved by the Animal Care and Use Committee of the University of Szeged. The brain tissues were immersion-fixed with 4% paraformaldehyde at 4 °C for 2 weeks. Paraffin-embedded, 4-μm sections were produced using a microtome (Leica Microsystems, Wetzlar, Germany) and mounted on sylanized slides. Hematoxylin-eosin staining was performed to assess the extent of neuronal lesions, which was determined by cell counting in most areas. In the cerebral cortex, however, neuropathology scores were determined (0–9) as described previously[23]. Briefly, in each region, 20 fields of view were assessed by two independent observers. In each field of view, the neuronal lesions were described as none, scattered, grouped/laminar or panlaminar. The neuropathology score was determined by the incidence of the most severe lesion observed. If the most severe lesions represented less than 20% of the total lesions, the scores were 1, 4, or 7; if 20%–50%, 2, 6, or 8; and if more than 50%, 3, 6, or 9. Thus, higher scores represented increasingly severe neuronal damage.

COX-2 immunohistochemistry was performed using the LEICA BOND-MAX automated immunostainer (Leica Microsystems, Wetzlar, Germany). The slides were dewaxed at 72 °C, and antigen retrieval was performed at pH 6. The slides were then incubated with a rabbit monoclonal antibody against COX-2 diluted at 1:100 (clone SP21, Labvision, Fre-

mont, California, USA) for 30 min followed by horseradish peroxidase-conjugated anti-rabbit antibody (EnVision®; Dako, Glostrup, Denmark). 3,3'-Diaminobenzidine (DAB) tetrahydrochloride solution was used for visualization, and the slides were then counterstained with hematoxylin to visualize the cell nuclei. The slides were dehydrated in an ascending alcohol series, cleared in xylene, covered with a coverslip, scanned in a slide scanner (Pannoramic MIDI, 3DHISTECH Ltd, Budapest, Hungary) and visualized on a personal computer using the Pannoramic Viewer software (3DHISTECH Ltd) at 20x magnification. Areas of interest were randomly selected, and photomicrographs were acquired from each region observed, including 10-10 images of the frontal, temporal, parietal and occipital cortex; 3-3 images of the CA1, CA3 subfields and the dentate gyrus of the hippocampus; 10-10 images of the thalamus and the basal ganglia; and 15 images of the cerebellar cortex for the study of Purkinje-cells. The cells were manually counted by two independent observers using ImageJ software (Wayne Rasband, NIH, Bethesda, Maryland, USA). Neurons were identified by their shape and size. The ratio of COX-2-immunopositive neurons relative to all neurons was determined, and the averages/cerebral areas/animals were counted and plotted on box plots using R 3.3.1 software (The R Foundation for Statistical Computing, Vienna, Austria). For statistical analysis, ANOVA on ranks followed by the Student-Newman-Keuls *post hoc* test was performed using SigmaPlot 12.0 (Systat Software Inc., Chicago, Illinois, USA). $P<0.05$ was considered statistically significant. The ratio of COX-2-immunopositive neurons was correlated with the previously determined histopathological score[23], and the result was plotted on a dot plot using R 3.3.1 software.

Based on the results of our COX-2 studies, the parietal cortex was selected for further studies. Tissue microarrays from the parietal cortex were produced from the paraffin-embedded tissue blocks of the second study (including the time control, 20 min asphyxia, and 20 min asphyxia+H_2 groups) using a custom-made stainless steel tissue puncher (3 mm). The microarrays were also sectioned at 4 μm, mounted on sylanized slides and processed for immunohistochemistry. To determine the extent of oxidative damage in the neurons, 8-OHdG immunohistochemistry was performed[23]. The slides were incubated with a mouse monoclonal primary antibody against 8-OHdG diluted at 1:200 (JaICA Inc, Fukuroi, Japan) for 20 min, followed by incubation with a horseradish peroxidase-conjugated rabbit anti-mouse secondary antibody for 15 min (n=6-6-6). Iba-1 immunohistochemistry was performed to assess microglial activation (n=7-6-6). Slides were incubated with rabbit anti-Iba-1 antibody (Wako Chemicals GmbH, Neuss, Germany) for 30 min, followed by horseradish peroxidase-conjugated anti-rabbit antibody (EnVision®; Dako, Glostrup, Denmark) for 15 min. In both cases, 3,3'-diaminobenzidine was used to visualize the immunostaining, and the slides were then counterstained with hematoxylin to visualize the cell nuclei. The slides were covered with coverslips, scanned in the slide scanner, and visualized on a personal computer using the Pannoramic Viewer software at x40 magnification. Homogeneous, strong nuclear 8-OHdG immunoreactivity indicated oxidative damage. The ratio of these nuclei to the total neuronal nuclei was determined using ImageJ software, similarly to the previously described method. The average/sample was plotted on box plots. The groups were compared with one-way ANOVA on ranks followed by the Student-Newman-Keuls *post hoc* test ($P<0.05$). Microglial activation was characterized by determining the so-called ramification index (RI)[33]. We applied a 0.20 mm×0.25 mm grid to the microphotographs of 3 randomly selected areas/sample at x40 magnification. The immunopositive cell bodies (CBD) in the grid were counted as well as the microglial branches (B) crossing the gridlines. From these data, the RI was defined according to the following equation: $RI=B^2/CBD$. The RI values for each field of view were plotted on box plots, and the groups were compared with one-way ANOVA on ranks followed by Dunn's *post hoc* test ($P=0.015$). Correlations were plotted and tested using R 3.3.1 software (Pearson's correlation, $P<0.05$).

Results

Neuronal COX-2 expression in the time controls

Neuronal COX-2 expression in the naïve animals was similar to our previous observations and showed marked regional differences: the highest percentages of COX-2-positive neurons were observed in the frontal and parietal cortices as described previously[22]. However, this regional expression pattern appeared markedly changed in the 24-h time controls, as COX-2 expression was significantly reduced in all neocortical regions compared with the naïve or 4-h survival animals (Figure 1). This reduction was found to be limited to the cortex, as the ratio of COX-2-immunopositive neurons remained unchanged in the hippocampus (Figure 1).

Effect of asphyxia on neuronal COX-2 expression

In the brain regions obtained from the study of animals exposed to 8-min asphyxia, there was no significant alteration in neuronal COX-2 expression (Figure 2), as no difference was noted between the time control and asphyxiated groups in any of the observed regions (Figure 2). In contrast, 20-min asphyxia elicited significant increases in neuronal COX-2 immunopositivity in the parietal and occipital cortices, as well as in the hippocampal CA3 region (Figure 2). Furthermore, the asphyxia-induced elevation of COX-2-immunopositive neurons was also observed in the frontal and temporal cortices and the basal ganglia, although these changes did not reach statistical significance in these regions (Figure 2). In the H_2-treated group, despite exposure to the same level of asphyxia, the ratio of COX-2-immunopositive cells was similar to that in the time control group (Figure 2). Notably, strong COX-2-immunopositive areas were only recorded in the asphyxia group (Figure 3). In contrast to the CA3 subfield, the hippocampal CA1 region and the dentate gyrus displayed low percentages of COX-2-immunopositive neurons in the time controls. In addition, the ratio of immunopositive neurons was unchanged by asphyxia, as these percentages were similar

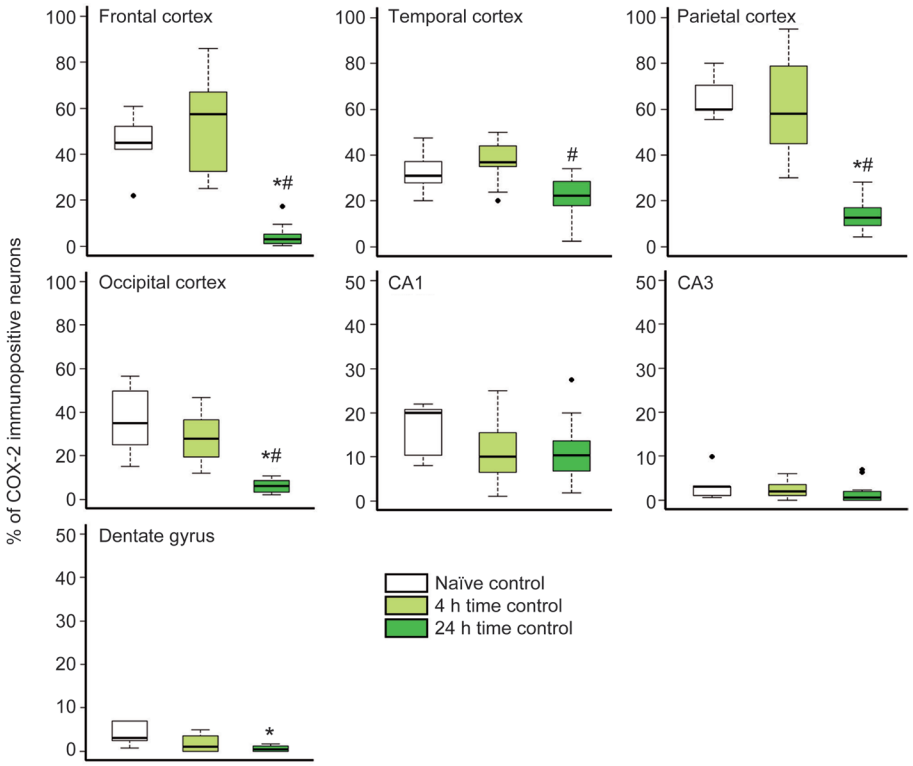

Figure 1. The ratio of neocortical COX-2-immunopositive neurons decreased over time under normoxic conditions in anesthetized time control animals. In the different cortical lobes, the percentages of COX-2-immunopositive cells determined in samples from naïve animals (brains harvested immediately after anesthesia, *n*=5) and from normoxic time controls with 4 h of survival after anesthesia (*n*=12) displayed similar COX-2 expression in accordance with previous data showing regional differences[22]. However, the percentage of COX-2-immunopositive neurons in the 24 h survival time control group (*n*=14) was significantly reduced compared with those of both the naïve and the 4 h time control groups in all neocortical regions. Interestingly, this reduction did not affect the CA1 and CA3 hippocampal subfields. ($^{*}P$<0.05 *vs* naïve animals, $^{\#}P$<0.05 *vs* 4 h time control; ANOVA on ranks, Dunn's *post hoc* test. Bold line, box, and whiskers represent the median, 25th–75th, and 10th–90th percentiles, respectively; black dots are outliers).

among all three groups. In a similar fashion, COX-2 was present in approximately 30% of the cerebellar Purkinje cells in all experimental groups (Figure 2).

Assessment of correlation between neuronal COX-2 expression and neuronal damage

As neuronal COX-2 expression was affected by 20-min asphyxia exposure only, we performed all subsequent studies on these animals. We first investigated whether the ratio of COX-2-immunopositive neurons correlated with the previously determined neuropathology scores[23] with higher scores reflecting more severe neuronal damage in the cortex (Figure 4). We found no correlation between the neuropathology scores and neuronal COX-2 expression (r=0.38; P<0.01); however, we clearly identified 3 expression patterns. Low neuropathology scores were always associated with low-moderate levels of neuronal COX-2 expression, and high neuropathology scores were associated either with high or with low COX-2 expression levels. Notably, low neuropathology score never coincided with high COX-2 expression levels (Figure 4).

Assessment of the correlation between neuronal COX-2 expression and oxidative DNA damage

In the parietal cortex, 20-min asphyxia significantly increased the ratio of 8-OHdG-immunopositive neuronal nuclei (Figure 5A) compared with both the time control and the H_2-treated asphyxia group, indicating the oxidative stress induced by asphyxia and the mitigating effect of molecular H_2 (Figure 5B). By assessing the correlation between the ratios of COX-2- and 8-OHdG-immunopositive neurons (Figure 5C), we found a marked tendency towards a positive correlation (r=0.71), considering data either from all groups or from the 20-min asphyxia group alone.

Assessment of the correlation between neuronal COX-2 expression and microglial activation

The Iba-1 immunohistochemistry results revealed the distribution of microglia in the parietal cortex (Figure 6A). Microglial activation is associated with reduced branching and the adoption of an amoeboid shape, and these changes were quantified by RI determination. We found that the RI was significantly lower in the group subjected to 20-min asphyxia than in the time control group (Figure 6B). However, there was no significant difference between the time controls and the H_2-treated

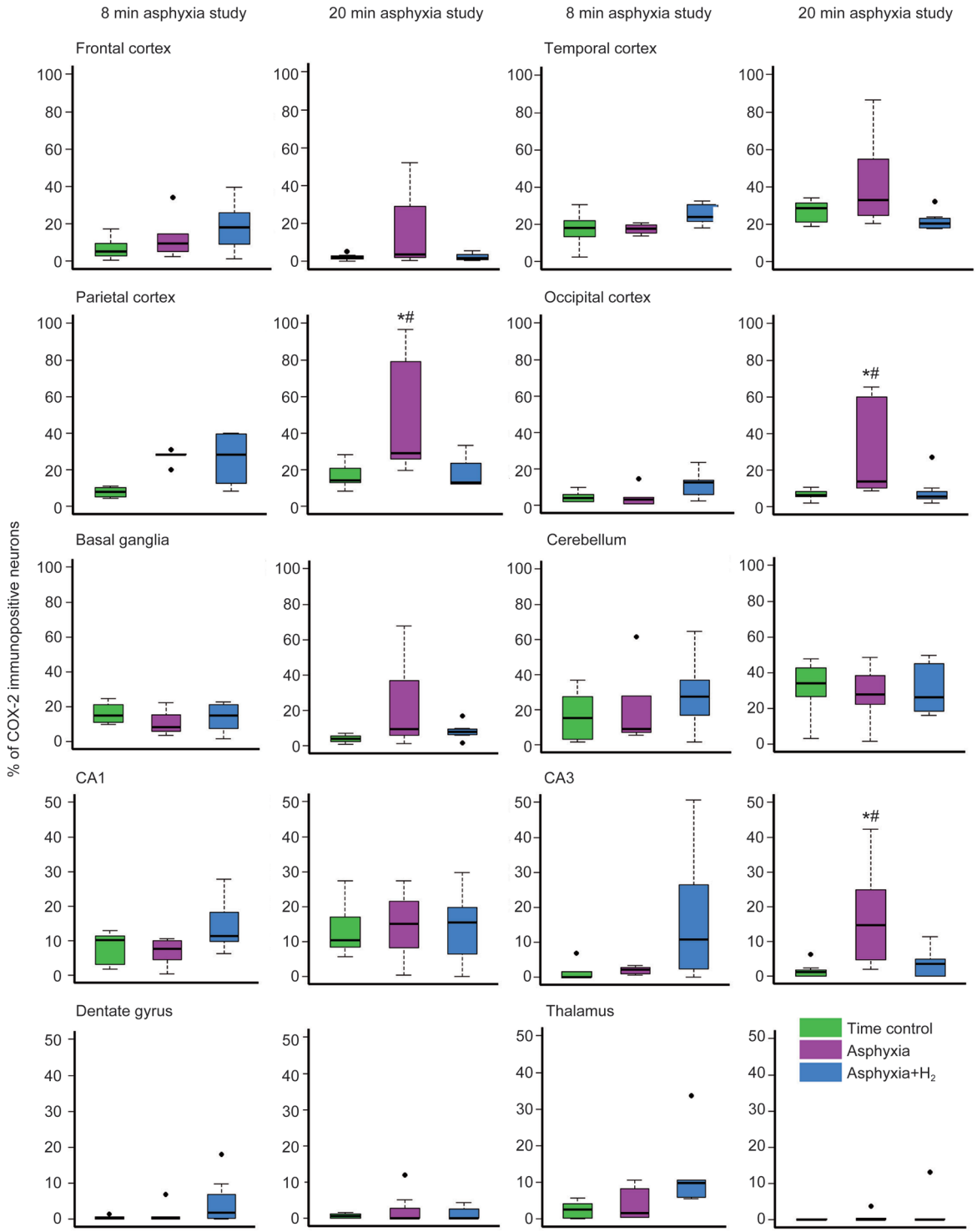

Figure 2. The effect of perinatal asphyxia and neuroprotective molecular H_2 on the ratio of COX-2-immunopositive neurons determined after 24 h of survival. Two levels of perinatal asphyxia of different durations (8 and 20 min) were studied, and both asphyxia groups (n=7-7) were compared with the corresponding time control (n=7-7) and H_2-treated asphyxia groups (n=7-7). In the first study using 8-min asphyxia, neuronal COX-2 expression was not significantly affected in either the asphyxia or the H_2-treated asphyxia group. On the other hand, in the second study, 20-min asphyxia elicited significant elevations in the ratios of COX-2-immunopositive neurons in the parietal and occipital cortices and in the hippocampal CA3 region. The trends towards increased COX-2 expression were also observed in the frontal and temporal cortices and the basal ganglia, although these differences did not reach statistical significance in these regions. The hippocampal CA1 region, dentate gyrus, and thalamus showed low immunopositivity, which was unaffected by both asphyxia and H_2 treatment. Approximately one-third of cerebellar Purkinje-cells were COX-2-immunopositive, and no marked differences were detected among the three groups. ($^{*}P$<0.05 *vs* time control. $^{\#}P$<0.05 *vs* asphyxia+H_2; ANOVA on ranks, Student-Newman-Keuls *post hoc* test. Bold line, box, and whiskers represent the median, 25th–75th, and 10th–90th percentiles, respectively; black dots are outliers).

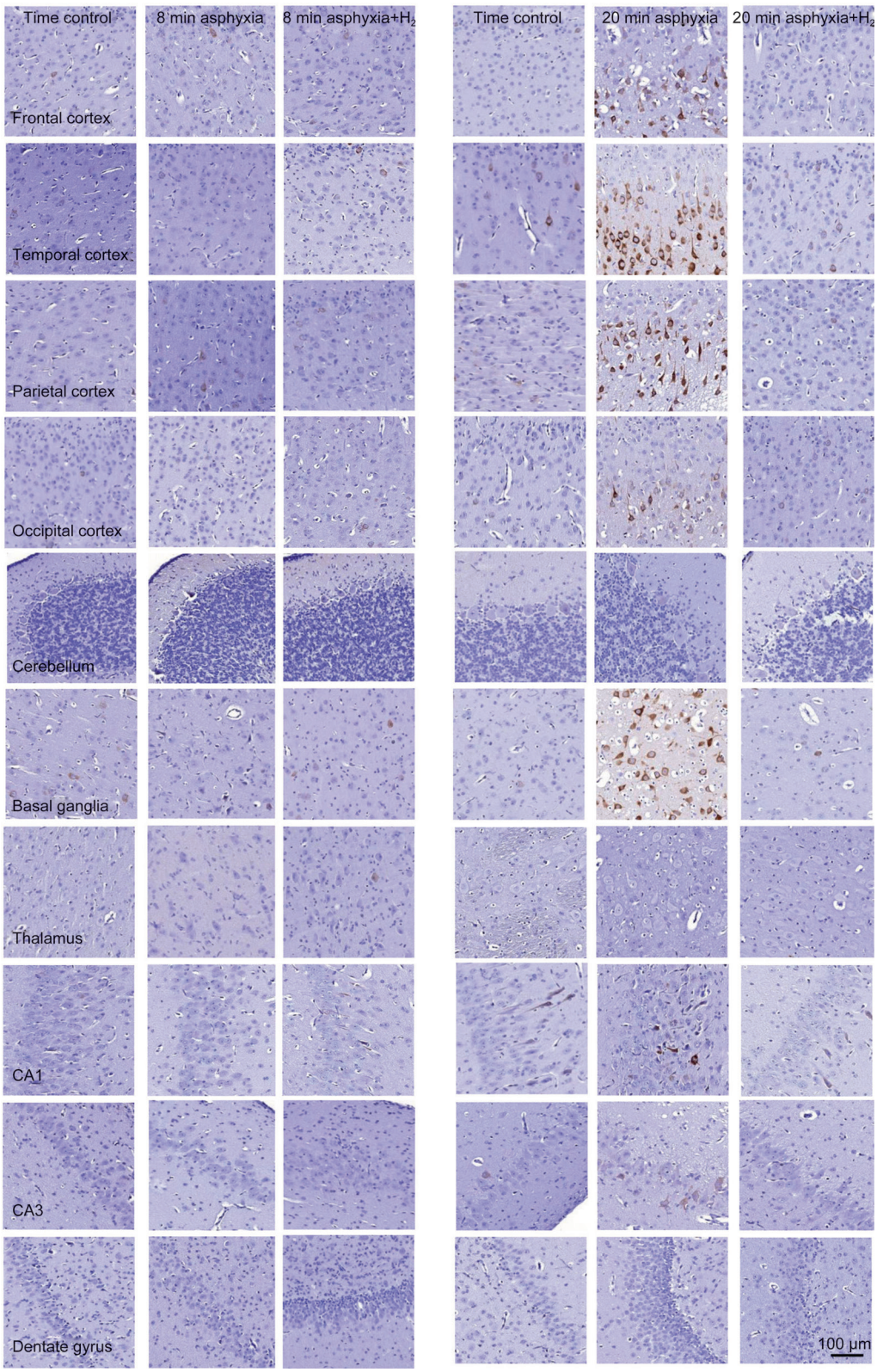

Figure 3. Representative photomicrographs (x20) showing cyclooxygenase-2 (COX-2)-immunopositive neurons (brown colored neurons) from the assessed brain regions in the matching time control, asphyxia and asphyxia+H_2 groups of the 8-min asphyxia and the 20-min asphyxia studies. The displayed fields of view were selected from the 10 analyzed fields of view of those animals that yielded the median values of the respective groups in Figure 2. No remarkable differences were detected among the experimental groups subjected to 8 min of asphyxia. The increased abundance of COX-2-immunopositive neurons was striking in virtually all neocortical areas, in the CA3 hippocampal region and in the basal ganglia from the 20-min asphyxia group.

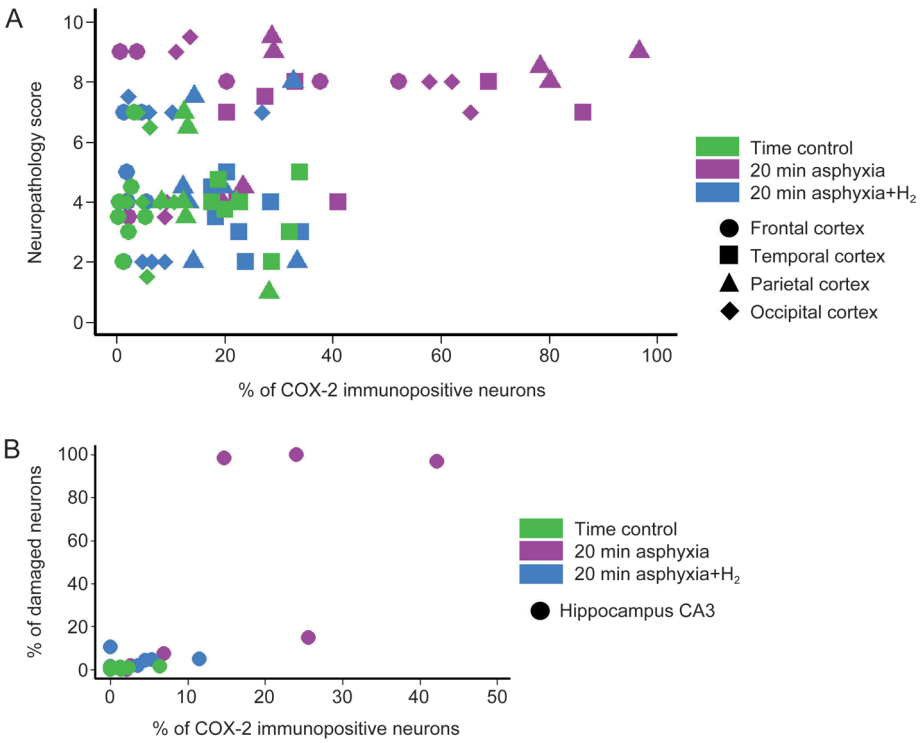

Figure 4. High ratios of COX-2-immunopositive neurons/total neurons are exclusively found in severely damaged cortical and hippocampal regions. (A) In the cortical regions of the normoxic time control group (n=7), the neuropathology scores were typically low and associated with low levels of COX-2-immunopositive neurons. Similar observations were made for the 20-min asphyxia+H_2 group (n=7) as well. However, in the 20-min asphyxia group (n=7), severe neuronal lesions may or may not be associated with high percentages of COX-2-immunopositive neurons. Importantly, high COX-2 immunopositivity was not associated with low neuropathology scores in any animals/regions. (B) In the hippocampal CA3 subfield, the highest number COX-2-immunopositive neurons was from the 20-min asphyxia group with largest degree of neuronal damage.

asphyxiated animals. When all data points were considered, the RI showed no correlation with neuronal COX-2 expression (r=-0.56, Figure 6C), but when data from only the 20-min asphyxia group were considered, a significant negative correlation (r=-0.75) was observed.

Discussion

The major findings of the present study are as follows: 1) neuronal COX-2 expression in the neocortical areas is greatly reduced in 24-h anesthetized time controls; 2) 20-min, but not 8-min, asphyxia exposure elevates the number of COX-2-positive neurons both in the cortex and the hippocampal CA3 subfield but not in the assessed subcortical areas or other hippocampal structures; 3) the effect of asphyxia on neuronal COX-2 abundance is associated and correlated with oxidative stress and microglial activation as shown by enhanced 8-OHdG staining and reduced RI, respectively; and 4) post-asphyxia administration of neuroprotective molecular H_2 prevents the upregulation of neuronal COX-2 expression in all sensitive brain regions with simultaneous reductions in oxidative stress and prevention of microglial activation.

This study is the first to describe the induction of neuronal COX-2 expression following asphyxia in a translational subacute piglet PA/HIE model. In our previous study[23], we extensively characterized the effect of 20-min asphyxia elicited in newborn (<1 day old) piglets by ventilation with a hypoxic-hypercapnic (6% O_2, 20% CO_2) gas mixture on hemodynamics, blood gases, metabolites, electroencephalogram and neuropathology. The applied insult resulted in alterations that matched both human pathology and naturally occurring birth asphyxia in swine[34] and corresponded to moderate to severe HIE in all of the animals. Our present results elucidated the confounding results from previous studies in which elevations in COX-2 levels were reported after 10 min of global cerebral ischemia but not 10 min of asphyxia[16]. Our current results suggest that this reported difference was due to the more severe hypoxic/ischemic insult elicited by global cerebral ischemia, and in the present study, the longer asphyxia duration rather than the shorter treatment elicited conditions similar to those observed with global ischemia, which resulted in the upregulation of COX-2.

In the present study, neuronal COX-2 abundance was conspicuously reduced in all neocortical areas of the 24-h time control animals compared with the values previously reported in our 4-h survival study[22]. This difference cannot be attributed to differences in methodology such as for COX-2 immunostaining or cell counting, as the values obtained from the naïve animals in the present study yielded virtually identical data to the previously published values. The decreased number of COX-2-expressing neurons may be in part explained

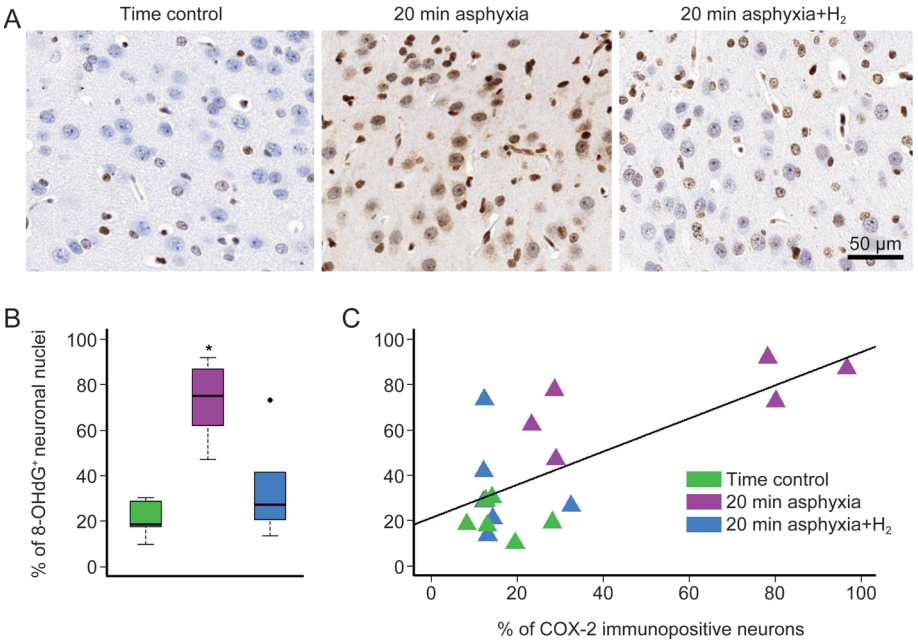

Figure 5. 8-OHdG immunopositivity in the parietal cortex of the matching time control, 20-min asphyxia and 20-min asphyxia+H_2 groups. Representative photomicrographs (A) demonstrate the oxidative damage of nuclei (×40) in the 20-min asphyxia group compared with the time control and the 20-min asphyxia+H_2 groups. The ratio of 8-OHdG-immunopositive neuronal nuclei/total neuronal nuclei (B) was markedly increased in the 20-min asphyxia group compared with time control and 20-min asphyxia+H_2 groups (n=6-6-6, ANOVA on ranks, Student-Newman-Keuls *post hoc* test, $^*P$<0.05; bold line, box, and whiskers represent the median, 25th-75th, and 10th-90th percentiles, respectively; black dots are outliers). Correlation analysis of the 8-OHdG and COX-2 immunopositivity (C) detected a significant tendency (Pearson's method, r=0.71, P<0.05).

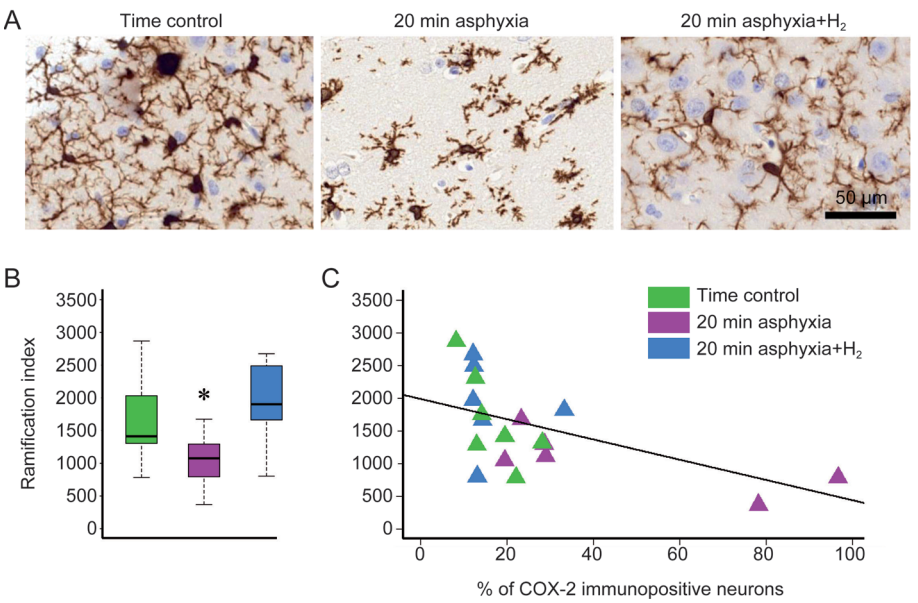

Figure 6. Iba-1 immunopositivity and microglial ramification index in the parietal cortex of the matching time control, 20-min asphyxia and 20-min asphyxia+H_2 groups. Representative photomicrographs (A) show that while in the time control and 20-min asphyxia+H_2 groups, the shape of the microglial cells becomes ramified, in the 20-min asphyxia group, the microglial cells become activated and start assuming a more amoeboid shape (×40). The ramification index (B) was evidently decreased in the 20-min asphyxia group compared with the time control group; however, the 20-min asphyxia+H_2 group was more similar to the time control group (n=7-6-6, ANOVA on ranks, Dunn's *post hoc* test, $^*P$=0.015). The correlation between the ramification index and neuronal COX-2 expression (% of total neurons) (C) considering all 3 groups was less pronounced (Pearson's method, r=-0.56, P<0.05); however, when regarding the 20-min asphyxia group only, a significant negative correlation was detected (r=-0.75).

by the inactivation of cortex due to anesthesia, as COX-2 expression is stimulated by neuronal activity[35]. The applied anesthetic/analgesic drugs could exert an inhibitory effect on COX-2 expression by interacting with the nuclear transcription factor NF-κB signaling pathway, which is a well-known transcriptional regulator of COX-2[36]. Although morphine has been reported to have ambiguous stimulatory and inhibitory effects on NF-κB activation[37, 38], midazolam is unequivocally known to inhibit the NF-κB pathway[39]. The applied anesthetic regimen was chosen to enhance the translational potential of our animal model, as morphine/midazolam analgesia/sedation is routinely used in the management of human neonates affected by PA/HIE[40]. Furthermore, experimental data suggested that morphine analgesia may be an important permissive factor by allowing neuroprotective therapies such as therapeutic hypothermia to be effective; mild hypothermia failed to exhibit neuroprotection in the absence of anesthesia and analgesia in newborn pigs[41]. Our current results suggested that this "supportive" analgesia may have a beneficial effect on neuronal survival in part through the attenuation of COX-2 expression. Our findings also suggested a time-dependent role of COX-2-derived ROS and prostanoids in the pathomechanism of HIE development in different brain regions, as COX-2 activity-dependent neuronal injury in the early reventilation/reoxygenation phase will be most likely pronounced in regions with high baseline COX-2 expression (especially the frontoparietal neocortex). However, in the delayed secondary energy failure phase, COX-2 will likely remain a more important pathogenic factor for neuronal injury in those areas where the asphyxia-induced elevation dominates the anesthesia-induced depression of COX-2 levels.

The present data thus suggested that at least in the neocortical areas, two factors affect neuronal COX-2 abundance. Long-term anesthesia tends to decrease the enzyme levels, whereas asphyxia elevates them. Both the increase in COX-2 levels and the increase in the level of neuronal injury were variable in the piglets subjected to asphyxia, in accordance with the spectrum of human HIE severity. We found that very high percentages of COX-2-immunopositive neurons were inevitably accompanied by the most severe types of cortical neuronal damage. In some cases, however, similarly high neuropathology scores coincided with rather low COX-2 immunopositivity. These areas may perhaps represent those severely damaged areas where the hypoxia/ischemia-induced translational blockade might have prevented the expression of COX-2. Thus, the areas displaying very high neuronal COX-2 levels may represent those areas that were still able after asphyxia to translate new proteins, and the deleterious effects of COX-2 may have contributed most in these areas to the observed neuronal damage.

In the present study, we assessed the effect of a neuroprotective (2.1%) concentration of H_2 on neuronal COX-2 expression. In addition to our previous studies[22-24], this concentration was found to be neuroprotective in a number of other disease models as well[25, 42, 43]. Inhaled H_2 can easily penetrate into the brain, as has been shown numerous times by the successful application of the so-called H_2-clearance technique to quantitatively determine cerebral blood flow in newborn pigs[44-46]. After rapid equilibration with the blood, the applied H_2 concentration likely resulted in approximately 10–20 μmol/L H_2 brain levels, as determined in both rats and humans[25, 47]. Our current results concerning the correlation of nuclear 8-OHdG immunoreactivity with COX-2 expression and the remarkable efficacy of molecular H_2 inhalation to attenuate elevations in both 8-OHdG and COX-2 levels after asphyxia suggest a role for ROS in the mechanism of COX-2 expression. 8-OHdG is used as a biomarker of oxidative modifications to DNA[48-50] and is one of the most studied catabolites. Guanine is the best electron donor that has the lowest oxidation potential among the DNA bases[49, 51]. 8-Hydroxylation in the guanine base occurs after an attack by hydroxyl radicals under oxidative stress[52]. Thus, elevations in the number of 8-OHdG-positive nuclei indirectly indicate significant oxidative stress imposed by hydroxyl radicals. Importantly, molecular H_2 was originally described as a selective hydroxyl radical scavenger[25], and thus, the efficacy of H_2 to attenuate elevations in 8-OHdG levels after asphyxia further confirms the presence of significant oxidative stress perhaps characterized by significant production of hydroxyl radicals in our present PA/HIE piglet model. The connection between this oxidative stress and the observed induction of COX-2 expression may be the activation of NF-κB, which is a transcription factor known to be induced by ROS and inhibited by antioxidants[53]. The general physiological functions of NF-κB include the regulation of apoptosis, cell growth, cellular stress responses and intracellular signaling[54]. NF-κB affects various brain functions as well as neuronal development, inflammation and neurodegeneration[55]. Brain injury has been shown to increase NF-κB activity[56]. The COX-2 gene is a neuronal target of NF-κB[36], and therefore the asphyxia-induced increase in neuronal COX-2 expression is very likely mediated via NF-κB. Indeed, a very recent report in neonatal rats demonstrated reduced NF-κB activation in H_2-treated rat pups, which lends experimental support to our hypothesis[57]. Our results with Iba-1 immunohistochemistry that was used to visualize microglia to determine the RI as an indicator of microglial activation are also in favor of the above-mentioned mechanism. We found that microglia were activated by asphyxia only but not by asphyxia followed by H_2. As microglial activation has also been reported to be accompanied by NF-κB activation[58], hydroxyl radicals may have activated the microglia by promoting NF-κB activity in the present study.

The efficacy of molecular H_2 to prevent increases in COX-2 levels after asphyxia suggest that the ROS responsible for triggering COX-2 induction were produced during the early reventilation/reoxygenation phase, as H_2 was administered only in the first four hours of survival. This is interesting, as ROS may arise at later time points as well, for instance from mitochondria during the secondary energy failure[59], from COX activity itself [60], or from the activated microglia[61].

Conclusion

In our translational HIE model, PA-induced increases in neu-

ronal COX-2 expression were dependent on regional vulnerability and on the severity of asphyxia. ROS are known to trigger COX-2 expression, and in turn, COX-2 activity is also an important source of ROS after PA[22, 62]. One of the limitations of the present study was that although it showed changes in neuronal COX-2 abundance, it could not directly demonstrate the changes in neuronal COX activity. However, the demonstrated increases in oxidative DNA damage and microglial activation may also indirectly signal enhanced COX-2 activity via the effects of ROS and neuroinflammation. Furthermore, these mechanisms indicate the development of a vicious cycle where ROS-inflicted changes (COX-2 induction, neuroinflammation triggered by microglial activation, and ROS-inflicted mitochondrial damage) lead to progressive neuronal injury. Molecular H_2 appears to interrupt this vicious cycle when applied immediately during the early reoxygenation phase after asphyxia.

We conclude that H_2 remains a promising neuroprotective agent to combat HIE development. H_2-induced neuroprotection involves not only direct scavenging of ROS but also the inhibition of deleterious neuronal COX-2 induction in vulnerable neurons.

Acknowledgments

This study was supported by grants from the Hungarian Brain Research Program (No KTIA_13_NAP-A-I/13) and from the EU-funded Hungarian grant EFOP-3.6.1-16-2016-00014. János NÉMETH was supported by the "Nemzeti Tehetség Program" of the "Emberi Erőforrás Támogatáskezelő" from the Hungarian Ministry of Human Capacities.

Author contribution

Viktória VARGA participated in animal experiments, evaluated the immunostaining results, analyzed the data and wrote the paper. Orsolya OLAH designed the study, participated in animal experiments, evaluated the immunostaining results, and analyzed the data. János NEMETH participated in animal experiments, evaluated the immunostaining results, and analyzed the data. Valéria TOTH-SZUKI participated in animal experiments and research management. Viktória KOVACS and Gábor REMZSO participated is animal experiments. Ferenc DOMOKI designed the study, participated in animal experiments, analyzed the data and wrote the paper.

References

1 Thornberg E, Thiringer K, Odeback A, Milsom I. Birth asphyxia: incidence, clinical course and outcome in a Swedish population. Acta Paediatr 1995; 84: 927-32.
2 Pierrat V, Haouari N, Liska A, Thomas D, Subtil D, Truffert P. Prevalence, causes, and outcome at 2 years of age of newborn encephalopathy: population based study. Arch Dis Child Fetal Neonatal Ed 2005; 90: F257–61.
3 Vannucci RC, Perlman JM. Interventions for perinatal hypoxic-ischemic encephalopathy. Pediatrics 1997; 100: 1004–14.
4 Smith WL, Dewitt DL. Prostaglandin endoperoxide H synthases-1 and -2. Adv Immunol 1996; 62: 167–215.
5 Smith WL, DeWitt DL, Garavito RM. Cyclooxygenases: structural, cellular, and molecular biology. Annu Rev Biochem 2000; 69: 145–82.
6 Kaufmann WE, Andreasson KI, Isakson PC, Worley PF. Cyclooxygenases and the central nervous system. Prostaglandins 1997; 54: 601–24.
7 Yamagata K, Andreasson KI, Kaufmann WE, Barnes CA, Worley PF. Expression of a mitogen-inducible cyclooxygenase in brain neurons: regulation by synaptic activity and glucocorticoids. Neuron 1993; 11: 371–86.
8 Peri KG, Hardy P, Li DY, Varma DR, Chemtob S. Prostaglandin G/H synthase-2 is a major contributor of brain prostaglandins in the newborn. J Biol Chem 1995; 270: 24615–20.
9 Weerasinghe GR, Coon SL, Bhattacharjee AK, Harry GJ, Bosetti F. Regional protein levels of cytosolic phospholipase A_2 and cyclooxygenase-2 in Rhesus monkey brain as a function of age. Brain Res Bull 2006; 69: 614–21.
10 Yang H, Chen C. Cyclooxygenase-2 in synaptic signaling. Curr Pharm Des 2008; 14: 1443–51.
11 Hahn T, Heinzel S, Plichta MM, Reif A, Lesch KP, Fallgatter AJ. Neurovascular coupling in the human visual cortex is modulated by cyclooxygenase-1 (COX-1) gene variant. Cereb Cortex 2011; 21: 1659–66.
12 Lecrux C, Toussay X, Kocharyan A, Fernandes P, Neupane S, Levesque M, *et al*. Pyramidal neurons are "neurogenic hubs" in the neurovascular coupling response to whisker stimulation. J Neurosci 2011; 31: 9836–47.
13 Strauss KI, Barbe MF, Marshall RM, Raghupathi R, Mehta S, Narayan RK. Prolonged cyclooxygenase-2 induction in neurons and glia following traumatic brain injury in the rat. J Neurotrauma 2000; 17: 695–711.
14 Dash PK, Mach SA, Moore AN. Regional expression and role of cyclooxygenase-2 following experimental traumatic brain injury. J Neurotrauma 2000; 17: 69–81.
15 Domoki F, Veltkamp R, Thrikawala N, Robins G, Bari F, Louis TM, *et al*. Ischemia-reperfusion rapidly increases COX-2 expression in piglet cerebral arteries. Am J Physiol 1999; 277: H1207–14.
16 Dégî R, Bari F, Thrikawala N, Beasley TC, Thore C, Louis TM, *et al*. Effects of anoxic stress on prostaglandin H synthase isoforms in piglet brain. Dev Brain Res 1998; 107: 265–76.
17 Seibert K, Zhang Y, Leahy K, Hauser S, Masferrer J, Perkins W, *et al*. Pharmacological and biochemical demonstration of the role of cyclooxygenase 2 in inflammation and pain. Proc Natl Acad Sci U S A 1994; 91: 12013–7.
18 Choi SH, Aid S, Bosetti F. The distinct roles of cyclooxygenase-1 and -2 in neuroinflammation: implications for translational research. Trends Pharmacol Sci 2009; 30: 174–81.
19 Fathali N, Ostrowski RP, Lekic T, Jadhav V, Tong W, Tang J, *et al*. Cyclooxygenase-2 inhibition provides lasting protection against neonatal hypoxic-ischemic brain injury. Crit Care Med 2010; 38: 572–8.
20 Toti P DFC, Schürfeld K, Stumpo M, Bartolommei S, Lombardi A, Petraglia E, Buonocore G. Cyclooxygenase-2 immunoreactivity in the ischemic neonatal human brain. An autopsy study. J Submicrosc Cytol Pathol 2001; 33: 245–9.
21 Dobbing J, Sands J. Comparative aspects of the brain growth spurt. Early Hum *Dev* 1979; 3: 79–83.
22 Olah O, Nemeth I, Toth-Szuki V, Bari F, Domoki F. Regional differences in the neuronal expression of cyclooxygenase-2 (COX-2) in the newborn pig brain. Acta Histochem Cytochem 2012; 45: 187–92.
23 Nemeth J, Toth-Szuki V, Varga V, Kovacs V, Remzso G, Domoki F. Molecular hydrogen affords neuroprotection in a translational piglet model of hypoxic-ischemic encephalopathy. J Physiol Pharmacol 2016; 67: 677–89.
24 Domoki F, Olah O, Zimmermann A, Nemeth I, Toth-Szuki V, Hugyecz M, *et al*. Hydrogen is neuroprotective and preserves cerebrovascular reactivity in asphyxiated newborn pigs. Pediatr Res 2010; 68: 387–92.

25 Ohsawa I, Ishikawa M, Takahashi K, Watanabe M, Nishimaki K, Yamagata K, *et al*. Hydrogen acts as a therapeutic antioxidant by selectively reducing cytotoxic oxygen radicals. Nat Med 2007; 13: 688–94.
26 Cai J, Kang Z, Liu K, Liu W, Li R, Zhang JH, *et al*. Neuroprotective effects of hydrogen saline in neonatal hypoxia–ischemia rat model. Brain Res 2009; 1256: 129–37.
27 Cai J, Kang Z, Liu WW, Luo X, Qiang S, Zhang JH, *et al*. Hydrogen therapy reduces apoptosis in neonatal hypoxia–ischemia rat model. Neurosci Lett 2008; 441: 167–72.
28 Fu Y, Ito M, Fujita Y, Ito M, Ichihara M, Masuda A, *et al*. Molecular hydrogen is protective against 6-hydroxydopamine-induced nigrostriatal degeneration in a rat model of Parkinson's disease. Neurosci Lett 2009; 453: 81–5.
29 Qu J, Gan YN, Xie KL, Liu WB, Wang YF, Hei RY, *et al*. Inhalation of hydrogen gas attenuates ouabain-induced auditory neuropathy in gerbils. Acta Pharmacol Sin 2012; 33: 445–51.
30 Nagata K, Nakashima-Kamimura N, Mikami T, Ohsawa I, Ohta S. Consumption of molecular hydrogen prevents the stress-induced impairments in hippocampus-dependent learning tasks during chronic physical restraint in mice. Neuropsychopharmacology 2008; 34: 501–8.
31 Iketani M, Ohsawa I. Molecular hydrogen as a neuroprotective agent. Curr Neuropharmacol 2017; 15: 324–31.
32 Olah O, Toth-Szuki V, Temesvari P, Bari F, Domoki F. Delayed neurovascular dysfunction is alleviated by hydrogen in asphyxiated newborn pigs. Neonatology 2013; 104: 79–86.
33 Faulkner S, Bainbridge A, Kato T, Chandrasekaran M, Kapetanakis AB, Hristova M, *et al*. Xenon augmented hypothermia reduces early lactate/N-acetylaspartate and cell death in perinatal asphyxia. Ann Neurol 2011; 70: 133–50.
34 Randall GCB. The relationship of arterial blood pH and pCO_2 to the viability of the newborn piglet. Can J Comp Med 1971; 35: 141–6.
35 Niwa K, Araki E, Morham SG, Ross ME, Iadecola C. Cyclooxygenase-2 contributes to functional hyperemia in whisker-barrel cortex. J Neurosci 2000; 20: 763–70.
36 Kaltschmidt B, Linker RA, Deng J, Kaltschmidt C. Cyclooxygenase-2 is a neuronal target gene of NF-kappaB. BMC Mol Biol 2002; 3: 16.
37 Hou YN, Vlaskovska M, Cebers G, Kasakov L, Liljequist S, Terenius L. A μ-receptor opioid agonist induces AP-1 and NF-κB transcription factor activity in primary cultures of rat cortical neurons. Neurosci Lett 1996; 212: 159–62.
38 Cadet P, Rasmussen M, Zhu W, Tonnesen E, Mantione KJ, Stefano GB. Endogenous morphinergic signaling and tumor growth. Front Biosci 2004; 9: 3176–86.
39 Gupta SC, Sundaram C, Reuter S, Aggarwal BB. Inhibiting NF-κB activation by small molecules as a therapeutic strategy. Biochim Biophys Acta, Gene Regul Mech 2010; 1799: 775–87.
40 Roka A, Kelen D, Halasz J, Beko G, Azzopardi D, Szabo M. Serum S100B and neuron-specific enolase levels in normothermic and hypothermic infants after perinatal asphyxia. Acta Paediatr 2012; 101: 319–23.
41 Tooley J, Eagle R, Satas S, Thoresen M. Significant head cooling can be achieved while maintaining normothermia in the newborn piglet. Arch Dis Child Fetal Neonatal Ed 2005; 90: F262–F6.
42 Xin Y, Liu H, Zhang P, Chang L, Xie K. Molecular hydrogen inhalation attenuates postoperative cognitive impairment in rats. NeuroReport 2017; 28: 694–700.
43 Hayashida K, Sano M, Kamimura N, Yokota T, Suzuki M, Maekawa Y, *et al*. H_2 gas improves functional outcome after cardiac arrest to an extent comparable to therapeutic hypothermia in a rat model. J Am Heart Assoc 2012; 1: e003459. doi: 10.1161/JAHA.112.003459.
44 Park TS, Gidday JM, Gonzales E. Local cerebral blood flow response to locally infused 2-chloroadenosine during hypotension in piglets. Dev Brain Res 1991; 61: 73–7.
45 Gidday JM, Park TS. Effect of 2-chloroadenosine on cerebrovascular reactivity to hypercapnia in newborn pig. J Cereb Blood Flow Metab 1992; 12: 656–63.
46 Ruth VJ, Park TS, Gonzales ER, Gidday JM. Adenosine and cerebrovascular hyperemia during insulin-induced hypoglycemia in newborn piglet. Am J Physiol, Heart Circ Physiol 1993; 265: H1762–H8.
47 Ono H, Nishijima Y, Adachi N, Sakamoto M, Kudo Y, Kaneko K, *et al*. A basic study on molecular hydrogen (H_2) inhalation in acute cerebral ischemia patients for safety check with physiological parameters and measurement of blood H_2 level. Med Gas Res 2012; 2: 21.
48 Anjana Vaman VS, Tinu SK, Geetha CS, Lissy KK, Mohanan PV. Effect of fibrin glue on antioxidant defense mechanism, oxidative DNA damage and chromosomal aberrations. Toxicol Mech Methods 2013; 23: 500–8.
49 Villaño D, Vilaplana C, Medina S, Cejuela-Anta R, Martínez-Sanz JM, Gil P, *et al*. Effect of elite physical exercise by triathletes on seven catabolites of DNA oxidation. Free Radic Res 2015; 49: 973–83.
50 Hintsala HR, Jokinen E, Haapasaari KM, Moza M, RistimÄKi ARI, Soini Y, *et al*. Nrf2/Keap1 pathway and expression of oxidative stress lesions 8-hydroxy-2'-deoxyguanosine and nitrotyrosine in melanoma. Anticancer Res 2016; 36: 1497–506.
51 Nunomura A, Moreira PI, Castellani RJ, Lee HG, Zhu X, Smith MA, *et al*. Oxidative damage to RNA in aging and neurodegenerative disorders. Neurotox Res 2012; 22: 231–48.
52 Huang Q, Chen Z, Yang Y, Wang B, Li F, Zhan M. Content change and clinical significance of oxidation damage products 8-OHdG, 4-HNE and NTY in hemangioma tissue. Int J Clin Exp Pathol 2016; 9: 8847–57.
53 Campo GM, Avenoso A, Campo S, D'Ascola A, Traina P, Samà D, *et al*. The antioxidant effect exerted by TGF-1β-stimulated hyaluronan production reduced NF-kB activation and apoptosis in human fibroblasts exposed to FeSo4 plus ascorbate. Mol Cell Biochem 2008; 311: 167–77.
54 Hoffmann A, Levchenko A, Scott ML, Baltimore D. The IκB-NF-κB signaling module: temporal control and selective gene activation. Science 2002; 298: 1241–5.
55 O'Neill LAJ, Kaltschmidt C. NF-kB: a crucial transcription factor for glial and neuronal cell function. Trends Neurosci 1997; 20: 252–8.
56 Salminen A, Liu PK, Hsu CY. Alteration of transcription factor binding activities in the ischemic rat-brain. Biochem Biophys Res Commun 1995; 212: 939–44.
57 Shi Y, Wang G, Li J, Yu W. Hydrogen gas attenuates sevoflurane neurotoxicity through inhibiting nuclear factor kappa-light-chain-enhancer of activated B cells signaling and proinflammatory cytokine release in neonatal rats. Neuroreport 2017; 28: 1170–5.
58 Kaltschmidt C, Kaltschmidt B, Lannes-Vieira J, Kreutzberg GW, Wekerle H, Baeuerle PA, *et al*. Transcription factor NF-κB is activated in microglia during experimental autoimmune encephalomyelitis. J Neuroimmunol 1994; 55: 99–106.
59 Indo HP, Davidson M, Yen HC, Suenaga S, Tomita K, Nishii T, *et al*. Evidence of ROS generation by mitochondria in cells with impaired electron transport chain and mitochondrial DNA damage. Mitochondrion 2007; 7: 106–18.
60 Phaniendra A, Jestadi DB, Periyasamy L. Free radicals: properties, sources, targets, and their implication in various diseases. Indian J Clin Biochem 2015; 30: 11–26.
61 Block ML, Zecca L, Hong JS. Microglia-mediated neurotoxicity: uncovering the molecular mechanisms. Nat Rev Neurosci 2007; 8: 57–69.
62 Domoki F, Perciaccante JV, Puskar M, Bari F, Busija DW. Cyclooxygenase-2 inhibitor NS398 preserves neuronal function after hypoxia/ischemia in piglets. Neuroreport 2001; 12: 4065–8.

Publications related to the PhD thesis

II.

Life Sciences 192 (2018) 1–8

Contents lists available at ScienceDirect

Life Sciences

journal homepage: www.elsevier.com/locate/lifescie

Active forms of Akt and ERK are dominant in the cerebral cortex of newborn pigs that are unaffected by asphyxia

Viktória Kovács*, Valéria Tóth-Szűki, János Németh, Viktória Varga, Gábor Remzső, Ferenc Domoki

Department of Physiology, University of Szeged, School of Medicine, Szeged, Hungary

ARTICLE INFO

Chemical compounds studied in this article:
Akt1/2 kinase inhibitor A-6730 (PubChem CID: 16218954) and the MAPK/ERK kinase (MEK) inhibitor U0126 monoethanolate (PubChem CID: 16218944) both from Sigma Aldrich (St. Louis, MO, USA).

Keywords:
Hypoxic-ischemic encephalopathy
Perinatal asphyxia
Translational piglet model

ABSTRACT

Aims: Perinatal asphyxia (PA) often results in hypoxic–ischemic encephalopathy (HIE) in term neonates. Introduction of therapeutic hypothermia improved HIE outcome, but further neuroprotective therapies are still warranted. The present study sought to determine the feasibility of the activation of the cytoprotective PI-3-K/Akt and the MAPK/ERK signaling pathways in the subacute phase of HIE development in a translational newborn pig PA/HIE model.

Main methods: Phosphorylated and total levels of Akt and ERK were determined by Western blotting in brain samples obtained from untreated naive, time control, and PA/HIE animals at 24–48 h survival (n = 3–3–6,respectively). PA (20 min) was induced in anesthetized piglets by ventilation with a hypoxic/hypercapnic (6% $O_2$20%CO_2) gas mixture. Furthermore, we studied the effect of topically administered specific Akt1/2 and MAPK/ERK kinase inhibitors on Akt and ERK phosphorylation (n = 4–4) in the cerebral cortex under normoxic conditions.

Key findings: PA resulted in significant neuronal injury shown by neuropathology assessment of haematoxylin/eosin stained sections. However, there were no significant differences among the groups in the high phosphorylation levels of both ERK and Akt in the cerebral cortex, hippocampus and subcortical structures. However, the Akt1/2 and MAPK/ERK kinase inhibitors significantly reduced cerebrocortical Akt and ERK phosphorylation within 30 min.

Significance: The major finding of the present study is that the PI-3-K/Akt and the MAPK/ERK signaling pathways appear to be constitutively active in the piglet brain, and this activation remains unaltered during HIE development. Thus, neuroprotective strategies aiming to activate these pathways to limit apoptotic neuronal death may offer limited efficacy in this translational model.

1. Introduction

According to the World Health Organization's estimates, perinatal asphyxia (PA) affects 4 neonates out of 1000 live births [1]. The neuronal injury triggered by PA may lead to the so-called hypoxic-ischemic encephalopathy (HIE) in the survivors leading to lifelong neurodevelopmental disorders. The neuronal injury eliciting HIE is no longer considered as a single “event” during PA but rather an evolving process that lasts for days after the resolution of the asphyxia. Correspondingly, mild whole body hypothermia applied in the first 2–3 days after PA is currently the only effective therapy to mitigate HIE severity [2]. However, hypothermia cannot cure HIE alone, and thus clearly further therapies are needed that can augment the neuroprotection afforded by cooling.

The newborn piglet is an established large animal model of the term neonate because of its gyrencephalic brain, developmental stage, body size, cerebrovascular regulation and its cerebral glucose metabolic rate are similar to the term human neonate [3]. We have recently created and characterized a piglet PA/HIE model that resulted in moderate/severe brain damage in most of the animals [4]. This model faithfully reproduces all major hallmarks of human PA/HIE, and can be used to assess the molecular mechanisms of HIE development, and to identify appealing targets for neuroprotective interventions. One of these may be the brain-derived neurotrophic factor (BDNF) signaling pathway. BDNF is a member of the neurotrophic factor family that plays an important role in regulating neural proliferation, differentiation and survival [5,6]. The neuroprotective actions of BDNF are mediated through the phosphatidylinositide 3-kinases (PI-3-K) and the mitogen-activated

* Corresponding author at: Department of Physiology, University of Szeged, School of Medicine, 10. Dóm tér, Szeged 6720, Hungary.
E-mail address: kovacs.viktoria.1@med.u-szeged.hu (V. Kovács).

https://doi.org/10.1016/j.lfs.2017.11.015
Received 19 May 2017; Received in revised form 3 November 2017; Accepted 10 November 2017
Available online 11 November 2017
0024-3205/

protein kinase (MAPK) pathways [7]. The PI-3-K pathway activates the kinase Akt, one of its direct downstream protein kinase effectors, which regulates multiple biological processes including cell survival, proliferation, growth, and glycogen metabolism [8,9]. Similarly, MAPK-s also regulates widespread cellular processes including cell survival, and apoptosis. Extracellular signal-regulated kinase (ERK) is an anti-apoptotic MAPK, as its downstream pathways are usually linked to growth factor action: cellular differentiation and proliferation. Thus, ERK usually promotes cell survival [10]. Maintaining the delicate balance between the simultaneously active and inactive kinases is critical in determining cell fate [11]. There are both *in vitro* and *in vivo* studies providing evidence that BDNF-supported neuronal survival is mediated *via* the activation of the ERK pathway [12,13], while others have shown that rather the PI-3-K pathway is involved [14]. Therefore, it appears that growth factor-mediated protection of neurons can occur *via* different pathways depending on various factors such as cell types, environmental conditions, and cellular stimuli. However, the potential *in vivo* role of these pathways in the neuronal injury/survival during HIE has not yet been previously studied in a PA/HIE large animal model.

Therefore, the major objective of the present study was to determine the *in vivo* activation of the PI-3-K/Akt and the MAPK/ERK signaling pathways under normoxic conditions and over the course of HIE development (24–48 h). The results emanating from these studies urged us to test also if cortical kinase activities can be *in vivo* modified by specific inhibitors.

2. Materials and methods

2.1. Experimental groups

All necessary permits to perform the *in vivo* animal experiments including the approval from the Institutional Animal Care and Use Committee have been obtained preceding the experiments. Animal care and handling were in accordance with the National Institutes of Health guidelines. The levels of activated ERK and Akt kinases have been determined in the following experimental groups (Fig. 1): (1) untreated animals without any interventions (n = 3); (2) normoxic time controls (n = 3) with 24 or 48 h of survival (n = 1–2, respectively); (3) animals undergoing 20 min PA (n = 6) also with 24 or 48 h of survival (n = 3–3, respectively); (4) non-asphyxiated animals treated topically with the MAPK/ERK kinase (MEK) inhibitor U0126 monoethanolate (n = 4); and (5) non-asphyxiated animals treated topically with the Akt1/2 kinase inhibitor A-6730 (n = 4) onto the cerebral cortex. The detailed procedures applied to the different groups are given in the subsequent paragraphs.

2.2. Animals

Newborn (< 24 h old) male Large-White piglets (weighing between 1.5 and 2.5 kg, n = 20) were used in the present study, they were delivered to the laboratory on the morning of the experiments from a local company (Pigmark Ltd., Co., Szeged, Hungary). The animals were anesthetized with an intraperitoneal injection of sodium thiopental (45 mg/kg; Sandoz, Kundl, Austria). The animals were placed on a heating pad. The skin was disinfected, and the animals were intubated through a tracheotomy. Then the piglets were artificially ventilated with warmed, humidified medical air (21% O_2, balance N_2) at a frequency of 30–35 breaths/min, using a pressure controlled ventilator applying peak inspiratory pressure = 120–135 mmH_2O. Aseptic technique was followed during all aspects of the animal surgery. With the exception of the untreated animals, the right carotid artery and femoral vein were cannulated with catheters. To maintain anesthesia/analgesia the mechanically ventilated animals were given a bolus injection of morphine (100 μg/kg; Teva, Petach Tikva, Israel) and midazolam (250 μg/kg; Torrex Pharma, Vienna, Austria), then were infused with morphine (10 μg/kg/h), midazolam (250 μg/kg/h) and fluids (5% glucose, 0.45% NaCl 3–5 ml/kg/h) throughout the whole experiment. The wounds were closed and covered with warm compress to minimize heat and fluid losses.

2.3. Experimental PA/HIE

The piglets between the time control and the asphyxia groups were randomized with coin flip. The animals were placed into a neonatal incubator (SPC 78-1; Narco Air-Shields, Inc., Hatboro, Pa., USA). Oxygen saturation, mean arterial blood pressure (MABP) through the arterial catheter, heart rate (HR), and ECG were continuously monitored using a Hewlett-Packard M1094 monitor (Palo Alto, California, USA) and recorded online (MecifView, Arlington, Mass., USA). Core temperature was maintained rigorously between 38.5 ± 0.5 °C with a servo-controlled heating pad. Prophylactic antibiotics were given intravenously (penicillin: 50 mg/kg/12 h, Teva, Petah Tikva, Israel and gentamicin: 2.5 mg/kg/12 h, Sanofi, Paris, France) and the urinary bladder was tapped by suprapubic puncture every 12 h of survival. Arterial blood gases, along with blood sugar and lactate levels were determined (~300 μl/sample; EPOC Blood Analysis, Epocal Inc., Ottawa, Canada) at defined intervals to monitor the effect of PA and to keep the values in their respective physiological ranges during the

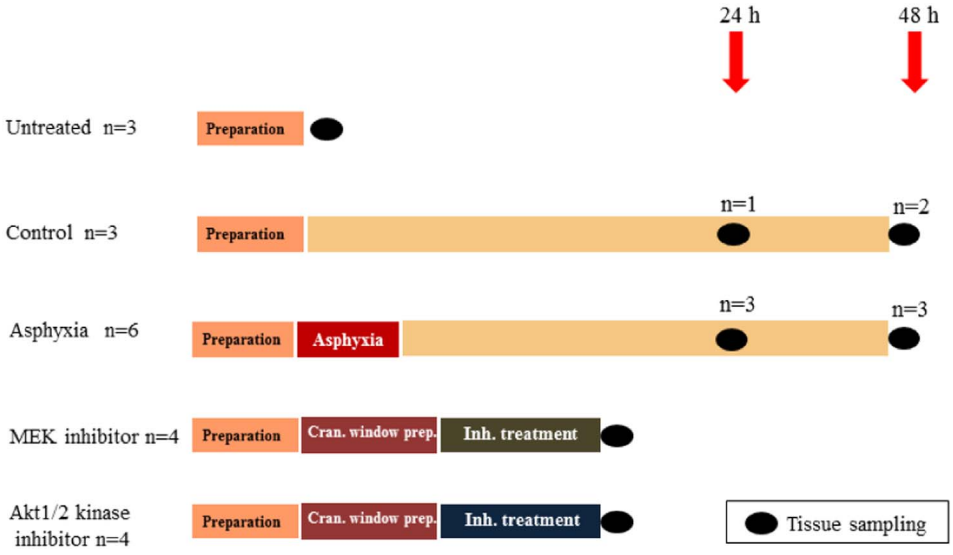

Fig. 1. Experimental protocol. Untreated animals served as naïve controls; Control animals were anesthetized, ventilated, and monitored, but not subjected to asphyxia. Asphyxia animals were like Controls but were exposed to 20 min asphyxia. The animals in the MEK and Akt1/2 kinase inhibitor groups were fitted with closed cranial windows and the respective drugs were applied locally onto the cerebral cortex.

survival period.

PA was induced by ventilation with a hypoxic/hypercapnic gas mixture containing 6% O_2 and 20% CO_2 for 20 min while respiratory rate was reduced from 30 to 15 breaths/min, and intravenous glucose administration was suspended. Arterial blood gases were also determined to check the severity of PA at the end of asphyxia (blood sample was taken at the 18th min of asphyxia). Reventilation was commenced with medical air throughout the survival period.

2.4. The study of ERK and Akt kinase inhibitors

In these groups, the head of the anesthetized, mechanically ventilated animals were fixed in a stereotactic frame. Monitoring of physiological parameters was similar to the previous groups. After retraction of the scalp, a circular craniotomy was made in the left frontoparietal region, where after careful removal of the dura mater, a stainless steel closed cranial window with three needle ports was inserted. The cranial window was sealed with bone wax, cemented in place with dental acrylic, and was filled with artificial cerebrospinal fluid (aCSF; containing KCl 220 mg/l, $MgCl_2$ 132 mg/l, $CaCl_2$ 221 mg/l, NaCl 7710 mg/l, urea 402 mg/l, dextrose 665 mg/l, and $NaHCO_2$ 2066 mg/l, warmed to 37 °C and equilibrated with a gas mixture containing 6% O_2, 6.5% CO_2 and 87.5% N_2). There was a 45 min stabilization period allowed after the implantation of the cranial window before commencing the experiments.

Both the MEK inhibitor U0126 and the Akt1/2 kinase inhibitor A-6730 drugs were prepared similarly: first a 10 mM stock solution was produced in dimethyl-sulfoxide (DMSO) that was further diluted in aCSF to obtain 10 μM drug solutions (final DMSO concentration was 0.01%). In the respective experimental groups, the drugs were applied topically onto the cerebral cortex with continuous superfusion through one of the injectable ports at a rate of 0.5 ml/min for 40 min. The other two ports allowed continuous efflux of the aCSF. Immediately after the completion of the drug treatment, the animals were euthanized with 300 mg Na-pentobarbital (Release®, WDT, Garbsen, Germany). The cortex below the cranial window as well as the corresponding contralateral untreated cortex were collected and processed as described in the following section.

2.5. Western blot analysis

At the end of the respective experimental periods (Fig. 1), both carotid arteries were catheterized in the distal direction, and the brains were perfused through them with cold (4 °C) physiological saline. The brains were gently removed from the skull, and tissue samples were snap frozen in liquid N_2, and stored at − 80 °C before Western-blot analysis.

Thawed samples were homogenized and harvested in ice-cold lysis buffer (50 mM Tris-base, pH 7.4, 150 mM NaCl, 10% glycerol, 1 mM EGTA, 1 mM Na-orthovanadate, 5 μM $ZnCl_2$, 100 mM NaF, 10 μg/ml aprotinin, 1 μg/ml leupeptin, 1 mM phenylmethylsulfonyl fluoride (PMSF), 1% Triton X-100). The homogenate was centrifuged at 40,000 × *g* at 4 °C for 30 min and the protein concentration of the supernatant was determined (Bio-Rad Protein Assay Dye Reagent Concentrate, Bio-Rad, Hercules, CA, USA).

Samples prepared from equal amounts (50 μg) of protein were mixed with Laemmli buffer (1 M Tris-HCl, pH 6.8, glycerol, SDS, 100 mM EDTA, 100 mM EGTA and 1% bromophenol blue) and denatured by boiling. Subsequently, they were loaded for 12% SDS-containing polyacrylamide gel and separated based on molecular size. The gels were electroblotted for polyvinylidene difluoride (PVDF) membranes (Hybond-P, GE Healthcare, United Kingdom).

Detection of the protein of interest was carried out by first blocking the membrane in 3% nonfat dry milk in Tris Buffered Saline -Tween (10 mM Tris-base, 150 mM NaCl, 0.2% Tween-20, pH 8.0; TBS-Tween). Membranes were probed overnight at 4 °C with antibodies recognizing the following antigens: phospho-p44/42 MAP kinase to detect phospho-ERK1/2, total p44/42 MAP kinase, anti-Akt and phospho-Akt (Ser473), (Cell Signaling Technology, Danvers, MA, USA), diluted 1:1000 in the blocking solution. Excess antibody was removed by five washes of TBS-Tween. Membranes were incubated with a horseradish-peroxidase (HRP)-conjugated goat anti-rabbit secondary antibody (Cell Signaling Technology, Danvers, MA, USA) diluted 1:1000 in blocking solution at room temperature for 2 h. Five washes in TBS-Tween were followed by detection of the enhanced chemiluminescent signal (WesternBright ECL, Advansta, USA) on X-ray films. The relative protein expressions were determined using densitometry (ImageJ software, National Institutes of Health, USA). Each experiment has been performed at least three times. Values are expressed as mean ± S.E.M.

2.6. Histology

Brain samples collected for histology were immersion-fixed in 4 °C, 4% paraformaldehyde solution for two weeks then processed further. From the cerebral cortex, paraffin embedded 4 μm sections were stained with haematoxylin-eosin. The slides were evaluated by two independent researcher blinded to the experimental protocol with light microscopy (Leica Microsystems, Wetzlar, Germany). The degree of cerebrocortical neuronal damage in the frontoparietal region was graded on a 10-step scale from 0 to 9 using our previously established scoring system [15,4]. Briefly, four pattern of neuronal injury (none; scattered; grouped; panlaminar) was determined in 20–20 non-overlapping fields of vision in the frontal region. Then, final score (0–9) were given to the region based on the most severe level of damage seen for a particular region.

2.7. Statistical analysis

Results were plotted using SigmaPlot (v12.0, Systat Software Inc., San Jose, CA., USA). Core temperature, saturation, HR and MABP as well as arterial blood gas and metabolic parameters were expressed as mean ± S.E.M.

Statistical comparisons include one-way analysis of variance (ANOVA) as well as two-way repeated measures ANOVA followed by the Holm-Sidak *post-hoc* test for pairwise comparisons. Neuropathology scores were expressed as median, 25–75 percentiles. For non-parametric data Mann-Whitney *U* test was applied. p values < 0.05 were considered to be significant.

3. Results

3.1. In vivo observations

At the beginning of the experiments, piglets in both the control and the asphyxia group had similar, physiological values of core temperature (38.6 ± 0.1 and 38.6 ± 0.1 °C), oxygen saturation (91 ± 3 and 97 ± 3%), heart rate (133 ± 10 and 150 ± 14 1/min), and MABP (68 ± 7 and 65 ± 9 mmHg), respectively. Also, arterial blood pH, blood gases and metabolites were similar and within the normal range for these and the untreated group as well (Table 1).

Asphyxia elicited marked increases in HR and MABP (peak values were 200 ± 60 1/min and 94 ± 18 mmHg, respectively) and large drop in oxygen saturation (to 27 ± 1%). Correspondingly, the blood gas analysis performed at the end of the asphyxia period revealed severe hypoxemia, acidosis due to both hypercapnia and elevated blood lactate levels, and hyperglycemia (Table 1). Reventilation restored oxygenation quickly, and the assessed physiological parameters all returned toward baseline levels and they were not then statistically different from the corresponding values of the control group with the exception of blood glucose and lactate levels. These remained significantly elevated at 1 h of reventilation but then returned to baseline values by 4 h of reventilation. (Fig. 2, Table 1). Then, the assessed

Table 1
Arterial blood gas and metabolite analysis in the different groups. Arterial blood pH, partial pressures of carbon dioxide, partial pressures of oxygen, as well as blood glucose- and lactate levels were in the normal ranges at baseline conditions in all three groups. Asphyxia resulted in severe hypoxemia, hypercapnia, acidosis, hyperglycemia and elevations in lactate indicating severe mixed respiratory and metabolic acidosis. Reventilation quickly restored blood gases, however, and blood sugar and lactate levels were still elevated at 1 h compared to controls, and normalized only by 4 h after reventilation. The values then remained in the physiological range and there was no difference between the experimental groups at any later time points (data beyond 20 h are not shown). Data are shown as mean ± S.E.M. Level of significance (p) was set at 0.05. *vs. baseline; †vs. asphyxia at given time point.

Arterial pH	Base	Asph.	1 h	4 h	8 h	12 h	16 h	20 h
Untreated	7.55 ± 0.09							
Control	7.51 ± 0.04	NA	7.51 ± 0.04	7.49 ± 0.02	7.5 ± 0.1	7.52 ± 0.07	7.54 ± 0.09	7.53 ± 0.08
Asphyxia	7.55 ± 0.05	6.87 ± 0.01*	7.47 ± 0.06	7.51 ± 0.06	7.31 ± 0.42	7.49 ± 0.08	7.48 ± 0.11	7.53 ± 0.04

Arterial pCO_2 (mmHg)	Base	Asph.	1 h	4 h	8 h	12 h	16 h	20 h
Untreated	35.3 ± 8.9							
Control	37.1 ± 6	NA	39.7 ± 7.3	43.3 ± 4.4	41.7 ± 14.2	39.2 ± 13.6	37.7 ± 8.2	38.6 ± 7.7
Asphyxia	36.5 ± 4.6	164.3 ± 31*	35.1 ± 5.4	41.4 ± 6.3	37.4 ± 17.6	38.8 ± 7.9	43.1 ± 12.5	40.8 ± 16.2

Arterial pO_2 (mmHg)	Base	Asph.	1 h	4 h	8 h	12 h	16 h	20 h
Untreated	76.7 ± 17.4							
Control	52.9 ± 4	NA	52.5 ± 5.9	58.4 ± 7.9	52.5 ± 2.4	51.3 ± 2.8	53.1 ± 4	53.8 ± 2.2
Asphyxia	63.5 ± 9.6	20 ± 6.2*	60.4 ± 7.7	60.9 ± 10.5	58.6 ± 9.4	60 ± 7.2	65.8 ± 5.3	70.3 ± 7.8

Blood glucose (mmol/l)	Base	Asph.	1 h	4 h	8 h	12 h	16 h	20 h
Untreated	5.5 ± 1.9							
Control	5.3 ± 0.2	NA	4.8 ± 0.9	5.7 ± 1.7	5.5 ± 2.4	4.3 ± 2.1	4.5 ± 0.7	5.1 ± 0.8
Asphyxia	5.8 ± 0.9	9 ± 1.2*	7.3 ± 1.1*	5.6 ± 0.6	4.1 ± 0.8*	4.6 ± 0.9*	4.7 ± 0.9*	4.6 ± 0.8*

Blood lactate (mmol/l)	Base	Asph.	1 h	4 h	8 h	12 h	16 h	20 h
Untreated	2 ± 1.3							
Control	2.2 ± 0.8	NA	1.2 ± 0.1	1.1 ± 0.4	1.3 ± 0.7	1.3 ± 0.7	1.5 ± 1	1.5 ± 0.6
Asphyxia	1.6 ± 0.7	7.4 ± 0.7*	7.7 ± 2.2*,†	1.5 ± 0.6	1.2 ± 0.5	1.2 ± 0.4	1.1 ± 0.4	1.1 ± 0.3

physiological parameters remained in the respective physiological ranges and were statistically not different from the time control group during the rest of the survival period.

3.2. Neuropathology

Asphyxia resulted in severe neuronal damage similar to previously reported values confirming HIE development. In the frontoparietal cortex, the neuropathology scores were significantly higher as compared to the values of the normoxic (combined untreated/time control animals) groups: the scores were 7; 6; 8 *versus* 1; 1; 4 *(median; 25th;75th percentiles; asphyxiated *versus* normoxic animals, respectively; n = 5–5, *p = 0,008, Mann-Whitney U test).

3.3. Activation of ERK/Akt signaling pathways

Total ERK levels in the frontoparietal cortex were remarkably similar in all experimental groups. In addition, the levels of phosphorylated ERK (P-ERK) were also similar to the total levels; therefore the ratio of the P-ERK to total ERK was typically between 80 and 100% indicating high degree of activation of the pathway (Fig. 3.) The results concerning total and phosphorylated Akt (P-Akt) levels, the ratio of P-Akt to total Akt levels were remarkably high and there were no statistical differences among the groups, despite a slight tendency of activation by asphyxia (Fig. 3.)

High degree of ERK and Akt phosphorylation in the frontoparietal cortex was also demonstrated in the samples taken from the control side in our short-term experiments (Fig. 4). However, under normoxic conditions, local, topical *in vivo* treatment with the MEK inhibitor U0126 and the Akt1/2 kinase inhibitor A-6730 resulted in significant inhibition of ERK and Akt phosphorylation, respectively (Fig. 4).

The ratios of P-ERK/total ERK and the P-Akt/total Akt in the other assessed brain regions were remarkably similar to the values determined in the neocortex (Fig. 5). In the untreated as well as in the 48 h asphyxia animals, the phosphorylation ratios were remarkably high and there were no statistical differences among the groups, indicating no effect of asphyxia.

4. Discussion

The most important novel findings of the present study are the following: (1) we could assess activation levels of two signaling pathways important for neuronal survival in a large animal model of HIE; (2) we found that both ERK and Akt are constitutively phosphorylated/active in the cerebral cortex and all other assessed brain regions of newborn pigs irrespective of the length of anesthesia and/or exposure to asphyxia; (3) we proved that the high cerebrocortical ERK and Akt phosphorylation levels under normoxic conditions can be *in vivo* modulated by specific inhibitors.

The pathophysiology of HIE is not yet fully understood, however, in recent years the neuronal injury during HIE is increasingly being viewed as a multi-step process consisting of distinct pathomechanisms characteristic of the successive phases of HIE development. These phases include (1) the primary energy failure during the PA stress, (2) the reoxygenation/reperfusion injury associated with the reventilation/resuscitation efforts, and (3) the so-called “secondary energy failure” triggered perhaps by accumulated mitochondrial damage and associated clinically with bouts of apnoe periods and seizures [16]. During the primary energy failure of PA, the lack of oxygen and the reduction of blood flow shifts cellular metabolism from an aerobic to a less

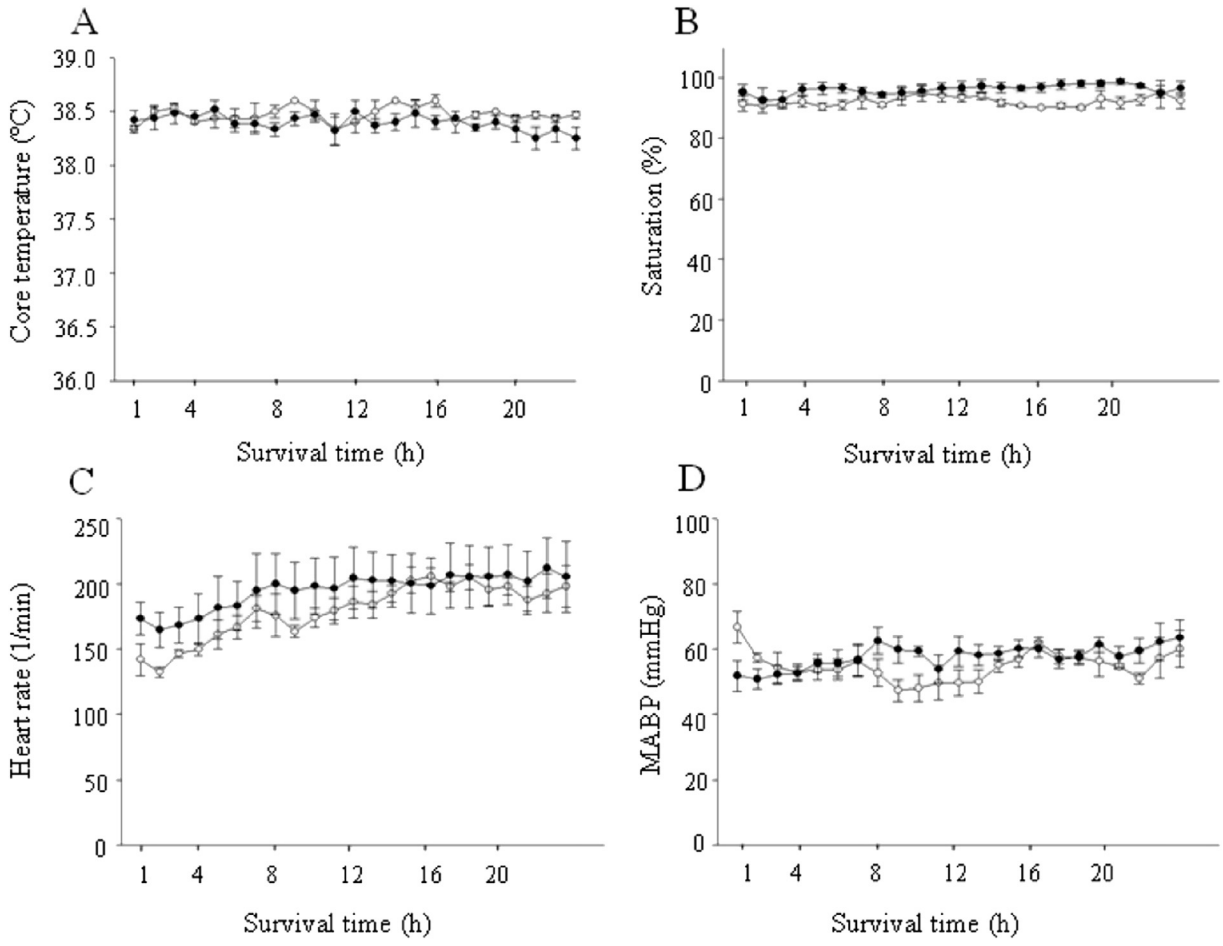

Fig. 2. Core temperature (Panel A), oxygen saturation (Panel B), heart rate (Panel C), and mean arterial blood pressure (MABP) (Panel D) data in the control and in the asphyxia groups during the first 24 h survival period. There were no significant differences between the groups in the monitored parameters either in the first or the second (data not shown) 24 h period. Data are shown as mean ± S.E.M.

efficient anaerobic pathway, resulting in the depletion of NAD^+ stores, decrease in ATP levels, and lactate accumulation [17]. ATP depletion will soon lead to the depression of neuronal activity soon followed by anoxic depolarization. Anoxic depolarization is characterized by the loss of transmembrane ionic gradients eliciting the accumulation of intracellular Na^+, H^+, and Ca^{2+} ions causing edema and worsening tissue acidosis [18,19], the unregulated release of excitatory amino acids along with the inhibition of astrocytic uptake can also contribute to excitotoxic damage *via* the *N*-methyl-D-aspartate (NMDA) receptor [20,21]. Upon reventilation/reoxygenation, the high energy phosphate levels and the transmembrane ionic gradients are gradually restored, but the initially still increased intracellular and intramitochondrial Ca^{2+} levels will activate a host of intracellular proteases and nucleases, as well as enzymatic and non-enzymatic synthesis of reactive oxygen species (ROS). These alterations will trigger mitochondrial dysfunction [17] and DNA fragmentation [22] setting the stage for further delayed and programmed neuronal cell death during the secondary energy failure stage. Based on the above delineated sequence of events, rational neuroprotective therapies aimed to mitigate neuronal injury of HIE should focus on (1) shortening the duration of asphyxia, (2) administration of cytoprotective/antioxidant agents simultaneously with the resuscitation to limit reoxygenation/reperfusion injury, and (3) to implement neuroprotective interventions before the neuronal injury related to secondary energy failure occurs. These options can and should be combined to maximize their neuroprotective potential, but perhaps the third option has the largest translational feasibility as there is usually a latent phase between the restoration of brain energy metabolism upon reoxygenation and the onset of secondary energy failure that offers at least a 5–6 h long therapeutic window for interventions.

In the current experiments, we used a large animal (piglet) PA/HIE model that was previously characterized [4] and now confirmed to present all the major metabolic hallmarks of PA also observed in humans at birth (hypoxemia, hypercapnia and lactic acidosis), and to develop HIE shown by neuropathology scores. This model has been successfully implemented to show neuroprotection afforded by reventilation with gas mixture containing 2.1% molecular hydrogen, likely mitigating the oxidative stress-induced neuronal damage associated with reoxygenation/reperfusion [4]. Another attractive neuroprotective target would be the prevention of neuronal cell death through the activation of antiapoptotic signaling pathways. This approach could be used in the latent phase after reoxygenation but before the onset of secondary energy failure as although necrosis can be observed within minutes, apoptosis takes more time to develop [23]. For instance, exogenous or endogenous BDNF could exert neuroprotection through stimulation of neuronal survival and inhibition of apoptosis in this period. BDNF might be involved in the endogenous neuroprotective response after PA, as BDNF mRNA levels detected at 48 h survival were significantly increased in all brain areas compared to naïve animals in a newborn piglet HIE model [24]. Furthermore, exogenous BDNF was found neuroprotective in a rat neonatal hypoxic-ischemic brain injury model [13]. Neuroprotection elicited by intracerebroventrical administration of BDNF to postnatal day 7 rat pups was causally linked to pronounced and rapid increases in the phosphorylation/activation of ERK and Akt kinases lasting up to at least 12 h. Furthermore, ERK activation was specifically shown to reduce apoptotic neuronal death assessed with cleaved caspase 3 immunohistochemistry [13].

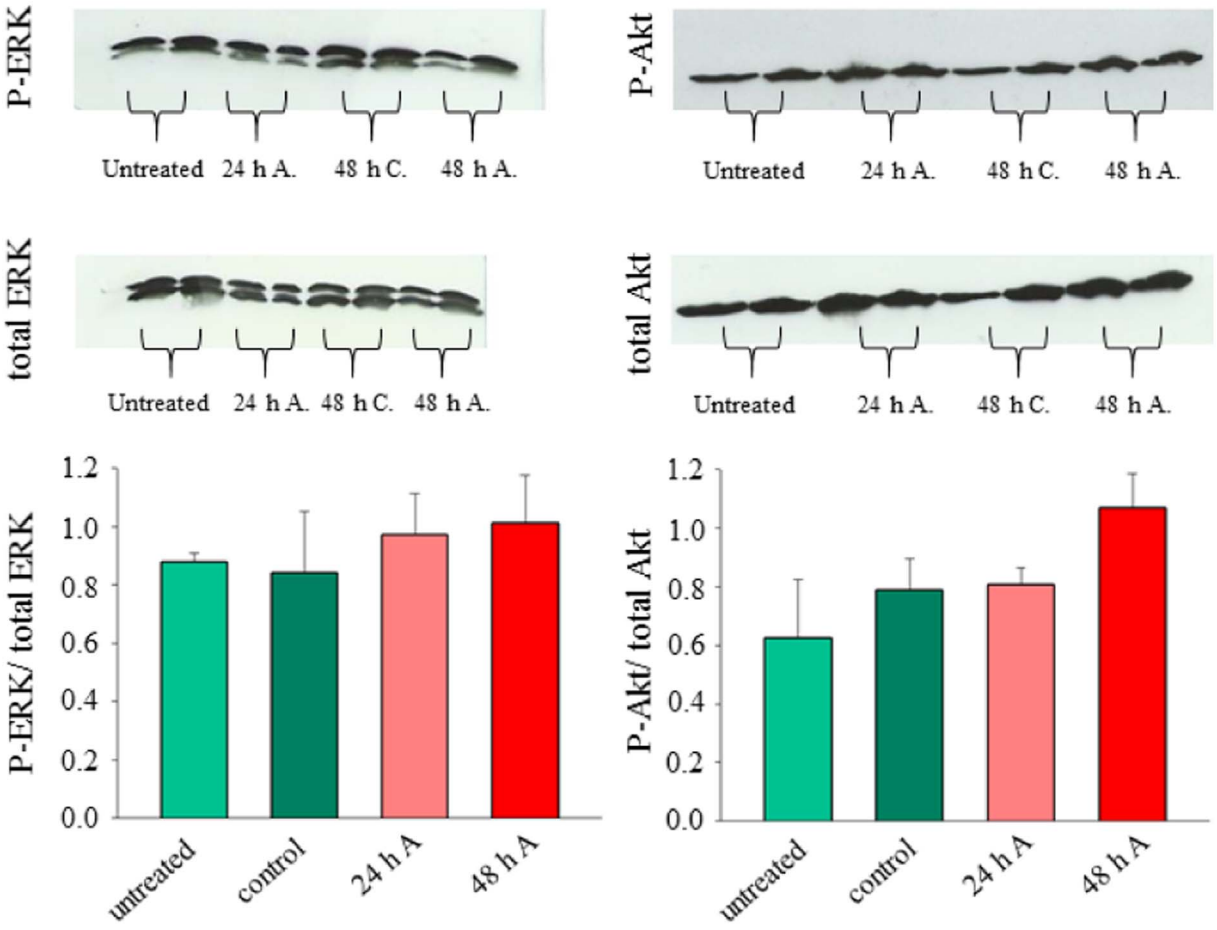

Fig. 3. Ratio of phosphorylated (P-ERK, P-Akt) and levels of total ERK and Akt in the cerebral cortex of the different experimental groups (bar graphs) with representative blots. There were no significant differences among the different groups. *Untreated* – untreated group; *Control*, *C* – time control animals without asphyxia; *A* – asphyxia group, 24 h–48 h – length of survival. Data are shown as mean ± S.E.M.

In addition to BDNF, other growth factors such as basic fibroblast growth factor have been identified as a factor promoting cell survival and neurogenesis, through activation of the ERK pathway [25,26]. In addition, Cohen-Armon et al. demonstrated that ERK2 phosphorylation can be modulated by PolyADP-ribose polymerase-1 (PARP-1) which catalyze a posttranslational modification of nuclear proteins by polyADP-ribosylation [27]. PARP-1 activation could play a role in our model as it has been found to be induced by hypoxia in newborn piglets [28]. The importance of the activation of the PI3K/Akt signaling pathway has been demonstrated in an adult rat stroke model, where cerebral infarct was elicited with permanent middle cerebral artery occlusion (pMCAO). Again, BDNF could reduce infarct size that was associated with the phosphorylation of Akt. Wortmannin, a selective PI3K inhibitor, could reverse the increment in p-Akt level and the afforded neuroprotection [29]. The transient elevation in p-Akt levels was also noted in adult mice within hours of MCAO, and this endogenous activation was regarded as neuroprotective [30].

Our current study yielded markedly different results concerning the phosphorylation levels of both ERK and Akt. Unlike in the previously cited adult or P7 neonatal rodent studies [13,29,30], ERK and Akt

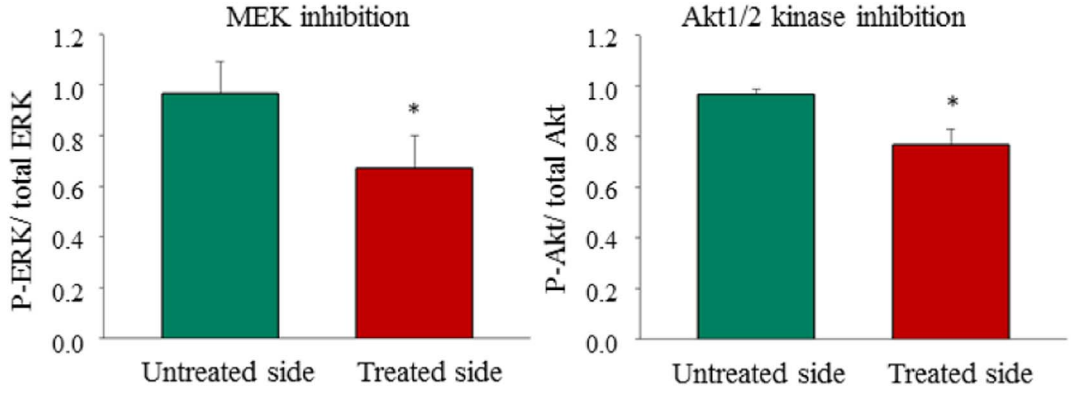

Fig. 4. Ratio of phosphorylated (P-ERK, P-Akt) and levels of total ERK and Akt in the normoxic, non-asphyxiated cerebral cortex after inhibition with the MEK inhibitor U0126 and the Akt1/2 kinase inhibitor A-6730, respectively. Both inhibitor significantly reduced phosphorylation compared to the contralateral untreated side. *$p < 0.05$ compared to the untreated side. Data are shown as mean ± S.E.M.

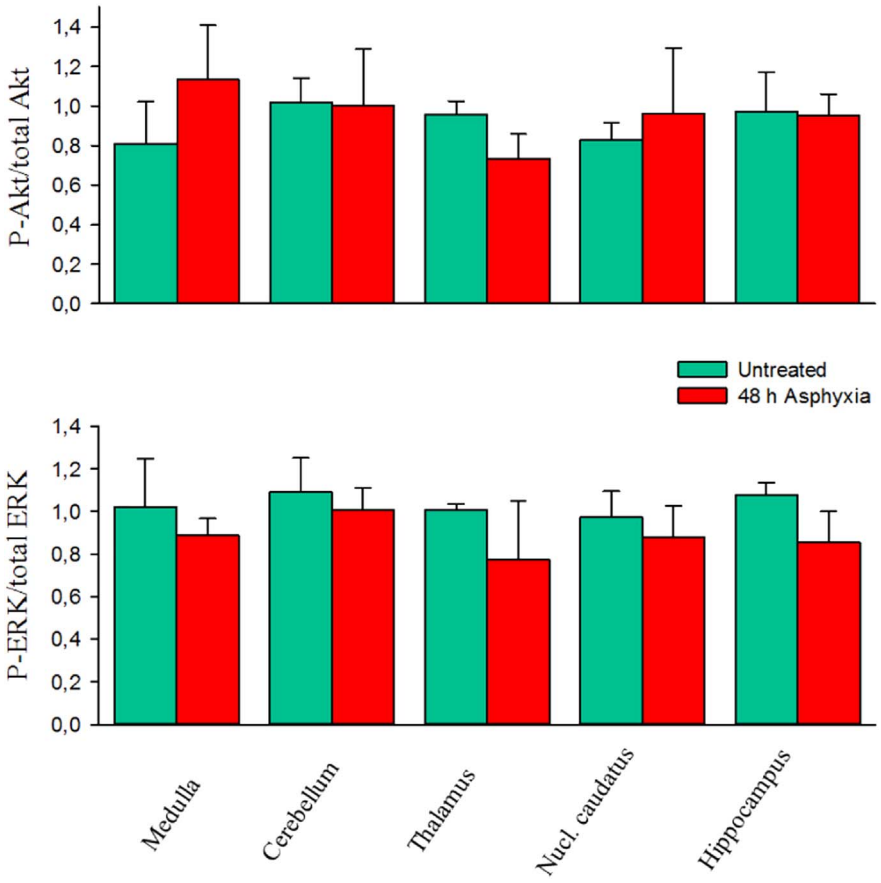

Fig. 5. Ratio of phosphorylated (P-ERK, P-Akt) and of total ERK and Akt levels in the assessed brain regions from the untreated and 48 h asphyxia groups (n = 3–3). Assessment of the different brain regions yielded essentially similar data: both ERK and Akt displayed high degree of phosphorylation that was unaffected by asphyxia, there were no significant differences among the different groups. *Untreated* – untreated group; *48 h Asphyxia* – asphyxia group with 48 h period of survival. Data are shown as mean ± S.E.M.

phosphorylation was virtually complete also in the cortex of untreated naïve animals, and it was not changed significantly either in the normoxic time controls or the animals subjected to PA for at least 48 h. This high degree of baseline phosphorylation/activation of untreated animals was also observed in virtually all of the assessed brain regions, not only in the neocortex, but also in the hippocampus, the caudate nucleus, the thalamus, cerebellum, and the medulla oblongata suggesting a general phenomenon. Similarly, high phosphorylation levels were maintained also at 48 h after asphyxia. Our pharmacological experiments proved that these findings cannot be simply attributed to technical limitations. We could show in the neocortex, where local pharmacological treatment through the closed cranial window was possible that the MEK and Akt1/2 kinase inhibitors could reduce rapidly and statistically significantly the ratio of the phosphorylated forms of ERK and Akt, respectively. The background of this substantial difference is unknown, but one can assume to be associated with the fact that the piglets in the present study were indeed in the perinatal period: they were all born < 24 h before the experiments. Vaginal delivery even under physiological conditions is associated with mild asphyxia and perhaps this physiological amount of cerebral hypoxia is enough to trigger the observed activation of ERK and Akt. This situation may be in sharp contrast with most of the neonatal rodent HIE models. In these models P7–P8 pups are used because brain maturity is closest to the term human baby at this postnatal age [31]. However, our results suggest that in these models the effects of delivery on cerebral function may have already likely faded, and the activation levels of ERK and Akt are significantly different from the immediate perinatal period. These results question the efficacy of therapeutic interventions aiming to activate these antiapoptotic signaling pathways to obtain neuroprotection. This suggestion is in line with the recent findings of an elegant study. Robertson et al. studied melatonin-induced neuroprotection in a very similar newborn piglet 48 h survival HIE model. Although melatonin was found neuroprotective, however, significant anti-apoptotic effect of melatonin using cleaved caspase-3 immunohistochemistry could not be shown in the cerebral cortex [32].

5. Conclusion

We demonstrated in a translational newborn piglet model of PA/HIE that the endogenous activations levels of ERK and Akt kinases critical in antiapoptotic signaling are already high in the cerebral cortex and all other assessed brain regions under baseline conditions and would not significantly change up to 48 h following asphyxia capable to induce significant neuronal injury. We propose that further activation of these signaling pathways is difficult, and this limitation should be taken into consideration when designing rational neuroprotective treatments to mitigate the long term adverse effects of HIE.

Conflict of interest statement

The authors declare that there are no conflicts of interest.

Acknowledgments

The study was supported by grants from the Hungarian Brain Research Program (KTIA_13_NAP-A-I/13) and from the EU-funded Hungarian grant EFOP-3.6.1-16-2016-00014. János Németh was supported by the “Nemzeti Tehetség Program” of the “Emberi Erőforrás Támogatáskezelő” from the Hungarian Ministry of Human Capacities.

References

[1] H.M. Aslam, S. Saleem, R. Afzal, U. Iqbal, S.M. Saleem, M.W.A. Shaikh, N. Shahid, Risk factors of birth asphyxia, Ital. J. Pediatr. 40 (2014) 94, http://dx.doi.org/10.1186/s13052-014-0094-2.

[2] D. Azzopardi, P. Brocklehurst, D. Edwards, H. Halliday, M. Levene, M. Thoresen, A. Whitelaw, The TOBY study. Whole body hypothermia for the treatment of perinatal asphyxial encephalopathy: a randomised controlled trial, BMC Pediatr. 8 (2008) 17, http://dx.doi.org/10.1186/1471-2431-8-17.
[3] S.A. Book, L.K. Bustad, The fetal and neonatal pig in biomedical research, J. Anim. Sci. 38 (1974) 997–1002.
[4] J. Nemeth, V. Toth-Szuki, V. Varga, V. Kovacs, G. Remzso, F. Domoki, Molecular hydrogen affords neuroprotection in a translational piglet model of hypoxic-ischemic encephalopathy, J. Physiol. Pharmacol. 67 (2016) 677–689.
[5] F. Marmigère, F. Rage, L. Tapia-Arancibia, GABA-glutamate interaction in the control of BDNF expression in hypothalamic neurons, Neurochem. Int. 42 (2003) 353–358.
[6] L. Minichiello, A.M. Calella, D.L. Medina, T. Bonhoeffer, R. Klein, M. Korte, Mechanism of TrkB-mediated hippocampal long-term potentiation, Neuron 36 (2002) 121–137, http://dx.doi.org/10.1016/S0896-6273(02)00942-X.
[7] M. Meng, W. Zhiling, Z. Hui, L. Shengfu, Y. Dan, H. Jiping, Cellular levels of TrkB and MAPK in the neuroprotective role of BDNF for embryonic rat cortical neurons against hypoxia in vitro, Int. J. Dev. Neurosci. 23 (2005) 515–521.
[8] D.P. Brazil, J. Park, B.A. Hemmings, PKB binding proteins. Getting in on the Akt, Cell 111 (2002) 293–303.
[9] R.S. Duman, B. Voleti, Signaling pathways underlying the pathophysiology and treatment of depression: novel mechanisms for rapid-acting agents, Trends Neurosci. 35 (2012) 47–56, http://dx.doi.org/10.1016/j.tins.2011.11.004.
[10] M. Hetman, A. Gosdz, Role of extracellular signal regulated kinases 1 and 2 in neuronal survival, Eur. J. Biochem. 271 (2004) 2050–2055, http://dx.doi.org/10.1111/j.1432-1033.2004.04133.x.
[11] S.Y. Park, H. Lee, J. Hur, S.Y. Kim, H. Kim, J.-H. Park, S. Cha, S.S. Kang, G.J. Cho, W.S. Choi, K. Suk, Hypoxia induces nitric oxide production in mouse microglia via p38 mitogen-activated protein kinase pathway, Brain Res. Mol. Brain Res. 107 (2002) 9–16, http://dx.doi.org/10.1016/S0169-328X(02)00421-7.
[12] X. Sun, H. Zhou, X. Luo, S. Li, D. Yu, J. Hua, D. Mu, M. Mao, Neuroprotection of brain-derived neurotrophic factor against hypoxic injury in vitro requires activation of extracellular signal-regulated kinase and phosphatidylinositol 3-kinase, Int. J. Dev. Neurosci. 26 (2008), http://dx.doi.org/10.1016/j.ijdevneu.2007.11.005.
[13] B.H. Han, D.M. Holtzman, BDNF protects the neonatal brain from hypoxic-ischemic injury in vivo via the ERK pathway, J. Neurosci. 20 (2000) 5775–5781.
[14] H. Lu, X. Liu, N. Zhang, X. Zhu, H. Liang, L. Sun, Y. Cheng, Neuroprotective effects of brain-derived neurotrophic factor and noggin-modified bone mesenchymal stem cells in focal cerebral ischemia in rats, J. Stroke Cerebrovasc. Dis. 25 (2016) 410–418, http://dx.doi.org/10.1016/j.jstrokecerebrovasdis.2015.10.013.
[15] O. Oláh, V. Tóth-Szűki, P. Temesvári, F. Bari, F. Domoki, Delayed neurovascular dysfunction is alleviated by hydrogen in asphyxiated newborn pigs, Neonatology. 104 (2013) 79–86, http://dx.doi.org/10.1159/000348445.
[16] K.J. Hassell, M. Ezzati, D. Alonso-Alconada, D.J. Hausenloy, N.J. Robertson, New horizons for newborn brain protection: enhancing endogenous neuroprotection, Arch. Dis. Child. Fetal Neonatal Ed. 100 (2015) F541–52, http://dx.doi.org/10.1136/archdischild-2014-306284.
[17] Y. Chen, E. Engidawork, F. Loidl, E. Dell'Anna, M. Goiny, G. Lubec, K. Andersson, M. Herrera-Marschitz, Short- and long-term effects of perinatal asphyxia on monoamine, amino acid and glycolysis product levels measured in the basal ganglia of the rat, Brain Res. Dev. Brain Res. 104 (1997) 19–30.
[18] B. Lubec, M. Chiappe-Gutierrez, H. Hoeger, E. Kitzmueller, G. Lubec, Glucose transporters, hexokinase, and phosphofructokinase in brain of rats with perinatal asphyxia, Pediatr. Res. 47 (2000) 84–88.
[19] E. Engidawork, Y. Chen, E. Dell'Anna, M. Goiny, G. Lubec, U. Ungerstedt, K. Andersson, M. Herrera-Marschitz, Effect of perinatal asphyxia on systemic and intracerebral pH and glycolysis metabolism in the rat, Exp. Neurol. 145 (1997) 390–396, http://dx.doi.org/10.1006/exnr.1997.6482.
[20] Y. Numagami, A.B. Zubrow, O.P. Mishra, M. Delivoria-Papadopoulos, Lipid free radical generation and brain cell membrane alteration following nitric oxide synthase inhibition during cerebral hypoxia in the newborn piglet, J. Neurochem. 69 (1997) 1542–1547.
[21] V. Degos, G. Loron, J. Mantz, P. Gressens, Neuroprotective strategies for the neonatal brain, Anesth. Analg. 106 (2008) 1670–1680, http://dx.doi.org/10.1213/ane.0b013e3181733f6f.
[22] W. Akhter, Q.M. Ashraf, S.A. Zanelli, O.P. Mishra, M. Delivoria-Papadopoulos, Effect of graded hypoxia on cerebral cortical genomic DNA fragmentation in newborn piglets, Biol. Neonate 79 (2001) 187–193 (47089).
[23] E. Bonfoco, D. Krainc, M. Ankarcrona, P. Nicotera, S.A. Lipton, Apoptosis and necrosis: two distinct events induced, respectively, by mild and intense insults with N-methyl-D-aspartate or nitric oxide/superoxide in cortical cell cultures, Proc. Natl. Acad. Sci. U. S. A. 92 (1995) 7162–7166.
[24] L. Olson, S. Faulkner, K. Lundströmer, A. Kerenyi, D. Kelen, M. Chandrasekaran, U. Ådén, L. Olson, X. Golay, H. Lagercrantz, N.J. Robertson, D. Galter, Comparison of three hypothermic target temperatures for the treatment of hypoxic ischemia: mRNA level responses of eight genes in the piglet brain, Transl Stroke Res 4 (2013) 248–257, http://dx.doi.org/10.1007/s12975-012-0215-4.
[25] K. Takami, M. Iwane, Y. Kiyota, M. Miyamoto, R. Tsukuda, S. Shiosaka, Increase of basic fibroblast growth factor immunoreactivity and its mRNA level in rat brain following transient forebrain ischemia, Exp. Brain Res. 90 (1992) 1–10.
[26] P. Morales, J.L. Fiedler, S. Andrés, C. Berrios, P. Huaiquín, D. Bustamante, S. Cardenas, E. Parra, M. Herrera-Marschitz, Plasticity of hippocampus following perinatal asphyxia: effects on postnatal apoptosis and neurogenesis, J. Neurosci. Res. 86 (2008) 2650–2662, http://dx.doi.org/10.1002/jnr.21715.
[27] M. Cohen-Armon, L. Visochek, D. Rozensal, A. Kalal, I. Geistrikh, R. Klein, S. Bendetz-Nezer, Z. Yao, R. Seger, DNA-independent PARP-1 activation by phosphorylated ERK2 increases Elk1 activity: a link to histone acetylation, Mol. Cell 25 (2007) 297–308, http://dx.doi.org/10.1016/j.molcel.2006.12.012.
[28] O.P. Mishra, W. Akhter, Q.M. Ashraf, M. Delivoria-Papadopoulos, Hypoxia-induced modification of poly (ADP-ribose) polymerase and dna polymerase beta activity in cerebral cortical nuclei of newborn piglets: role of nitric oxide, Neuroscience 119 (2003) 1023–1032.
[29] H. Huang, R. Zhong, Z. Xia, J. Song, L. Feng, Neuroprotective effects of Rhynchophylline against ischemic brain injury via regulation of the Akt/mTOR and TLRs signaling pathways, Molecules 19 (2014) 11196–11210, http://dx.doi.org/10.3390/molecules190811196.
[30] M. Shibata, T. Yamawaki, T. Sasaki, H. Hattori, J. Hamada, Y. Fukuuchi, H. Okano, M. Miura, Upregulation of Akt phosphorylation at the early stage of middle cerebral artery occlusion in mice, Brain Res. 942 (2002) 1–10, http://dx.doi.org/10.1016/S0006-8993(02)02474-5.
[31] J. Dobbing, J. Sands, Comparative aspects of the brain growth spurt, Early Hum. Dev. 3 (1979) 79–83, http://dx.doi.org/10.1016/0378-3782(79)90022-7.
[32] N.J. Robertson, S. Faulkner, B. Fleiss, A. Bainbridge, C. Andorka, D. Price, E. Powell, L. Lecky-Thompson, L. Thei, M. Chandrasekaran, M. Hristova, E.B. Cady, P. Gressens, X. Golay, G. Raivich, Melatonin augments hypothermic neuroprotection in a perinatal asphyxia model, Brain 136 (2013) 90–105, http://dx.doi.org/10.1093/brain/aws285.